



TEXAS TECH UNIVERSITY

Multidisciplinary Research in Transportation

Minimize Premature Distresses in Continuously Reinforced Concrete Pavement

Sureel Saraf, Pangil Choi, Sungwoo Ryu,
Tewodros Ghebrab, Moon C. Won

Texas Department of Transportation

Research Project #: 0-6687
Research Report #: 0-6687-1
www.techmrt.ttu.edu/reports.php

May 2014

NOTICE

The United States Government and the State of Texas do not endorse products or manufacturers. Trade or manufacturers' names appear herein solely because they are considered essential to the object of this report.

1. Report No. FHWA/TX-14-0-6687-1	2. Government Accession No.:	3. Recipient's Catalog No.:	
4. Title and Subtitle: Minimize Premature Distresses in Continuously Reinforced Concrete Pavements		5. Report Date: August 2013	
7. Author(s): Sureel Saraf, Pangil Choi, Sungwoo Ryu, Soojun Ha, Tewodros Ghebrab, Moon C. Won		8. Performing Organization Report No. 0-6687-1	
9. Performing Organization Name and Address: Texas Tech University College of Engineering Box 41023 Lubbock, Texas 79409-1023		10. Work Unit No.(TRAIS):	
		11. Contract or Grant No.: Project 0-6687	
12. Sponsoring Agency Name And Address Texas Department Of Transportation Research and Technology Implementation Office P.O. Box 5080 Austin, TX 78763-5080		13. Type of Report and Period Cover: Technical Report 09/2011-08/2013	
		14. Sponsoring Agency Code:	
15. Supplementary Notes: Project performed in cooperation with Texas Department of Transportation and the Federal Highway Administration			
16. Abstract: The long-term performance of continuously reinforced concrete pavement (CRCP) has been quite satisfactory in Texas, providing an important network of highways with heavy truck traffic and minimal maintenance. Field evaluations of the performance of CRCP in Texas reveal that a substantial portion of distresses is not necessarily due to structural deficiencies of CRCP. Rather, many distresses appear to be due to construction and material related issues and to a lesser extent, imperfections in design details. Since these distresses occur long before structural distresses develop, they are considered premature distresses. The most effective way to prevent or minimize premature distresses is to identify the mechanisms of distresses, develop appropriate special provisions to existing specifications or special specifications, and modify existing design standards. Distresses at transverse construction joints (TCJs) were one of the most frequently observed and efforts were made to identify the mechanisms of those distresses and develop or improve design standards or specifications. Field evaluations of concrete and steel behavior near TCJs were made using various gages. The analysis of the data indicates that the current practice of placing additional tie bars at TCJs, along with poor construction practices, are the major causes of the distress. There is a large difference in the behavior of reinforcement between additional tie bars and longitudinal steel that is continuous through transverse construction joints. The premise that additional tie bars at TCJs will behave the same way as longitudinal steel, thus reducing steel stresses of longitudinal steel at TCJs, keeping the joint widths tight, and improving TCJ performance, is not necessarily correct. Also, the use of additional tie bars makes the consolidation of concrete at TCJs difficult due to the reduced spacing between longitudinal reinforcing steel. Not placing additional tie bars at TCJs, and the use of relief transverse saw cut joints near TCJs, along with improved construction practices at TCJs, will minimize the distresses.			
17. Key Words: CRCP, punchout, transverse construction joint, premature distresses	18. Distribution Statement No Restrictions. This document is available to the public through the National Technical Information Service, Springfield, VA 22161, www.ntis.gov		
19. Security Classif. (of this report) Unclassified	20. Security Classif. (of this page) Unclassified	21. No. Of Pages 140	22. Price

**Minimize Premature Distresses in Continuously Reinforced Concrete
Pavements**

By

Sureel Saraf

Pangil Choi

Sungwoo Ryu

Soojun Ha

Tewodros Ghebrab

Moon C. Won

Research Report Number 0-6687-1

Project Number 0-6687

Conducted for the Texas Department of Transportation

Center for Multidisciplinary Research in Transportation
Texas Tech University

AUTHOR'S DISCLAIMER

The contents of this report reflect the views of the authors who are responsible for the facts and the accuracy of the data presented herein. The contents do not necessarily reflect the official view of policies of the Texas Department of Transportation or the Federal Highway Administration. This report does not constitute a standard, specification, or regulation.

PATENT DISCLAIMER

There was no invention or discovery conceived or first actually reduced to practice in the course of or under this contract, including any art, method, process, machine, manufacture, design or composition of matter, or any new useful improvement thereof, or any variety of plant which is or may be patentable under the patent laws of the United States of America or any foreign country.

ENGINEERING DISCLAIMER

Not intended for construction, bidding, or permit purposes.

TRADE NAMES AND MANUFACTURERS' NAMES

The United States Government and the State of Texas do not endorse products or manufacturers. Trade or manufacturers' names appear herein solely because they are considered essential to the object of this report.

ACKNOWLEDGMENTS

This research study was sponsored by the Texas Department of Transportation in cooperation with the Federal Highway Administration. The authors express their gratitude to Mr. Andy Naranjo, project director, PMC members, and RTI Research Engineer, Mr. Wade Odell. In addition, the authors acknowledge the support provided by the TxDOT District personnel for construction of test sections.

TABLE OF CONTENTS

Chapter 1 Introduction.....	1
Chapter 2 Premature Distresses in CRCP	3
2.1 Distresses at Transverse Construction Joints	5
2.2 Distresses Due to Slab Movement at Transverse Construction Joints	7
2.3 Distresses Due to Construction / Material Quality at Transverse Construction Joints	8
2.4 Y and Narrow Transverse Cracks	10
2.5 Distresses Due to Slab Expansion.....	12
2.6 Debonding and Large Joint Width at Transverse Construction Joint	13
2.7 Distresses at Gore Areas	15
2.8 Distresses at Longitudinal Joints.....	17
2.9 Premature Distress Types in Other States	18
2.9.1 Illinois DOT	18
2.9.2 California DOT (Caltrans).....	21
2.9.3 Virginia DOT	21
2.9.4 Louisiana DOT	23
2.9.5 Oklahoma DOT	23
2.10 Summary	24
Chapter 3 Identification of Premature Distress Mechanisms at Transverse Construction Joint in New CRCP	25
3.1 Site Selection for Field Testing.....	26
3.2 Test Sections on US 82 in Lubbock District.....	28
3.2.1 LBB-I Test Section – Testing Plan and Gage Setup	29
3.2.2 LBB-II Test Section – Testing Plan and Gage Setup	32
3.2.3 Steel Strain Behavior near TCJ in Lubbock District.....	35
3.2.4 Concrete Strain Behavior near TCJ in Lubbock District.....	40

3.2.5 Longitudinal Slab Movement at LBB-I TCJ.....	47
3.3 Test Section on IH 20 in Brownwood District.....	48
3.3.1 BWD-I Test Section – Testing Plan and Gage Setup.....	50
3.3.2 Steel Strain Behavior near TCJ at BWD-I Test Section.....	52
3.3.3 BWD-II Test Section – Testing Plan and Gage Setup	57
3.3.4 Concrete Strain at Junction of Transverse Construction Joint and Longitudinal Construction Joint – BWD-II TCJ.....	60
3.3.5 Slab Movement at Free Edge at BWD-II Test Section	64
3.3.6 Relationship Between Crackmeter Movement and Concrete Strain Change	67
3.3.7 Vertical Slab Movement at BWD-II TCJ.....	68
3.4 Effect of Construction Season on Concrete Strain near Transverse Construction Joint	69
3.5 Test Section on IH 35 in Waco District	72
3.5.1 Steel Strain Behavior near TCJ in Waco District.....	75

Chapter 4 Identification of Premature Distress Mechanisms at Transverse Construction Joint in Existing CRCP81

4.1 Large Joint Width Section on IH 10 in the El Paso District.....	81
4.1.1 ELP-I and ELP-II Test Section – Testing Plan and Gage Setup	82
4.1.2 Crackmeter Data from IH 10 in the El Paso District.....	83
4.2 Large Joint Width Section on IH 40 in Childress District	87
4.2.1 IH-40 Test Section in Childress – Testing Plan and Gage Setup	90
4.2.2 Crackmeter Data from IH 40 in Childress District.....	91
4.3 Construction and Material Issue at Transverse Construction Joint.....	94
4.3.1 Construction Practice at Transverse Construction Joint.....	94
4.3.2 Concrete Properties near the Transverse Construction Joint.....	96
4.4 Coefficient of Thermal Expansion and Dynamic Modulus of Elasticity at Y and Narrow Crack Sections.....	102
4.4.1 Y-Cracks on IH 10 in El Paso District	105
4.5 Test Section on FM 1938 in the Ft. Worth District.....	106
4.5.1 FTW-I and FTW-II Test Sections - Testing Plan and Gage Setup.....	107
4.5.2 Concrete Strain Behavior at FTW-I and FTW-II Test Section	108
4.6 Distress Mechanisms at Longitudinal Joint	114

Chapter 5 Conclusions and Recommendations	117
5.1 Conclusions.....	117
5.2 Recommendations.....	118
References	120
Appendix A: Special Provision to Item 360.....	121
Appendix B: Revised Design Standards for CRCP.....	122

LIST OF FIGURES

Figure 2. 1 CRCP Distress Classification in Texas (Won, 2012).....	3
Figure 2. 2 Distress at TCJ.....	5
Figure 2. 3 Distress at TCJ.....	5
Figure 2. 4 Distress at CRCP Interface.....	5
Figure 2. 5 Distress at Repair TCJ.....	5
Figure 2. 6 Distress at 2 ft. from TCJ.....	6
Figure 2. 7 CRCP Design Details - CPR (B) - 61 (MOD).....	6
Figure 2. 8 Distresses at Repair Joint - US 59 in the Atlanta District.....	7
Figure 2. 9 Distresses at Repair Joint - US 59 in the Atlanta District.....	7
Figure 2. 10 Slab Movement Experimentation (Nam, 2005).....	8
Figure 2. 11 Slab Movement on US 287 in Wichita Falls (Nam, 2005).....	8
Figure 2. 12 Surface Voids at TCJ.....	9
Figure 2. 13 Surface Voids on US 287 in Wichita Falls.....	9
Figure 2. 14 Concrete Placement at TCJ.....	9
Figure 2. 15 Concrete Consolidation at TCJ.....	9
Figure 2. 16 Y-Crack on US 287 in the Wichita Falls District.....	10
Figure 2. 17 Core Taken From Y-Crack on US 287 in the Wichita Falls District.....	10
Figure 2. 18 Y-Crack on US 59 in the Atlanta District.....	11
Figure 2. 19 Core Taken at Y-Crack on US 59 in the Atlanta district.....	11
Figure 2. 20 Coring at Y-Crack Location.....	11
Figure 2. 21 Horizontal Cracking at Y-Crack Location.....	11
Figure 2. 22 Bent Stapling-bar at Longitudinal Joint on IH 45 in the Houston District.....	12
Figure 2. 23 Bent Tie-Bar at Repair Section on Loop 610 in the Houston District.....	12
Figure 2. 24 Distress at TCJ on IH 10 in the El Paso District.....	13
Figure 2. 25 Distress at TCJ on IH 10 in the El Paso District.....	13
Figure 2. 26 TCJ Width on IH 10 in the El Paso District.....	14
Figure 2. 27 TCJ on IH 10 in the El Paso District.....	14
Figure 2. 28 Distress at TCJ on IH 40 in the Childress District.....	14
Figure 2. 29 TCJ Width on IH 40 in the Childress District – Morning.....	14
Figure 2. 30 TCJ Width on IH 40 in the Childress District - Evening.....	15
Figure 2. 31 Debonding Between Steel and Concrete on IH 40 in the Childress District.....	15
Figure 2. 32 Distress at Gore Area Due to Different Edge Support Conditions.....	16
Figure 2. 33 Deflection Testing at Pavement Edge With Tied Concrete Shoulder.....	16
Figure 2. 34 Deflection Testing at Pavement Edge.....	16
Figure 2. 35 Deflections at Pavement Edge For Two Different Shoulder Types.....	17
Figure 2. 36 The Effect of Edge Condition and Slab Support From Westergaard Equation.....	17
Figure 2. 37 Distresses Near LCJ.....	18
Figure 2. 38 Distresses Near LWJ.....	18

Figure 2. 39 Distress at CRCP/CPCD.....	19
Figure 2. 40 Distress at CRCP/CPCD.....	19
Figure 2. 41 Distress in CRCP Next to CIP-PCP on IH 35 in Hillsboro.....	20
Figure 2. 42 Construction of CRCP Tied to CRCP on US 59 in the Atlanta District	20
Figure 2. 43 Cross-Section of Cement Stabilized Drainable Base (Photo Courtesy of M. Mueller)	21
Figure 2. 44 Distress Associated With Steel Placed Too High.....	21
Figure 2. 45 CRCP Const. With Mechanical Steel Placement	22
Figure 2. 46 Distress Associated With Reinforcing Steel Placed Too High	22
Figure 2. 47 Y-crack (Photo courtesy of M. Elfino).....	23
Figure 2. 48 Entrapped Air in Concrete From Y-Crack (Photo courtesy of M. Elfino).....	23
Figure 2. 49 Distress At Transverse Construction Joint (Photo courtesy of M. Elfino).....	23
Figure 2. 50 Lack of Concrete Consolidation at Header Area (Photo courtesy of M. Elfino)	23
Figure 3. 1 Test Section Locations for Studying CRCP behavior	26
Figure 3. 2 Location Map of Test Sections in Lubbock District.....	28
Figure 3. 3 Lubbock Test Section Layout.....	29
Figure 3. 4 Existing Slab at LBB-I Test Section.....	30
Figure 3. 5 Header Installed After Placing Female Tie-bars at Existing Slab at LBB-I Test Section	30
Figure 3. 6 Male Tie-Bars Inserted After Removing the Headers at Morning construction side at LBB-I.....	30
Figure 3. 7 Steel Placement at LBB-I Test Section	30
Figure 3. 8 Gage Layout at LBB-I Test Section	31
Figure 3. 9 Steel Strain Gage Installation at LBB-I Test Section.....	32
Figure 3. 10 Vibrating Wire Gage Installation at LBB-I Test Section	32
Figure 3. 11 Steel Placement at LBB-II Test Section	33
Figure 3. 12 Gage Installation Plan at LBB-II Test Location	34
Figure 3. 13 VWSG Installation at LBB-II Evening Test Section	35
Figure 3. 14 VWSG at LBB-II Morning Section With No Additional Steel at Transverse Construction Joint	35
Figure 3. 15 VWSG at LBB-II Morning Section With Additional Steel at Transverse Construction Joint	35
Figure 3. 16 Concrete Finishing at LBB-II Morning Test Section.....	35
Figure 3. 17 Early Age Steel Strain Behavior at LBB-I Test Section.....	37
Figure 3. 18 Later Age Steel Strain Behavior at LBB-I Test Section	37
Figure 3. 19 Early Age Steel Strain Behavior at LBB-II Test Section	39
Figure 3. 20 Steel Strain Behavior at LBB-II Test Section After 5 Weeks Since Construction....	40
Figure 3. 21 Concrete Strain Variation at LBB-I in January 2012.....	42
Figure 3. 22 Concrete Strain Variation at LBB-I in February 2012.....	42
Figure 3. 23 Concrete Strain Variation at LBB-I in June 2012.....	43

Figure 3. 24 Concrete Strain Variation at LBB-I in April 2013	43
Figure 3. 25 Rate of Concrete Strain Change at 1 ft.....	45
Figure 3. 26 Rate of Concrete Strain Change at 2 ft.....	46
Figure 3. 27 Rate of Concrete Strain Change at 4 ft.....	46
Figure 3. 28 Crackmeter Installation at LBB-I Test Section.....	47
Figure 3. 29 Slab Movement at LBB-I Test Section	48
Figure 3. 30 Location Map of Test Sections in Brownwood District	49
Figure 3. 31 Brownwood Test Section Layout.....	50
Figure 3. 32 Gage Installation Plan at BWD-I Test Location	51
Figure 3. 33 Concrete Placement at BWD-I Evening Test Section.....	51
Figure 3. 34 Protecting VWSGs at BWD-I Evening Test Section	51
Figure 3. 35 Concrete Placement at BWD-I Morning Test Section.....	52
Figure 3. 36 Concrete Finishing at BWD-I Morning Test Section.....	52
Figure 3. 37 Early Age Steel Strain at BWD-I Test Section	53
Figure 3. 38 Later Age Steel Strain at BWD-I Test Section	54
Figure 3. 39 Steel Strain at BWD-I Right After Construction.....	55
Figure 3. 40 Steel Strain at BWD-I-3 Months After Construction.....	55
Figure 3. 41 Steel Strain at BWD-I-5 Months After Construction.....	56
Figure 3. 42 Steel Strain at BWD-I-7 Months After Construction.....	56
Figure 3. 43 Gage Installation Plan at BWD-II Test Location.....	57
Figure 3. 44 VWSG Installation at BWD-II Evening Test Section.....	58
Figure 3. 45 Concrete Placement at BWD-II Evening Section.....	58
Figure 3. 46 Finishing at BWD-II Evening Test Section.....	58
Figure 3. 47 Crackmeter Installation Locations at BWD-II Test Section.....	59
Figure 3. 48 Crackmeters Installed to Measure Longitudinal Slab Movement at BWD-II Test Section	59
Figure 3. 49 Vertical Crackmeter Installed at the Free Slab Edge at BWD-II Test Section.....	60
Figure 3. 50 Reference Crackmeter Attached to Measure Invar Movement at BWD-II Test Section	60
Figure 3. 51 Concrete Strain Variation at BWD-II Test Section.....	61
Figure 3. 52 BWD-II Concrete Strain Comparison Before Morning Side Placement.....	62
Figure 3. 53 BWD-II Concrete Strain Comparison After Morning Side Placement.....	62
Figure 3. 54 Daily Strain Variation Near and Away	64
Figure 3. 55 Daily Slab Movement Along the Transverse Construction Joint at BWD-II	65
Figure 3. 56 Average Longitudinal Movement of the Slab	66
Figure 3. 57 Slab Movement and Concrete Strain Variation Near the Junction of LCJ and TCJ.....	67
Figure 3. 58 Slab Movement and Concrete Strain Variation Away from the Junction of LCJ and TCJ.....	68
Figure 3. 59 Vertical Slab Movement at the Free Edge of the Slab	69
Figure 3. 60 Rate of Concrete Strain Change at TCJ – LBB-I Test Section.....	70

Figure 3. 61 Rate of Concrete Strain Change at LBB II TCJ - Winter Construction.....	71
Figure 3. 62 Rate of Concrete Strain Change at BWD I TCJ - Summer Construction.....	71
Figure 3. 63 Location Map of Test Sections in Waco District.....	72
Figure 3. 64 Waco Test Section Layout.....	73
Figure 3. 65 Steel Strain Gage Installation Plan at Waco Test Location.....	74
Figure 3. 66 Steel Strain Gage Installation Near Transverse Construction Joint	75
Figure 3. 67 Tie-Bar Diameter Smaller than Longitudinal Steel.....	75
Figure 3. 68 Steel Strain Gage Lead Wire Protected by PVC Pipes and Embedded in the Asphalt Base.....	75
Figure 3. 69 Embedded PVC Pipes Carrying SSG Lead Wires Covered With Cold-Mix Asphalt	75
Figure 3. 70 Steel Strain at 34 in. From Longitudinal Construction Joint.....	78
Figure 3. 71 Steel Strain at 77 in. From Longitudinal Construction Joint.....	78
Figure 3. 72 Steel Strain at 110 in. From Longitudinal Construction Joint	79
Figure 3. 73 Steel Strain at 132 in. From Longitudinal Construction Joint	79
Figure 4. 1 Location Map of Test Sections in El Paso District.....	81
Figure 4. 2 Distance Between Consecutive Transverse Construction Joints in El Paso District ..	81
Figure 4. 3 Distresses at ELP-I Test Section	82
Figure 4. 4 Wide Transverse Construction Joint Width at ELP-I Test Section	82
Figure 4. 5 Transverse Construction Joint Condition at ELP-II Test Section.....	82
Figure 4. 6 Narrow Transverse Construction Joint Width at ELP-II Test Section.....	82
Figure 4. 7 Crackmeter Installation Across Transverse Construction Joint at ELP-I Test Section	83
Figure 4. 8 Crackmeter Installation Across Transverse Construction Joint at ELP-II Test Section	83
Figure 4. 9 Movement of Bad Transverse Construction Joint on IH 10 in El Paso – Day 1	85
Figure 4. 10 Movement of Bad Transverse Construction Joint on IH 10 in El Paso – Day 7	85
Figure 4. 11 Movement of Good Transverse Construction Joint on IH 10 in El Paso – Day 1....	86
Figure 4. 12 Movement of Good Transverse Construction Joint on IH 10 in El Paso – Day 7....	86
Figure 4. 13 Location Map of Test Section in the Childress District.....	87
Figure 4. 14 Concrete Disintegration Near Transverse Construction Joint at Childress District Test Section.....	87
Figure 4. 15 Distresses Near Transverse and Longitudinal Construction Joint Intersection at Childress Test Section	88
Figure 4. 16 Distresses near Longitudinal Construction Joint at Childress Test Section	88
Figure 4. 17 Transverse Construction Joint Width in the Morning at Childress Test Section	89
Figure 4. 18 Transverse Construction Joint Width in the Evening at Childress Test Section	89
Figure 4. 19 Transverse Construction Joint Width at Childress Test Section in February 2011...	89
Figure 4. 20 Transverse Construction Joint Width at Childress Test Section in March 2013	89
Figure 4. 21 Concrete Deterioration at Inside Shoulder of TCJ – Childress Test Section	90
Figure 4. 22 Concrete Deterioration at Outside Shoulder of TCJ – Childress Test Section	90

Figure 4. 23 Steel Slipping Out of Concrete at Transverse Construction Joint	90
Figure 4. 24 Crackmeter Installation at Outside Shoulder – Childress Test Section	91
Figure 4. 25 Crackmeter Installation at Inside Shoulder – Childress Test Section	91
Figure 4. 26 Location of MIRA 3-D Section.....	91
Figure 4. 27 Delamination Near Transverse Construction Joint on IH 40 in Childress	91
Figure 4. 28 Slab and Joint Movement at Transverse Construction Joint on IH 40 in Childress – Outside Shoulder	93
Figure 4. 29 Slab and Joint Movement at Transverse Construction Joint on IH 40 in Childress – Inside Shoulder	93
Figure 4. 30 First Truck of Concrete Arrives at BWD-I Test Section	95
Figure 4. 31 Manual Placement of Concrete At the Transverse Construction Joint – Morning... 95	95
Figure 4. 32 Auto-Float Stuck in Concrete Due to Mis-alignment of Paver.....	95
Figure 4. 33 Manual Finishing of Concrete at BWD-I Test Section	95
Figure 4. 34 Finishing Process Becomes Difficult as Concrete Hardens	95
Figure 4. 35 Uneven Slab Edge.....	95
Figure 4. 36 Coring Locations at BWD-II Transverse Construction Joint.....	96
Figure 4. 37 BWD-II Coring Location 1 and MIRA Scan	97
Figure 4. 38 BWD-II Coring Location 2 and MIRA Scan	97
Figure 4. 39 BWD-II Coring Location 3 and MIRA Scan	98
Figure 4. 40 Unit Weight of Cores Taken at BWD-II Section.....	99
Figure 4. 41 Dynamic Young's Modulus (Dry) of Cores Taken at BWD-II Section.....	99
Figure 4. 42 Surface Condition of Coring Location on US 287 in Wichita Falls	100
Figure 4. 43 Core Taken at Location B1 on US 287 in Wichita Falls	100
Figure 4. 44 Core Taken at Location B2 on US 287 in Wichita Falls	100
Figure 4. 45 Core Taken at Location G1 on US 287 in Wichita Falls	100
Figure 4. 46 Unit Weight of Cores Taken on US 287 in Wichita Falls	101
Figure 4. 47 Dynamic Young's Modulus (Dry) of Cores Taken on US 287 in Wichita Falls	102
Figure 4. 48 Y-cracks on US 287 in the Wichita Falls District	103
Figure 4. 49 Y-Crack on Top of Transverse Steel on US 287 in the Wichita Falls District.....	103
Figure 4. 50 Y-Crack on IH 35 in the Laredo District	103
Figure 4. 51 Distress Due to Y-Crack on IH 35 in the Laredo District	103
Figure 4. 52 Narrow Cracks on US 287 in the Wichita Falls District.....	104
Figure 4. 53 Narrow Cracks on US 287 in the Wichita Falls District.....	104
Figure 4. 54 Distress Due to Narrow Cracks on IH 45 in the Dallas District	104
Figure 4. 55 Distress Due to Narrow Cracks on IH 45 in the Dallas District.....	104
Figure 4. 56 Coring Conducted at Y-crack Location on IH 10 in El Paso District – Location 1	106
Figure 4. 57 Y-crack at the Intersection of Longitudinal and Transverse Steel on IH 10 in El Paso District – Location 1	106
Figure 4. 58 Y-Crack on IH 10 in El Paso District – Location 2.....	106
Figure 4. 59 Core Taken at Y-crack Location 2 on IH 10 in El Paso District	106

Figure 4. 60 Vibrating Wire Strain Gage Installation at FTW-I Test Section	107
Figure 4. 61 Vibrating Wire Strain Gage Installation at FTW-II Test Section.....	107
Figure 4. 62 Crack Location at FTW-I Test Section	108
Figure 4. 63 Crack Location at FTW-II Test Section.....	108
Figure 4. 64 Concrete Strain Variation on FM 1938 Summer Section at 60-62 °F	109
Figure 4. 65 Concrete Strain Variation on FM 1938 Summer Section at 70-72 °F	109
Figure 4. 66 Concrete Strain Variation on FM 1938 Summer Section at 80-82 °F	110
Figure 4. 67 Concrete Strain Variation on FM 1938 Summer Section at 90-92 °F	110
Figure 4. 68 Concrete Strain Variation on FM 1938 Winter Section at 60-62 °F	112
Figure 4. 69 Concrete Strain Variation on FM 1938 Winter Section at 70-72 °F	112
Figure 4. 70 Concrete Strain Variation on FM 1938 Winter Section at 80-82 °F	113
Figure 4. 71 Concrete Strain Variation on FM 1938 Winter Section at 90-92 °F	113
Figure 4. 72 LCJ Distresses on IH 27 in the Lubbock District.....	114
Figure 4. 73 Longitudinal Joint Condition on IH 40 in the Amarillo District	115
Figure 4. 74 Asphalt Overlay over CRCP on IH 40 in the Amarillo District	115
Figure 4. 75 LCJ Distress on IH 10 Eastbound in the El Paso District.....	116
Figure 4. 76 LCJ Distress on IH 10 Westbound in the El Paso District	116

LIST OF TABLES

Table 2. 1 Detailed Classification of Punchouts.....	4
Table 3. 1 Types of Gages and Testing Setup	25
Table 3. 2 Test Section Details	27
Table 3. 3 Daily Concrete Strain Variation at BWD-II Test Section	63
Table 3. 4 Slab Movement at Transverse Construction Joint	66
Table 4. 1 CoTE and Dynamic Modulus of Elasticity at Y and Narrow Transverse Cracks	105

Chapter 1 Introduction

The long-term performance of continuously reinforced concrete pavement (CRCP) has been quite satisfactory in Texas, providing an important network of highways with heavy truck traffic and minimal maintenance.

Extensive field performance evaluations of CRCP in Texas conducted under the TxDOT rigid pavement database project indicate that the majority of the distresses is not necessarily due to the deficiencies in the structural capacity of CRCP; rather, the majority of distresses is due to imperfections in materials and construction quality. Those distresses normally occur earlier than structural distresses caused by fatigue failure of concrete, and are termed premature distresses (PMDs). Traditional ways of strengthening the pavement system, such as the use of increased concrete slab thickness, do not reduce the frequency of PMDs.

The performance of CRCP repairs has not always been good and often the repairs done previously are re-repaired. The repair of these distresses usually involves undertaking partial or full depth repair. If the extent of the distresses is small usually due to spalling, asphalt patches are used as repair strategies. These methods are fairly complicated since they involve isolating the deteriorated area from the rest of the pavement by saw cutting, removing deteriorated concrete without causing damage to the adjacent concrete as well as subbase material, compacting the subbase and sub grade material, introducing tie-bars between the existing slab and the repair section to ensure good load transfer, and then ensuring a good bond between the newly placed concrete in the PCC patch and the existing pavement. Once the longitudinal steel is cut during the removal of deteriorated slab, it is difficult to maintain the continuity of the longitudinal steel. The repair of CRCP distresses is expensive and is not always effective in restoring the pavement condition. Also, traffic delays become a serious issue in areas of repairs since CRC pavements are usually used in areas with high traffic.

Hence, prevention of premature distresses in CRCP is the best course of action. The most effective way to prevent or minimize premature distresses is to identify the mechanisms of

distresses, develop appropriate special provisions to existing specifications or special specifications, and modify existing design standards.

This research focused on the correct identification of the premature and non-structural distresses in CRCP, identifying the concerned mechanisms and suggesting possible solutions. Thus, the two primary technical objectives in this research project are as follows:

- (1) Identify mechanisms of premature distresses in CRCP.
- (2) Improve/develop design details and/or specifications to minimize the incidence of premature distresses in CRCP.

The research conducted under this study is presented in five chapters. The organization of each chapter is as described below:

Chapter 2 discusses the various field investigations conducted to identify various premature and non-structural CRCP distresses and the classification thereof.

Chapter 3 explains the field and laboratory testing conducted to identify the mechanisms of premature distresses near the transverse construction joint. This chapter describes detailed data analyses to ascertain the behavior of steel and concrete leading to premature distresses in new CRCP.

Chapter 4 explains in detail the field testing conducted in existing CRCP to determine concrete material related issues causing premature distresses.

Chapter 5 enlists the conclusions derived from the data analysis and also recommends premature distress mitigation techniques.

Chapter 2 Premature Distresses in CRCP

CRCP field performance evaluations were conducted under TxDOT Research Project 0-6274: Project Level Performance Database for Rigid Pavements in Texas, II. Figure 2.1 illustrates the classification of CRCP distresses observed in Amarillo, Childress, Dallas, Fort Worth, Lubbock, Wichita Falls and Houston districts in Texas. About half of the CRCP distresses recorded are actually large surface defects. These defects are primarily due to the use of a specific aggregate type or poor finishing practice and hence do not fall into the category of structural defects. Also, Figure 2.1 shows that only about 14 percent of the total distresses are true punchouts. A higher percentage of distresses at 18 percent and 20 percent of the total distresses are either at the repair or transverse construction joints, respectively. Thus, most of the distresses – more than 85 percent – were non-structural and could be classified as premature distresses, which are related to the construction and materials quality issues.

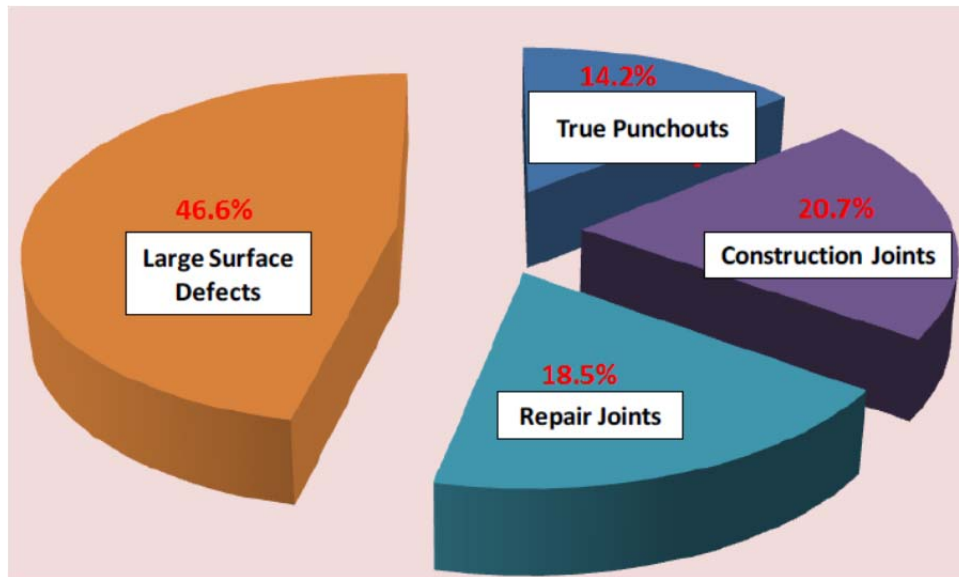


Figure 2. 1 CRCP Distress Classification in Texas (Won, 2012)

Table 2.1 presents the results of field evaluation of punchouts in Amarillo, Childress, Dallas, Fort Worth, Wichita Falls and Houston districts. Field surveys were conducted in each of these districts in order to investigate each of the punchouts recorded in the PMIS and classify them based on the potential causes. In Table 2.1, “PCH” indicates punchouts under wheel path or center of the lane. “E-PCH” denotes punchouts observed at pavement edge, some with pumping

evidence and some without. Similarly, “E-PCH-PTB” indicates edge punchouts with poor tie-bar, “PCH-CJ” indicates punchout at construction joints and “PCH-RJ” represents punchout at repair joints. Punchouts identified in the PMIS but that appear to be big size spalling that occurred due to poor concrete work are categorized as “BS-PCW”.

Table 2. 1 Detailed Classification of Punchouts

District	Punchout Classification						TOTAL
	PCH	E-PCH	E-PCH-PTB	PCH-CJ	PCH-RJ	BW-PCW	
AMARILLO	0	0	4	2	6	6	18
CHILDRESS	0	0	0	2	0	1	3
DALLAS	9	8	1	7	9	7	41
FT. WORTH	0	0	0	6	10	12	28
WICHITA FALLS	1	3	6	10	0	5	25
HOUSTON	1	0	0	21	18	77	117
SUB TOTAL	11	11	11	48	43	108	232
RATIO	4.7%	4.7%	4.7%	20.7%	18.5%	46.6%	

As shown in Table 2.1, amongst the punchouts evaluated, less than 15 percent comprise of punchouts that have been caused due to structural deficiency, namely PCH, E-PCH and E-PCH-PTB. The remaining 85 percent of the evaluated punchouts are the ones classified as being caused due to non-structural issues, such as construction, repair or material quality control. These distresses occur much earlier than the true punchouts caused by fatigue of concrete and hence are known as premature distresses. Identifying the causes of occurrence of premature distresses will help in undertaking mitigation strategies to prevent the occurrence of such distresses and help in further optimizing CRCP performance.

This chapter provides an overview of the distresses surveyed that are postulated to be due to causes other than structural deficiencies and classified as premature distresses. The probable causes for each distress type are also mentioned. In addition, surveys for identification of premature distresses in states outside Texas were sent out to officials of several state DOTs that use CRCP on a routine basis. Pavement engineers were requested to provide pictorial evidence and probable causes leading to the occurrence of premature distresses observed in their states. The feedback obtained from the state pavement officials is also discussed in this chapter.

2.1 Distresses at Transverse Construction Joints

As shown in Table 2.1, about 40 percent of the total punchouts surveyed were at the transverse construction joint (TCJ) or repair joint. Figures 2.2 and 2.3 illustrate the distresses observed at TCJs. These types of distresses were not only observed at TCJs in new construction projects, but also where new CRCP was connected to old CRCP as shown in Figure 2.4 or at repair TCJs as shown in Figure 2.5.

As illustrated in Figure 2.6, the distresses at TCJ are usually observed at a distance of two feet from the TCJ. Currently, 50% additional longitudinal steel is placed at the TCJs in the form of 50-in. long tie-bars. In Texas, CRCP design standards dating back as early as 1961 provide details of the use of tie-bars at TCJs as shown in Figure 2.7.



Figure 2. 2 Distress at TCJ



Figure 2. 3 Distress at TCJ



Figure 2. 4 Distress at CRCP Interface



Figure 2. 5 Distress at Repair TCJ



Figure 2. 6 Distress at 2 ft. from TCJ

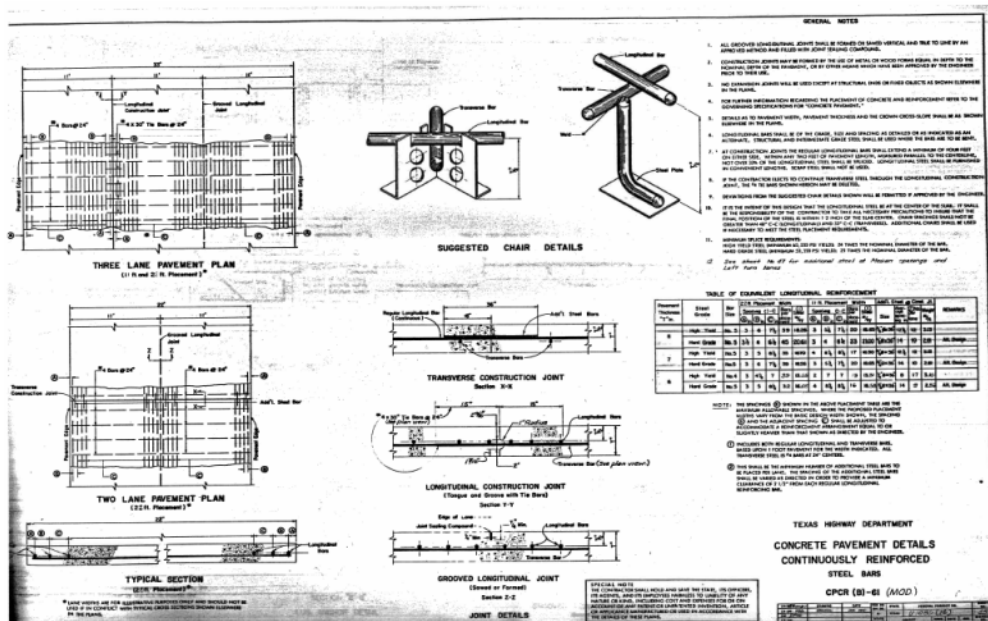


Figure 2. 7 CRCP Design Details - CPCRB (B) - 61 (MOD)

Although no documented evidence exists on the rationale behind the introduction of additional steel at the TCJs, the reasoning could have been that if the longitudinal steel amount is deficient, stresses at longitudinal steel at TCJs can be elevated above an allowable level. In early CRCP construction in Texas, longitudinal reinforcement was in the range of 0.47% to 0.52% which is lower than the values in use currently. In 1969, a new design standard was published and 0.6% longitudinal steel was provided as an option of two longitudinal steel percentages (0.5% and 0.6%). It is possible that at a low longitudinal steel amount, steel stress could increase above an allowable level at TCJs. In such situations, the widths of TCJs could be larger, with water getting

into the joint and resulting in corrosion of steel. However, the presence of distresses in the area where the additional steel ends, i.e. two feet from the TCJ, implies that the presence of additional steel at the TCJ plays a role in the occurrence of distresses near the TCJ.

Figures 2.8 and 2.9 represent full depth repair sections in the south bound direction on US 59 in the Atlanta district. This section of US 59 was originally constructed in 2001 in Cass County. The pavement thickness is 12 in. with 4-in. asphalt concrete pavement as base and 8-in. lime treated subgrade were used. additional steel with on hundred percent was placed in the repairs carried out in this section. As shown in Figures 2.8 and 2.9, distresses were observed near the repair joints.



Figure 2. 8 Distresses at Repair Joint - US 59 in the Atlanta District



Figure 2. 9 Distresses at Repair Joint - US 59 in the Atlanta District

However, 100% additional steel was replaced by use of 50% additional steel in the repairs carried out in the north bound direction for the same highway section. No distresses were observed in the section with 50% additional steel. This observation indicates that too much steel at TCJ may affect the quality of concrete consolidation at the TCJ and could be a probable cause for occurrence of distresses at TCJ.

2.2 Distresses Due to Slab Movement at Transverse Construction Joints

In order to evaluate concrete slab displacements at TCJs, field experimentation was carried out in 2005 (Nam, 2005). The concrete slab displacement in the longitudinal direction was measured at TCJ. This section was constructed on August 26, 2005 on US 287 in the Wichita Falls District. Four LVDTs (Linear Variable Differential Transducer) were placed in the longitudinal direction as shown in Figure 2.10. LVDT #4 was placed against a reference bar.

Three other LVDTs were installed directly against concrete at mid-depth of the slab. Figure 2.11 shows the concrete displacements and the temperature. Large ambient temperature variations with large contraction of concrete as much as 0.2 in. for two days were observed. The results from this study show that large concrete slab contraction was primarily due to drying shrinkage of concrete, and the contribution of temperature variation was relatively small. The large movement in the evening-placed side of the TCJ may lead to development of large stresses, cracking and potential distresses in the morning-placed side of the TCJ. By the time the concrete is placed on the morning side of the TCJ, the evening side is already stiff and the displacements in this previously placed side may lead to damages in the freshly placed concrete.



Figure 2. 10 Slab Movement Experimentation (Nam, 2005)

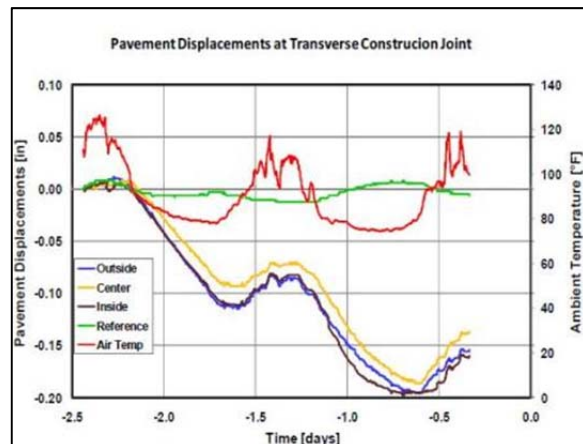


Figure 2. 11 Slab Movement on US 287 in Wichita Falls (Nam, 2005)

2.3 Distresses Due to Construction / Material Quality at Transverse Construction Joints

As shown in Figure 2.12 and Figure 2.13, surface distresses in the form of voids are observed at the TCJs. The cause of such distresses could be the quality of in-place concrete in these areas. The concrete used on either side of the TCJ is usually the first or the last batch of the concrete for

that particular day of construction. The quality of the concrete at the TCJ may vary slightly from the concrete quality in the rest of the slab. Also, concrete placement and consolidation at the TCJ is carried out manually since the slip-form paver cannot start or end the paving process right at the TCJ.



Figure 2. 12 Surface Voids at TCJ



Figure 2. 13 Surface Voids on US 287 in Wichita Falls

The manual operation employed during this process is illustrated in Figure 2.14 and Figure 2.15. Thus, the construction practice at the TCJ is different from the normal paving operation for the rest of the slab. In addition, a large amount of steel in the form of longitudinal steel and 50% additional steel is present near the TCJ. The presence of the dense amount of steel in this area may hinder the process of manual vibration near the TCJ and lead to improper consolidation. Also, during manual vibration the vibrator may hit the additional or longitudinal steel resulting in the migration of water into between the concrete and steel, which could lower bond strength and eventually cause distresses.



Figure 2. 14 Concrete Placement at TCJ



Figure 2. 15 Concrete Consolidation at TCJ

2.4 Y and Narrow Transverse Cracks

Transverse cracks develop in CRCP in order to relieve concrete stresses resulting from temperature and moisture variations and do not necessarily cause distresses. During the early usage of CRCP, large crack widths led to the occurrence of distresses at transverse cracks. Large crack widths were found to be due to splicing of longitudinal steel at the same transverse location and/or the use of insufficient longitudinal steel. Improvements such as staggered splicing and increasing the amount of longitudinal steel resulted in tight crack widths and substantially reduced the rate of distresses. However, certain transverse cracks that take a Y-shape or having quite narrow spacing were observed during visual surveys. These cracks could eventually lead to distresses and hence were included as premature distresses that need to be investigated.

Figure 2.16 shows cracks on a section on US 287 in the Wichita Falls District. The shape of cracking are not of typical transverse cracks in CRCP, as Y-cracks and cracks with quite narrow crack spacing are noted. The core shown in Figure 2.17 was taken at the Y-crack location represented in Figure 2.16. The core shows that the concrete between the two cracks forming the Y-crack is disintegrating. The ambient temperature in this location during construction was reported to be quite high.



Figure 2. 16 Y-Crack on US 287 in the Wichita Falls District



Figure 2. 17 Core Taken From Y-Crack on US 287 in the Wichita Falls District

Figure 2.18 represents a Y-crack on US 59 in the Atlanta district. Siliceous river gravel was used as a coarse aggregate in this section. A core taken at this section is represented in Figure 2.19.

The core shows delamination at a few inches from the surface of the slab. In this particular project, the contractor had trouble achieving required concrete strength due to the use of sand that was not clean. Distresses in the form of spalling may develop in this section in the future due to heavy truck traffic loads.

Figure 2.20 shows a Y-crack and Figure 2.21 illustrates the core taken at the Y-crack location. As shown in Figure 2.21, the core contains two horizontal cracks which may induce premature distresses in the form of partial-depth punchouts. The basic principle of CRCP design is based on the assumption of solid concrete that is bonded with longitudinal steel. Once this assumption is violated, the life of CRCP is reduced and premature distresses might develop.



Figure 2. 18 Y-Crack on US 59 in the Atlanta District



Figure 2. 19 Core Taken at Y-Crack on US 59 in the Atlanta district



Figure 2. 20 Coring at Y-Crack Location



Figure 2. 21 Horizontal Cracking at Y-Crack Location

2.5 Distresses Due to Slab Expansion

It has been traditionally assumed that concrete in CRCP is almost always in tension due to continued drying shrinkage of concrete and a temperature drop from the concrete setting temperature, except when concrete temperature is much higher than the setting temperature. Also, it is assumed that steel is in tension at transverse cracks. However, field surveys have revealed evidence suggesting that the slab actually expanded when a portion of the concrete slab was removed.

Figure 2.22 represents a section on IH 45 in the Houston District. This section shows the expansion of lane with respect to the other lane, when concrete was removed in one side for rehabilitation. The stapling bar installed at the longitudinal joint, initially straight, is bent due to the expansion of the slab. The expansion of the slab in this section was measured to be around 3.5 in., suggesting that the concrete in CRCP was under substantial compression.

Figure 2.23 illustrates the expansion of a slab cut for full-depth repair. This section is located on the frontage road of Loop 610 in the Houston District. The expansion of the slab was noted to be 0.5 in. This shows that the tie bar inserted into the existing concrete for full-depth repair was bent by the expansion of the existing concrete, pushing the concrete in the repaired section to disintegrate.



Figure 2. 22 Bent Stapling-bar at Longitudinal Joint on IH 45 in the Houston District



Figure 2. 23 Bent Tie-Bar at Repair Section on Loop 610 in the Houston District

Also, in several projects the crack width at the depth of the steel has been noted to be quite tight, supporting the fact that concrete in CRCP could be in compression instead of tension. Research studies conducted under TxDOT's project on terminal systems have concluded that CRCP slab movements due to temperature variations are limited to the end portions of the pavement near bridges. Slab movements at the middle portion of the pavement between bridges were found to be negligible. Concrete volume change restrained due to subbase friction could be responsible for negligible slab displacements.

2.6 Debonding and Large Joint Width at Transverse Construction Joint

If there is a sufficient bond between concrete and longitudinal steel and an adequate amount of longitudinal steel is used, the width of the TCJs in CRCP would be quite tight. However, in case of slow concrete strength development in the early ages due to low temperatures and/or large replacement of cement with supplementary cementitious materials, debonding between concrete and longitudinal steel might occur near the TCJs.

Figures 2.24 through 2.27 represent TCJ on IH 10 in the El Paso District. This section was constructed in 1995. The slab thickness is 13 in. and 4-in. Type B asphalt concrete pavement was used as subbase. The TCJ width in this section is around 2-in. Considerable movement of the slabs near the TCJ has resulted in the occurrence of distresses in both the lanes.



Figure 2. 24 Distress at TCJ on IH 10 in the El Paso District



Figure 2. 25 Distress at TCJ on IH 10 in the El Paso District



Figure 2. 26 TCJ Width on IH 10 in the El Paso District



Figure 2. 27 TCJ on IH 10 in the El Paso District

Figures 2.28 through 2.31 illustrate a section on IH 40 in the Childress District. This section exhibits distresses near the TCJ. The width of the TCJ at this section was measured in the morning and evening on November 2, 2012. The TCJ width decreased from 1/2 in. in the morning to 3/8 in. in the evening. The maximum and minimum temperature at this location on November 2, 2012 was 82 °F and 53 °F respectively. A zoomed-in view of the TCJ at this location provides evidence of steel slipping away from the concrete or occurrence of debonding between the steel and concrete. This provides evidence of debonding, and the resulting increase in TCJ width causing occurrence of distresses at the TCJ. CRCP segments in this area were removed and replaced due to expansion of subgrade soil containing gypsum due to lime stabilization. It appears that the restoration of the continuity of longitudinal reinforcement was not properly made.



Figure 2. 28 Distress at TCJ on IH 40 in the Childress District



Figure 2. 29 TCJ Width on IH 40 in the Childress District – Morning



Figure 2. 30 TCJ Width on IH 40 in the Childress District - Evening



Figure 2. 31 Debonding Between Steel and Concrete on IH 40 in the Childress District

2.7 Distresses at Gore Areas

Distresses are observed at gore areas where asphalt shoulder is used. Figure 2.32 shows distresses in the outside lane at the end of the concrete gore. When a CRCP section has two different shoulder types next to each other as shown in Figure 2.32, the edge of the CRCP slab at the transition between tied concrete and asphalt shoulders changes from Westergaard's so-called interior condition to an edge condition. The difference in slab deflections between the interior and edge conditions due to wheel load applications is considerable. Figure 2.33 shows deflection testing conducted on IH 35 in Denton County in the Dallas district.

Figure 2.33 shows the testing at the longitudinal joint with tied concrete shoulder, whereas Figure 2.34 shows the testing for asphalt shoulder. Figure 2.35 illustrates the measured deflection values. There is a large difference in deflections of CRCP slab with two different shoulder types. Figure 2.36 presents deflection values derived from Westergaard's equations for both interior and edge conditions for various modulus of subgrade reaction values. The modulus of subgrade reaction (k) varies from 100 psi/in. to 800 psi/in. The measured values are very close to those from Westergaard's equations at 300 psi/in. of k -value. The estimated k -value at this location is estimated at about 300 psi/in. Figure 2.36 shows a large difference in deflections between the

two loading conditions, regardless of k -values, even though the difference becomes smaller as k -value increases.



Figure 2. 32 Distress at Gore Area Due to Different Edge Support Conditions



Figure 2. 33 Deflection Testing at Pavement Edge With Tied Concrete Shoulder



Figure 2. 34 Deflection Testing at Pavement Edge With Asphalt Shoulder

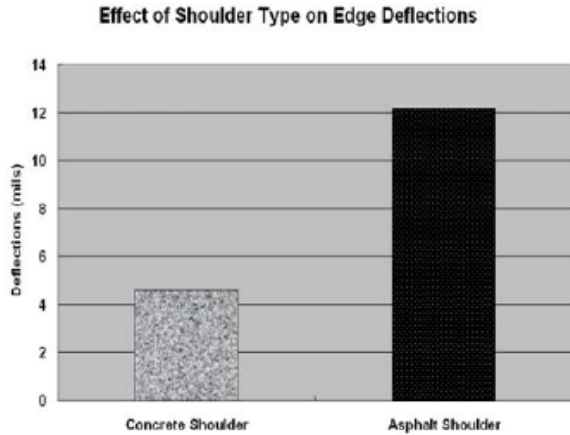


Figure 2. 35 Deflections at Pavement Edge For Two Different Shoulder Types

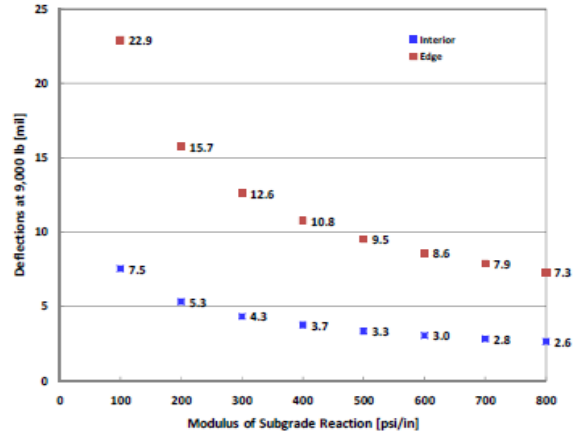


Figure 2. 36 The Effect of Edge Condition and Slab Support From Westergaard Equation

This large difference in deflection between the two loading conditions as wheel load is applied in this area will cause high local differential deflections (from 4.3 mils to 12.6 mils), which could lead to distresses. Since TxDOT started building CRCP with tied concrete shoulder, the frequency of this distress type will decrease significantly.

2.8 Distresses at Longitudinal Joints

Distresses at longitudinal construction joint (LCJs) or longitudinal warping joints (LWJs) are frequently observed. Figures 2.37 and 2.38 illustrate distresses observed at LCJ and LWJ, respectively. Until now, the distress shown in Figure 2.37 was classified as a punchout that resulted from short transverse crack spacing. Assuming that larger crack spacing would prevent this distress type, efforts were made in the past to minimize the occurrence of short crack spacing. However, there are many cracks with short spacing that do not develop into this type of distress. Field evaluations of this type of distress reveal that horizontal cracking is observed at the depth of the longitudinal steel. The distress shown in Figure 2.38 was investigated and horizontal cracking was observed at the depth of the longitudinal steel. Even though part of the distresses shown in Figures 2.37 and 2.38 are under the wheel path and when loading positively contributed to the progression of this distress, the longitudinal joint appears to play a role in the development of this distress type. Since this type of distress is rarely observed in CRCP with crushed limestone as a coarse aggregate in concrete, it is postulated that concrete volume change potential and possibly concrete modulus of elasticity plays a major role in development of this

distress. As TxDOT considers the use of jointed plain concrete pavement when the only aggregate type locally available has shown distresses in CRCP, which is quite often coarse aggregate type with a high CoTE, the frequency of this distress type might decrease in the future.



Figure 2. 37 Distresses Near LCJ



Figure 2. 38 Distresses Near LWJ

2.9 Premature Distress Types in Other States

State departments of transportation (DOTs) in Illinois, California, Virginia, Louisiana and Oklahoma were contacted to obtain information on their experiences with premature distress in CRCP.

2.9.1 Illinois DOT

Premature distress types identified in Illinois include:

- A.** Distress at CRCP main lanes tied with CPCD shoulder
- B.** Distresses caused by the use of cement stabilized drainable layer, and
- C.** Distresses caused by the use of #8 tie bars

A. Distresses at CRCP main lanes tied with CPCD shoulder: Figures 2.39 and 2.40 show distresses at CRCP outside lane tied with CPCD. This is on IH 70 at the Illinois and Indiana border.

David Lippert, P.E. of Illinois DOT states that the distresses occurred about five years after construction. Interestingly, this project had a 5-year warranty. Mr. Lippert also stated that no comprehensive investigation was conducted and the exact mechanism was not identified. He also mentioned that in Illinois, they use tied CPCD as a shoulder for CRCP, and this type of distress is not common. It appears that large slab movements near the transverse warping joints in CPCD shoulder could cause distresses in CRCP, when certain conditions are met, such as larger movements of CPCD due to insufficient base friction.



Figure 2. 39 Distress at CRCP/CPCD
(Photo courtesy of M. Plei)



Figure 2. 40 Distress at CRCP/CPCD
(Photo courtesy of M. Plei)

A similar type of distress occurred in Texas. Figure 2.41 shows a distress in CRCP tied to cast-in-place pre-stressed concrete pavement (CIP-PCP) on IH 35 in Hillsboro. Distress occurred in CRCP tied to CIP-PCP. In CIP-PCP, two layers of polyethylene sheets were placed under the concrete slab to reduce sub-base friction and pre-stress loss. Due to the reduced sub-base friction, CIP-PCP slab will move almost freely, resulting in large slab movement near the armor joint area. On the other hand, CRCP slab movements are quite limited due to the sub-base friction and the continuity of the longitudinal steel. Due to the differential slab movements of the two slabs that are tied together at the longitudinal joint by tie bars, distresses occurred.

In Texas, it is not common to use CPCD as a tied concrete shoulder for CRCP. Figure 2.42 shows construction of a CPCD turning lane tied to CRCP on US 59 in the Atlanta District.



Figure 2. 41 Distress in CRCP Next to CIP-PCP on IH 35 in Hillsboro



Figure 2. 42 Construction of CRCP Tied to CRCP on US 59 in the Atlanta District

Since the use of CPCD shoulder tied to CRCP is rather rare in Texas, this distress type shouldn't be a concern and was not investigated in this research study.

B. Distresses caused by the use of cement stabilized drainable layer: Figure 2.43 shows the cross-section of the cement stabilized open grade drainage course. This picture was taken in 2001, when the Illinois DOT first started using this layer under the concrete slab. Typical thickness of this layer in the actual pavement was 4-in. The nominal maximum coarse aggregate size was between $\frac{3}{4}$ -in. to 1 in. The use of this drainage layer resulted in distresses in CRCP in the form of “Depression” of CRCP slabs, and shear failures of tie bars at longitudinal joints. The subgrade materials underneath the drainable layer were liquefied under heavy wheel load and penetrated to the drainable layer resulting in localized depression of CRCP slabs. The localized depression also resulted in high shear stresses in and failures of tie bars at longitudinal joints. Illinois DOT banned the use of the drainable layer in CRCP. Since only a stabilized layer with no drainage considerations is used for CRCP in Texas, the distress caused by the use of drainable layer was not investigated in this research study.

C. Distresses caused by the use of #8 tie bars: Mr. Lippert stated that #8 bars were used as tied bars at longitudinal construction joints in the Chicago area, which resulted in distresses. Currently, the standard practice is to use #6 bars. In Illinois DOT, longitudinal steel is placed above the mid-depth of the slab (3.0 in from the top of steel to the top of the concrete surface when the slab is 8-in or less, or 3.5-in when the slab is larger than 8-in thick). The use of #8 bars

might not have had enough concrete cover for the #8 bar size. Placing longitudinal steel near the surface could have other consequences, as shown in Figure 2.44. Concrete spalled out at the location of the steel, exposing longitudinal steel. Since only #6 bars are used for tie bars in Texas, this issue was not investigated in this study.



Figure 2. 43 Cross-Section of Cement Stabilized Drainable Base (Photo Courtesy of M. Mueller)



Figure 2. 44 Distress Associated With Steel Placed Too High

2.9.2 California DOT (Caltrans)

Mr. Bill Fahnbach stated that in California, the oldest new CRCP is one year old, and no premature distresses were observed, except for numerous working cracks. Mr. Fahnbach's definition of "working cracks" are those that go through from the top to the bottom of the slab. He observed those cracks on the side of the CRCP. Since drying shrinkage and temperature variations are larger at the concrete surface than in the interior, transverse cracks normally go through the slab depth at the surface of the pavement side. At the inside of the pavement, most of the transverse cracks, if not all, are quite tight and become almost invisible at the depth of the longitudinal steel. Since working cracks are not a concern in Texas, they were not investigated in this study.

2.9.3 Virginia DOT

Premature distress types in Virginia include:

- A. Distresses due to the variation in the longitudinal steel depth
- B. Y-cracks, and
- C. Distresses at transverse construction joint

A. Distresses due to the variations in the longitudinal steel depth: Virginia DOT used to allow tube feeding for longitudinal steel, which resulted in the steel placement depths too high or low. Figures 2.45 and 2.46 show the CRCP construction with tube feeding of steel and distresses associated with longitudinal bars placed too close to the surface, respectively. This distress is similar to the distress shown in Figure 2.44. In Texas, steel is placed on chairs, and the variability of steel depth is quite small. Accordingly, the effect of steel depth was not investigated in this study.



Figure 2. 45 CRCP Const. With Mechanical Steel Placement
(Photo courtesy of M. Elfino)



Figure 2. 46 Distress Associated With Reinforcing Steel Placed Too High
(Photo courtesy of M. Elfino)

B. Y-Cracks: Figure 2.47 shows Y-cracks in CRCP. M. Elfino with Virginia DOT has the opinion that Y-cracks are caused due to entrapped air. He states that when he took cores at Y-crack locations, entrapped air was observed, as shown in Figure 2.48.

C. Distresses at transverse construction joints: Figure 2.49 shows a distress at a transverse construction joint. Mr. Elfino stated that poor consolidation of concrete near the joints, as shown in Figure 2.50, was partly responsible for the distress.



Figure 2. 47 Y-crack (Photo courtesy of M. Elfino)



Figure 2. 48 Entrapped Air in Concrete From Y-Crack (Photo courtesy of M. Elfino)



Figure 2. 49 Distress At Transverse Construction Joint (Photo courtesy of M. Elfino)

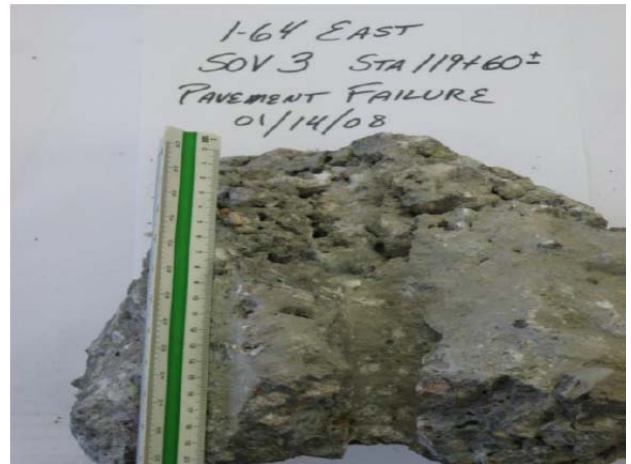


Figure 2. 50 Lack of Concrete Consolidation at Header Area (Photo courtesy of M. Elfino)

2.9.4 Louisiana DOT

Louisiana DOT built CRCP a few years ago, and distresses at transverse construction joints are the only distresses at this point.

2.9.5 Oklahoma DOT

The only recent CRCP section in Oklahoma is on IH 35, which was built within the past five years. No premature distresses have been observed, except for wide transverse cracks. Forensic

evaluations were conducted to identify the causes of wide cracks, and the findings were not available for this research study.

Efforts were made to identify premature distresses in other states that utilize CRCP. Some of the distresses are unique to specific states, and others are similar to those in Texas. Premature distresses that are caused by practices not common in Texas – those due to tying CPCD to CRCP, the use of drainable base, the use of #8 bars for tie bars, and the variations of steel depths – were not investigated in this study. Other premature distresses such as distresses at transverse construction joints were investigated in this study.

2.10 Summary

Based on the field evaluations of distresses recorded as punchouts in TxDOT PMIS, it appears that the majority of the distresses are premature distresses. Also observed is that premature distresses are construction/material related, not structural deficiency related. There are distresses caused by deficiencies in design details, such as distresses at gore areas. TxDOT, over the years, improved CRCP design and construction practices based on what worked and what did not. The frequency of distresses due to imperfections in design details will decrease. Based on the surveys in Texas and inputs from other states as discussed above, the major premature distresses can be classified as below:

- a. Distresses at Transverse Construction Joint
 - Due to Steel Design Issue
 - Due to Construction/ Material Issue
- b. Y-cracks and Narrow Transverse Cracks
- c. Distresses Due to Slab Expansion
- d. Debonding and Large Joint Width at Transverse Construction Joint
- e. Distresses at Longitudinal Joints

To further reduce premature distresses in CRCP, the distress mechanisms of premature distresses need to be identified and improvement in specification for construction and materials needs to be made.

Chapter 3 Identification of Premature Distress Mechanisms at Transverse Construction Joint in New CRCP

As described in Chapter 2, a number of premature distress types were identified during extensive field surveys. The probable causes for these premature distresses seem to be varied. In order to obtain a thorough understanding of the mechanistic behavior of CRCP leading to premature distresses, concrete strain gages, steel strain gages and gages for evaluating CRCP slab movements were installed during construction at various projects in Texas. Also, CRCP slab movements, Coefficient of Thermal Expansion (CoTE) and Dynamic Young's Modulus of Elasticity were evaluated for various existing CRCP sections.

Specific testing strategies for the study of each CRCP behavior type were employed. Since long-term evaluation of slab movement is needed in this study, concrete displacement gages that provide accuracy, high resolution, and long-term stability were used. Gages based on measuring the resonant frequency of vibrating wires and changes in resistance provide accurate and reliable long-term measurement (Window and Hollister, 1982; Larive et al., 1995). The detection of change in resistance in steel strain gages and transmission of change in frequency for vibrating wire technology can be transmitted over long cable lengths and provide stable measurements over long periods regardless of changes in resistance or length of leads. The type of gages and testing setup employed to study the various parameters of concrete are enlisted in Table 3.1.

Table 3. 1 Types of Gages and Testing Setup

Parameters To Be Studied	Type Of Gages/ Testing Setup	Model/ Make Of Apparatus
Concrete Strain at TCJ	Concrete Embedment Vibrating Wire Strain Gages [VWSG]	Model 4200/ Geokon Inc.
Steel Strain at TCJ	Steel Strain Gages [SSG]	Linear Pattern Stress Analyssi Strain Gages/ Micro-Measurements
CRCP Slab Movement	Displacement Transducers [Crackmeters]	Model 14420/ Geokon Inc.
Concrete Density	-	-
Dynamic Young's Modulus of Elasticity	As per ASTM C215-08	RT1 Resonant Frequency Test/ Olson Instruments
Coefficient of Thermal Expansion	As per TEX-428-A	Water Bath-1187P/VWR International DVRT Setup-HSG-DVRT-6/Microstrain Inc.

3.1 Site Selection for Field Testing

As discussed in Chapter 2, different premature distresses are postulated to be occurring for different reasons. Hence, various test sites were selected throughout Texas to conduct in-depth investigation of different premature types. As shown in Figure 3.1, at the locations marked in yellow i.e. Lubbock, Brownwood, Waco and Ft. Worth districts, on-going construction projects were selected for gage installation and monitoring of pavement behavior. The locations marked in blue in El Paso, Childress and Houston districts as shown in Figure 3.1 were already constructed pavement sections where gages were installed primarily to determine the CRCP behavior after many years of construction and service. In addition to this, collection of coring samples, field surveys, use of MIRA Tomographer for creating representation of internal concrete defects were employed at various other test sections which are discussed individually in detail.

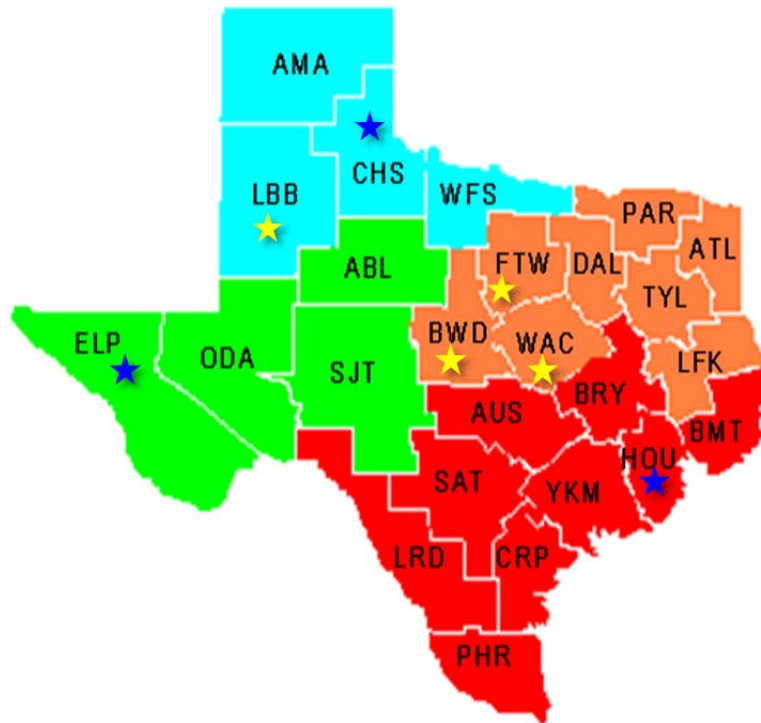


Figure 3. 1 Test Section Locations for Studying CRCP behavior

Table 3.2 lists the test sections for this research where gages were installed in new as well as existing CRCP projects. VWSGs, SSGs and crackmeters were installed at two transverse construction joints [TCJs] on US 82 East in the Lubbock district in December 2011. At the LBB-

I project, one side of the TCJ was placed on November 15, 2010 and the other side where gages were installed for this project was placed in the morning on December 15, 2011. The TCJ where paving stopped in the evening on December 15, 2011 was named as LBB-II test section. Paving resumed on the other end of the LBB-II TCJ in the morning on December 21, 2011. Gage installation was conducted at two TCJs during construction on IH 20 East in the Brownwood district during summer 2012. Gages were installed at BWD-I TCJ on the evening and morning construction sides on August 14, 2012 and August 16, 2012 respectively. BWD-II TCJ was placed three weeks later in a lane adjacent to the one where BWD-I was located. Paving in the evening side stopped on September 8, 2012 and resumed on the morning side on September 24, 2012 at BWD-II. The WAC TCJ was constructed on IH 35 in the Waco district on April 15, 2013.

Table 3. 2 Test Section Details

Section I.D.	Highway	District	Slab Thickness [in.]	Construction/ Gage Installation Date	Construction Time	Construction Season
LBB-I	US 82 E	LUBBOCK	13	11/15/2010	Existing	Winter
				12/15/2011	Morning	Winter
LBB-II	US 82 E	LUBBOCK	13	12/15/2011	Evening	Winter
				12/21/2011	Morning	
BWD-I	IH 20 W	BROWNWOOD	13	8/14/2012	Evening	Summer
				8/16/2012	Morning	
BWD-II	IH 20 W	BROWNWOOD	13	9/8/2012	Evening	Summer
				9/24/2012	Morning	
WAC	IH 35	WACO	13	4/15/2013	Morning	Spring
FTW-I	FM 1938	FT. WORTH	9	8/15/2010	-	Summer
FTW-II	FM 1938	FT. WORTH	9	3/17/2010	-	Winter
ELP-I	IH 10	EL PASO	13	7/12/2012	-	-
ELP-II	IH 10	EL PASO	13	7/12/2012	-	-
CHS	IH 40	CHILDRESS	15	11/2/2012	-	-

3.2 Test Sections on US 82 in Lubbock District

Figure 3.2 shows the location of the test sections constructed in the Lubbock district. Two TCJs, LBB-I and LBB-II, were selected in the same project for gage installation. The test section was constructed on US 82 east bound near the intersection of US 82 and IH 27.



Figure 3. 2 Location Map of Test Sections in Lubbock District

The overall layout of LBB-I and LBB-II test sections is given in Figure 3.3. As shown, the paving direction was east to west. Paving was carried out in the driving and passing lane, each 12 ft. wide at the same time and are referred to as Phase I construction. The 6 ft. inside shoulder and 10 ft. outside shoulder were paved at a later stage and are referred to as Phase II construction. LBB-I consisted of an existing pavement section constructed on November 15, 2010. On December 15, 2011, paving began in the morning on the other side of the TCJ at LBB-I. The area near LBB-I where paving began on December 15, 2011 is referred as LBB-I Morning Section and gage installation was carried out in this location. The location where paving stopped on December 15, 2011 in the evening is referred as LBB-II Evening Section. Paving resumed on the other side of LBB-II in the morning on December 21, 2011. Henceforth, either side of the

TCJs will be named after the “Name of the Section” and “Time of Concrete Placement (Morning/Evening)”.

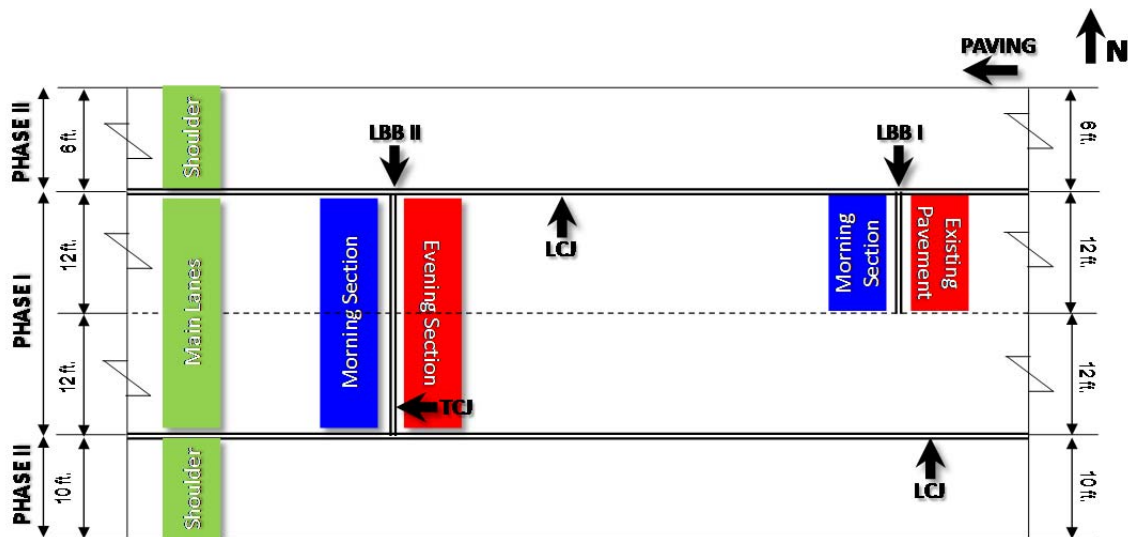


Figure 3. 3 Lubbock Test Section Layout

3.2.1 LBB-I Test Section – Testing Plan and Gage Setup

Figure 3.4 illustrates the condition of the existing pavement side of LBB-I test section. As shown in Figure 3.5, a header was placed at the end of construction on November 15, 2010. However, the longitudinal steel in this region was not extended to be spliced with longitudinal steel on the other side of the joint that would be constructed in the future. Also, 50% additional multi-piece tie-bars were installed during the construction of the transverse construction joint at the existing pavement. Female tie-bars were installed at the TCJ during construction and the header was placed at the end of construction.

On the morning side of LBB-I, the headers were removed and male-piece tie-bars were inserted onto female tie-bars as shown in Figure 3.6 before construction began on December 15, 2011. Consecutively, the longitudinal steel was spliced with the additional tie-bars instead of being continuous. Thus as shown in Figure 3.7, instead of following the standard configuration of continuous longitudinal steel, staggered splicing and 50% additional steel in the form of tie-bars, additional steel tie-bars at the design steel spacing were placed at the LBB-I TCJ.



Figure 3. 4 Existing Slab at LBB-I Test Section



Figure 3. 5 Header Installed After Placing Female Tie-bars at Existing Slab at LBB-I Test Section



Figure 3. 6 Male Tie-Bars Inserted After Removing the Headers at Morning construction side at LBB-I



Figure 3. 7 Steel Placement at LBB-I Test Section

LBB-I test section has specific significance to determine the effect of old and newly placed concrete on either side of the TCJ. Concrete and steel strain gage evaluation near LBB-I TCJ would help to ascertain the behavior of concrete and steel when the slab on the other side of the TCJ has already gained sufficient strength. Also, the individual movements of the new and existing slab would help to find the movement of the joint especially when the concrete on the morning side of the TCJ experiences drying shrinkage.

Figure 3.8 illustrates the plan and side view of the LBB-I test section. As shown, all longitudinal steel bars were connected to the male piece tie-bars on the morning side of the section. The male piece tie-bars are 25 in. in length. A total of nine SSGs were installed on the male tie-bars. Six of

those nine tie-bars were in turn spliced to longitudinal steel and the remaining three tie-bars acted as themselves. The SSGs were located at 1 ft, 6 ft. and 11 ft. from the inside longitudinal construction joint [LCJ]. Four VWSGs were also installed at this section. The VWSGs were installed at mid-depth of the slab. Three VWSGs were at a distance of 1 ft, 2 ft. and 4 ft. from the TCJ and 6 ft. from the LCJ. These three VWSGs were installed between the two longitudinal steel where an additional male tie-bar was also located. The fourth VWSG was installed in the succeeding spacing between two longitudinal steel without the presence of a male tie-bar.

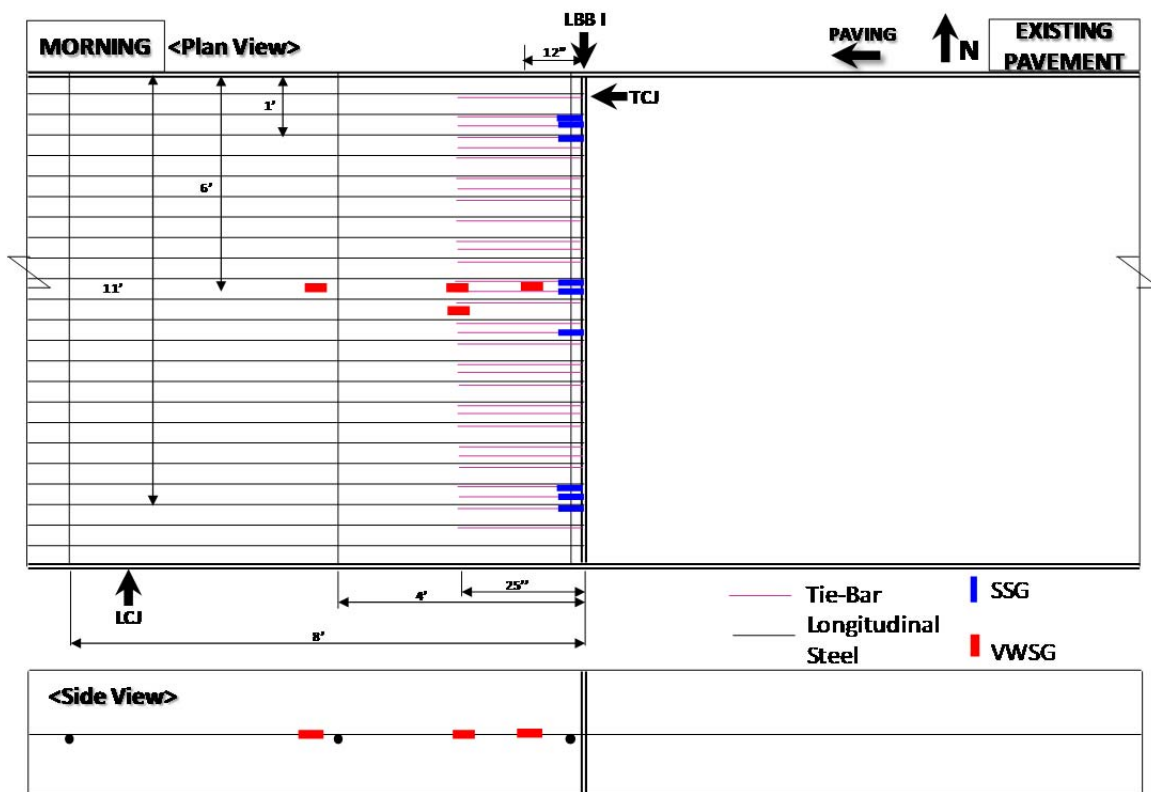


Figure 3. 8 Gage Layout at LBB-I Test Section

Figures 3.9 and 3.10 represent the gage installation of the SSGs and VWSGs at the LBB-I test section. As can be seen, the SSGs were installed on top of the male tie-bars right at the face of the existing slab at the TCJ. The VWSG installed at 2 ft. from the TCJ is right at the end of the tie-bar. The VWSG arrangement will help to determine the concrete strain near the face of the TCJ, at the end of the tie-bar and 4 ft. away from the TCJ. The VWSG installed at the location between two longitudinal steel where there is no tie-bar and 2 ft. away from the TCJ can be used to compare the difference in concrete strain at 2ft. from the tie-bar, with and without the use of

tie-bars between longitudinal steel. Paving was conducted in the morning on December 15, 2011 at 9 a.m. at the LBB-I section where gages were installed.



Figure 3. 9 Steel Strain Gage Installation at LBB-I Test Section

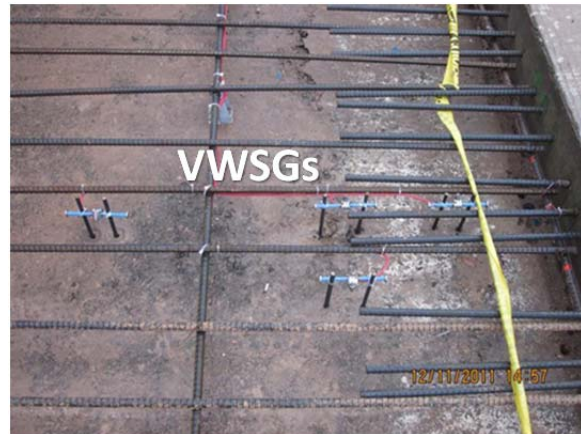


Figure 3. 10 Vibrating Wire Gage Installation at LBB-I Test Section

3.2.2 LBB-II Test Section – Testing Plan and Gage Setup

LBB-II transverse construction joint was constructed at the end of the paving on December 15, 2011. The “Evening Section” of LBB-II was where paving stopped on December 15, 2011 at 6:30 p.m. Paving began on the other side of the TCJ referred as the “Morning Section” on December 21, 2011 at 10 a.m.

In order to evaluate the effect of use of additional steel on the concrete and steel strain at the TCJ, different steel configurations were used at the LBB-II test section. As shown in Figure 3.11, in the inside lane of the test section, 50% additional steel was used at the TCJ in the form of alternately spaced tie-bars between longitudinal steel. However, in the outside lane, the additional tie-bars were removed and only longitudinal steel was present at the TCJ.



Figure 3. 11 Steel Placement at LBB-II Test Section

Figure 3.12 shows the layout of the LBB-II test location. The north lane (inside lane) has 50% additional steel in the form of 50 in. long tie-bars at the TCJ. The south side of the section (outside lane) has only longitudinal steel. Eleven SSGs were installed in the morning side of LBB-II on top of additional tie-bars and longitudinal steel. The SSGs installed on tie-bars were at a distance of 2 ft., 6 ft. and 10 ft. from the LCJ (inside free edge). SSGs on top of longitudinal steel were installed at a distance of 2 ft. 5ft., 6ft. and 10 ft. from the LCJ in the additional steel lane and at 14 ft., 18 ft. and 22 ft. from the LCJ in the non-additional steel lane. NAT refers to the location in the non-additional steel lane where VWSGs were installed longitudinally in the evening and morning sections. The NAT location is at a distance of 18 ft. from the LCJ. AT-1 and AT-2 locations are in the additional steel lane at a distance of 6 ft. and 5 ft. from the LCJ respectively. The AT-1 location has a tie-bar between two longitudinal steel, whereas there is no tie-bar between the two longitudinal steel at AT-2. At each of the locations NAT, AT-1 and AT-2, VWSGs were installed at 3ft. from the TCJ on the evening side and at 1ft., 2ft. and 4 ft. from the TCJ on the morning side.

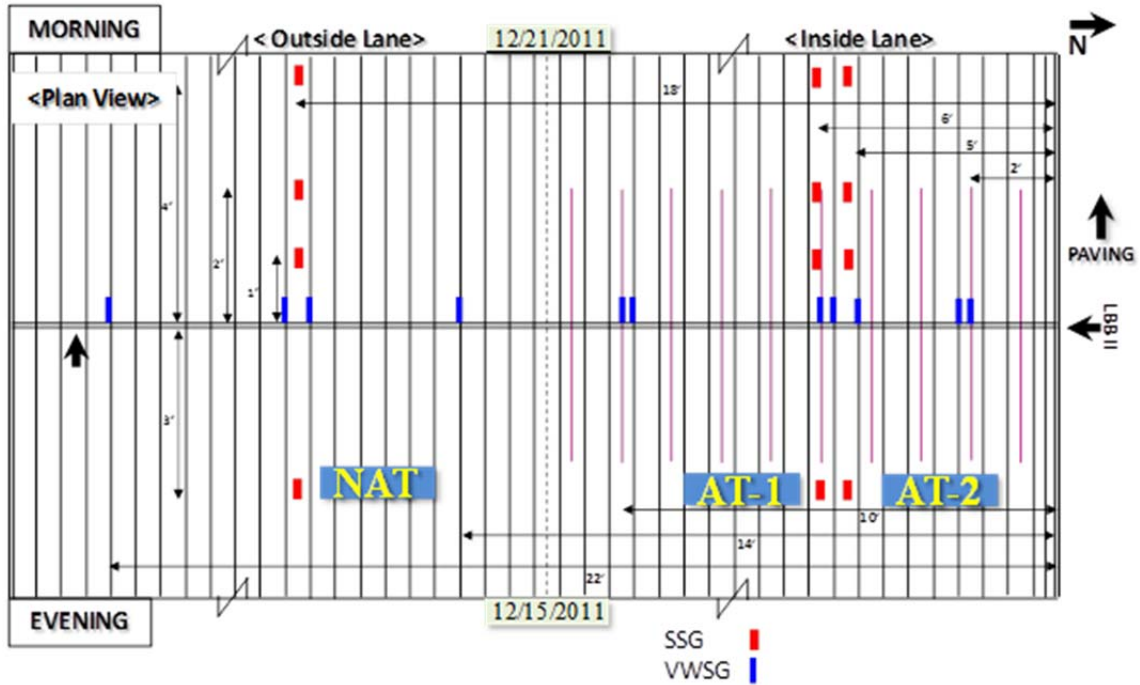


Figure 3.12 Gage Installation Plan at LBB-II Test Location

As shown in Figure 3.13, in the evening section at LBB-II VWSGs were installed at mid-depth of the slab at NAT, AT1 and AT2 locations. Figure 3.14 shows VWSG installation at 1 ft., 2ft. and 4ft. from the TCJ in the NAT section on the morning side of LBB-II and all three VWSGs were installed at mid-depth. Figure 3.15 shows the VWSG installation at the AT1 and AT2 locations. At AT1, VWSGs were installed at mid-depth and 1 in. from the top of the slab at 1 ft. and 4 ft. from the TCJ. At 2 ft. from the TCJ, VWSGs were installed at 1 in. from the base, at mid-depth and at 1 in. from the top of the slab. At AT-2 location, VWSGs at 1 ft., 2 ft. and 4 ft. from the TCJ were installed at mid-depth of the slab and 1 in. from the top. Figure 3.16 depicts the process of construction and finishing at the BWD-II Morning section on December 21, 2011.



Figure 3.13 VWSG Installation at LBB-II Evening Test Section

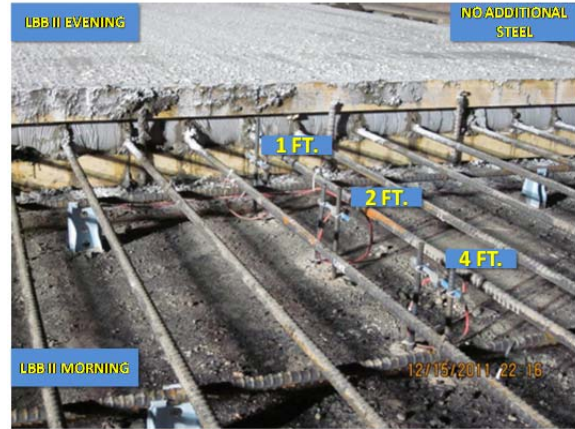


Figure 3.14 VWSG at LBB-II Morning Section With No Additional Steel at Transverse Construction Joint

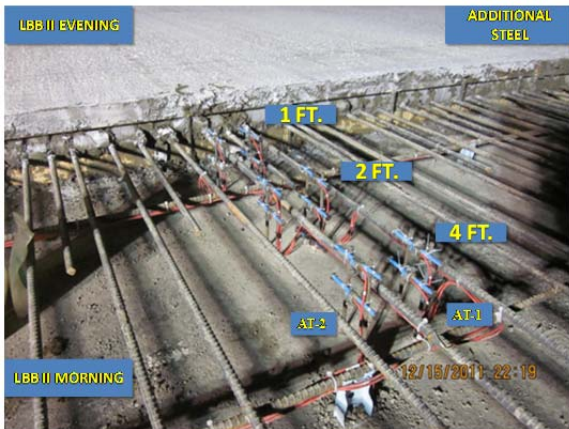


Figure 3.15 VWSG at LBB-II Morning Section With Additional Steel at Transverse Construction Joint



Figure 3.16 Concrete Finishing at LBB-II Morning Test Section

3.2.3 Steel Strain Behavior near TCJ in Lubbock District

Figure 3.17 and Figure 3.18 represent the steel strain behavior at LBB I TCJ in the early ages after construction and three months after construction, respectively. At the early ages, the concrete temperature drop from December 20, 2011 to December 24, 2011 was 22 °F overall, decreasing from 62 °F to 40 °F. This drop in concrete temperature is rather large. However, the variations in steel strains were minimal, which indicates that the steel strains at TCJ were relieved while the concrete temperature was decreasing, due to creep of concrete and the development of transverse cracks. On the other hand, daily variations in steel strains follow temperature variations quite well – in the morning when the concrete temperature is getting lower, steel strains move to the tension side, while in the afternoon when the concrete

temperature increases, steel strains move in the compression direction. This implies that daily concrete volume changes due to temperature variations affected steel stresses at TCJ, while the overall trend of concrete temperature variations during the several days did not have appreciable effects on steel stresses. Except for the steel strains on one of the tie-bars connected to the longitudinal steel at 12 ft. from the free edge of the pavement, those in the remaining gages were less than 3,000 micro strains. As shown in Figure 3.18, as the concrete temperature increased from 50 °F to 70 °F from March 21, 2012 to March 25, 2012, which is a rather large temperature increase, steel strain variations were relatively small. Also, it is noted that, compared with steel strains at the early ages shown in Figure 3.17, those at about three months after concrete placement decreased substantially, with steel strains in all the gages except one were in compression. Also, comparisons of steel strains at the same concrete temperature, for example at 60 °F (December 21, 2011) at the early ages and three months later (March 21, 2012), indicate significant decrease in steel strains for those three months. This finding has a technical significance, because in CRCP research, it is assumed that steel stresses at transverse cracks or at concrete discontinuities such as transverse construction joints, are maintained quite high, and crack widths could be large enough to decrease load transfer efficiency if steel stresses are excessive. The above assumption was made with the premise that concrete is elastic. It is well known that concrete exhibits visco-elastic behavior when subjected to slow loading such as gradual temperature variations. The information in Figures 3.17 and 3.18 indicates that the visco-elastic nature of concrete has effects on concrete slab behavior in CRCP and should be considered in a mechanistic analysis of CRCP behavior due to temperature and moisture variations.

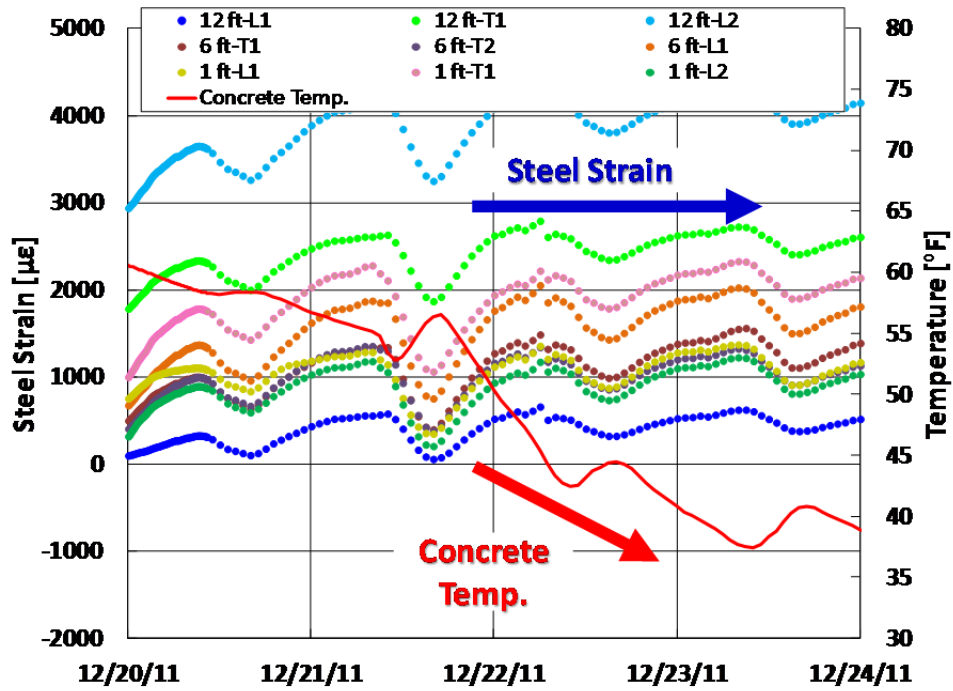


Figure 3. 17 Early Age Steel Strain Behavior at LBB-I Test Section

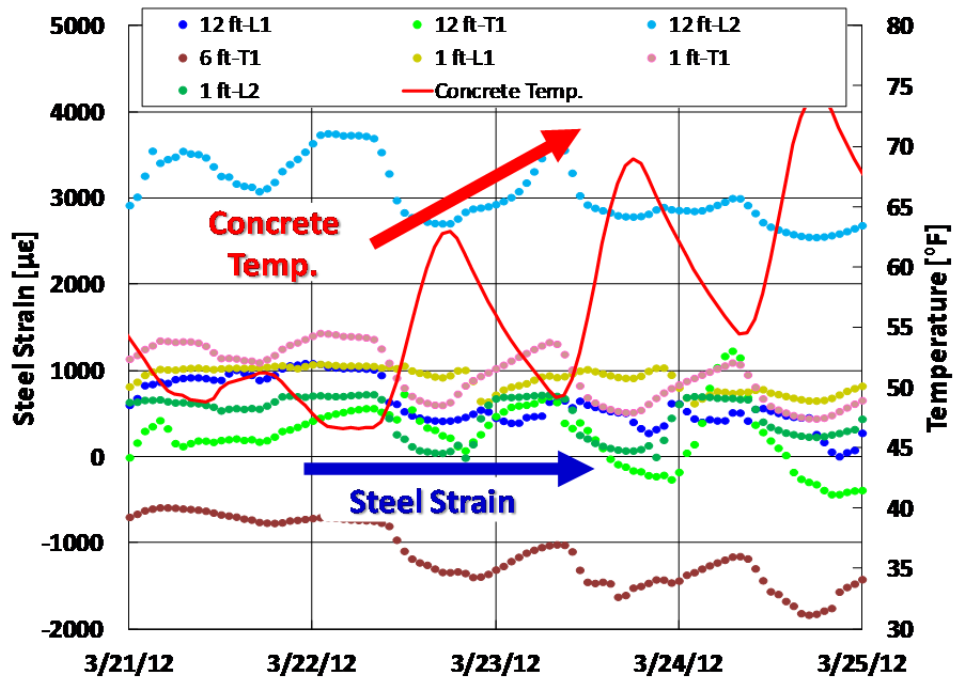


Figure 3. 18 Later Age Steel Strain Behavior at LBB-I Test Section

Figures 3.19 and 3.20 present the steel strain gage behavior at the LBB-II test section. The steel strain gages at LBB-II were installed at the morning side of construction at the TCJ on December 21, 2011. Figure 3.19 shows the steel strain variation with concrete temperature at LBB-II from December 26, 2011 to December 30, 2011. The prefix “NAT” and “AT” represent the steel strain gage locations in lanes without additional steel and with additional steel respectively. Also, whether the steel strain data is from the longitudinal steel or tie-bar is denoted by the use of “L” and “T” respectively in the legend. As the daily concrete temperature dropped, the steel strain in both the tie-bars and longitudinal steel went towards tension as the slab contracted. With increase in daily concrete temperature and expansion of the slab, the steel strain right at the transverse construction joint experienced compression.

From December 26, 2011 to December 29, 2011, the maximum concrete temperature remained steady at 52 °F. The steel strain daily variation during this duration was in accordance with the daily concrete temperature variation. Also, since no change in maximum concrete temperature was recorded, limited total steel strain drop was observed. The total steel strain behavior for longitudinal steel in the non-additional steel lane appears similar. The total steel strain observed in the longitudinal steel in the non-additional steel lane is higher than the total steel strain in the tie-bar and longitudinal steel in the lane with additional tie-bars. The maximum steel strains in the longitudinal steel on the non-additional steel side ranged between 1500-2000 micro strains and in the additional steel lane between 1200-1500 micro strains.

On December 27, 2011, as the concrete temperature dropped and the steel strains were increasing, a sudden drop in the total steel strain in all four locations can be observed. This sudden drop in the steel strain could be due to the formation of microscopic cracks in the concrete that would release the tensile stress in the longitudinal and additional tie-bars near the transverse construction joint.

The steel strain behavior at this location after five weeks since construction is illustrated in Figure 3.19. The total strain variation with daily concrete temperature variation from January 29, 2012 to February 2, 2012 is shown in Figure 3.20. The maximum concrete temperature during this duration increased from 52 °F to 56 °F. During this period, the steel strain gage located at 22

ft. on top of longitudinal steel in the non-additional lane showed minimal variation with temperature overall. The maximum steel strain on top of the longitudinal steel at 18 ft. in the non-additional steel lane showed movement towards the compressive side as the total steel strain dropped from 900 micro strains to 330 micro strains with increase in concrete temperature by 4°F. The maximum strain in longitudinal steel at 6 ft. in the additional steel lane also dropped from 1270 to 1200 micro strains. The highest compression was experienced by tie-bar at 10 ft. in the additional steel lane, where the total steel strain dropped from 500 micro strains in tension to 260 micro strains in compression.

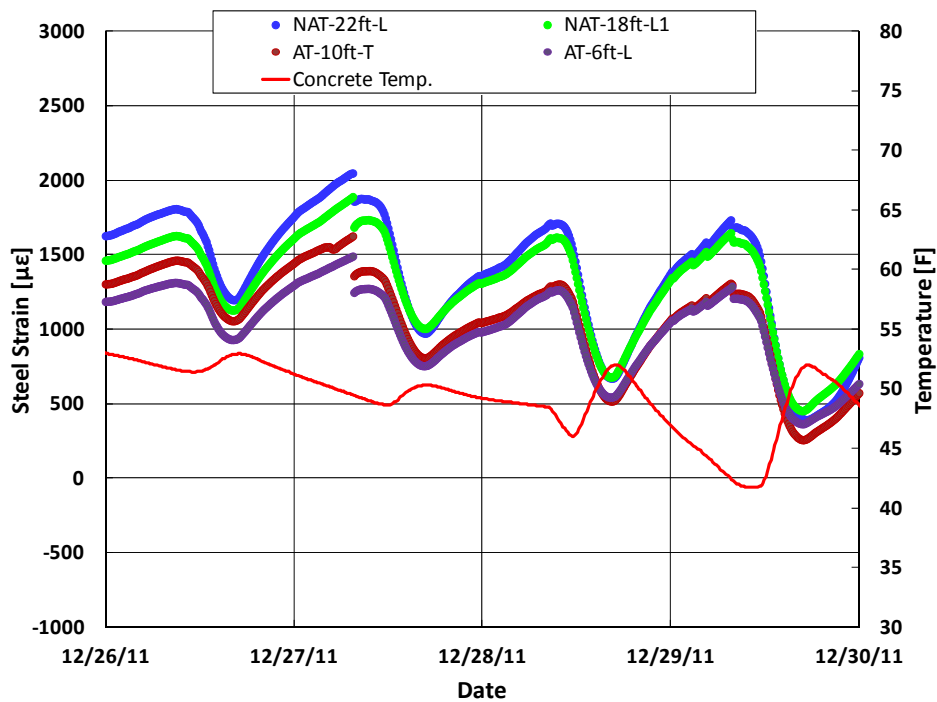


Figure 3. 19 Early Age Steel Strain Behavior at LBB-II Test Section

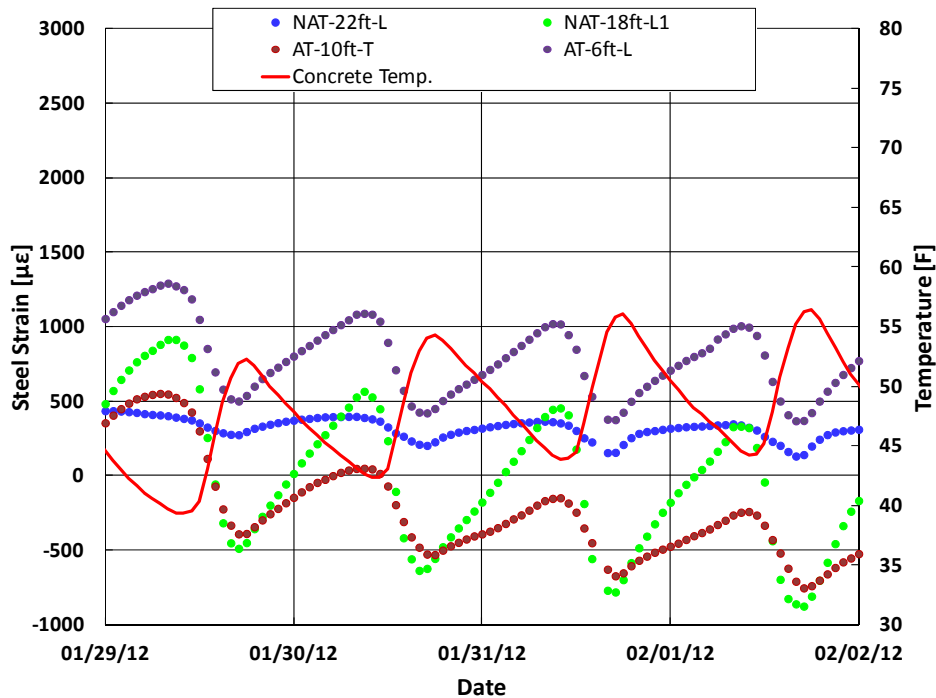


Figure 3. 20 Steel Strain Behavior at LBB-II Test Section After 5 Weeks Since Construction

3.2.4 Concrete Strain Behavior near TCJ in Lubbock District

VWSGs were installed at LBB-I test section as described in Section 3.2.1 to determine the behavior of concrete near the TCJ. The concrete strain variations at four locations over a period of more than one year are shown in Figures 3.21 through 3.24. VWSGs were installed at 1 ft., 2 ft., and 4ft. from the TCJ longitudinally between two longitudinal steel bars where additional tie-bar was located and are represented as “6 ft-T-M-1ft”, “6 ft-T-M-2ft” and “6 ft-T-M-4ft” respectively. One VWSG was also installed at 2 ft. from the TCJ between longitudinal steel bars where there was no additional tie-bar and is represented as “6 ft-NT-M-2 ft”.

Figure 3.21 represents the concrete strain variation at the above mentioned four locations from January 20, 2012 to January 24, 2012. The daily concrete temperature during this period varied between 45 °F and 55 °F. Concrete at all four locations experienced daily strain variation with change in daily temperature. As the concrete temperature decreased, the concrete strain decreased and with increase in concrete temperature and consecutive expansion of concrete in

the slab, the concrete strain increased. Also, the concrete strain in all four locations appeared to be in overall constant compression with maximum compressive strain of 100 micro strains.

As the maximum concrete temperature started to increase from 51 °F to 63 °F from February 20, 2012 to February 24, 2012, the total concrete strain at all four locations started to move towards the tensile side. Even as the temperature increased from 51 °F to 63 °F during this period, the daily concrete strain variation at all four locations was consistent with the daily change in concrete temperature.

Almost six months after construction, during summer June 2012, the behavior of concrete at all four locations was different as shown in Figure 3.23. During the period from June 20, 2012 to June 24, 2012, the concrete temperature varied between 85 °F to 105 °F. During this period, the concrete temperature underwent a daily variation of around 20 °F. However, contrary to the previous behavior of concrete at all four locations where concrete strain varied with change in concrete temperature, the concrete strain at all four locations remained steady individually.

Figure 3.24 displays the concrete strain variation at the four locations near the TCJ at LBB-I. The period depicted in Figure 3.24 is during spring 2013 between April, 11 2013 and April 15, 2013. The maximum concrete temperature during this period varied between 75 °F and 85 °F. During this period, the daily concrete strain variation in accordance with daily variation of concrete temperature seems to have resumed. Also, concrete strain at each location has gone into considerable compression overall. The highest compression in concrete is observed at a distance of 2 ft. from the TCJ where the additional tie-bar is located between the longitudinal steel. As the concrete temperature increased beyond 85 °F during summer 2012, the daily concrete strain variation ceased to exist. As the temperature increased, the concrete expanded. However, at the transverse construction joint when slabs from both sides expand, a terminal stage may be attained when there is no further space at the transverse construction joint for the slabs to expand. This may be manifested in a negligible change in concrete strain with daily temperature variation as shown in Figure 3.23. Once the concrete temperature drops in winter and the concrete shrinks, the daily variation is again resumed and can be seen as displayed in data for spring 2013 in Figure 3.24.

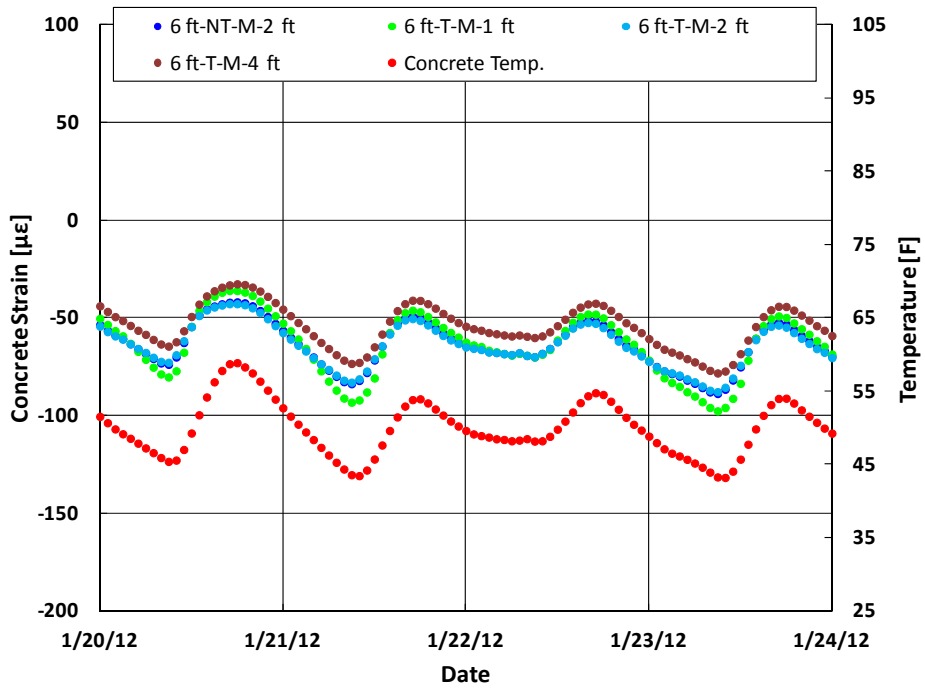


Figure 3. 21 Concrete Strain Variation at LBB-I in January 2012

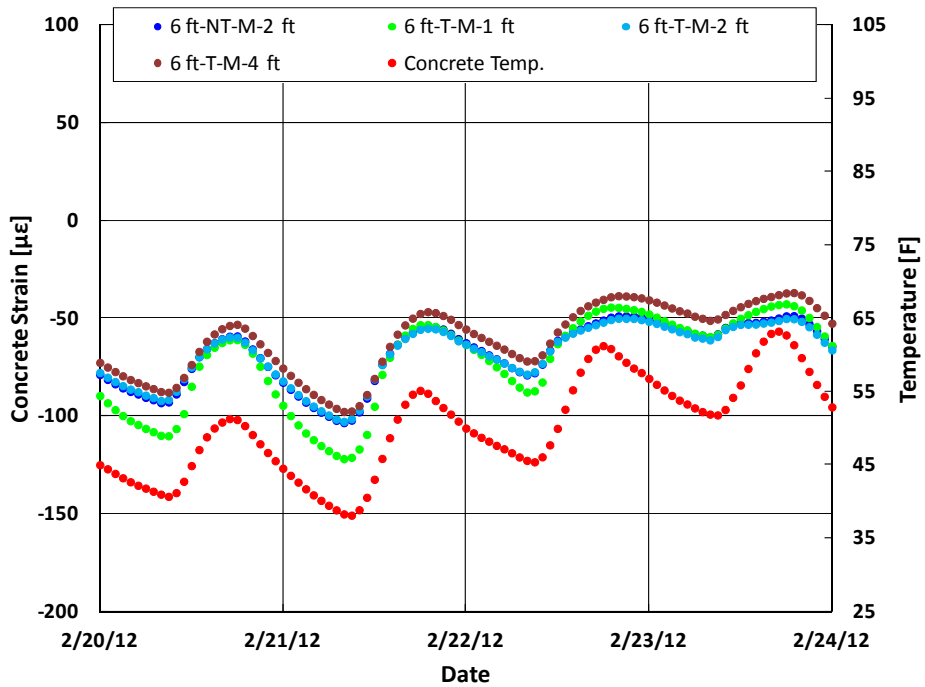


Figure 3. 22 Concrete Strain Variation at LBB-I in February 2012

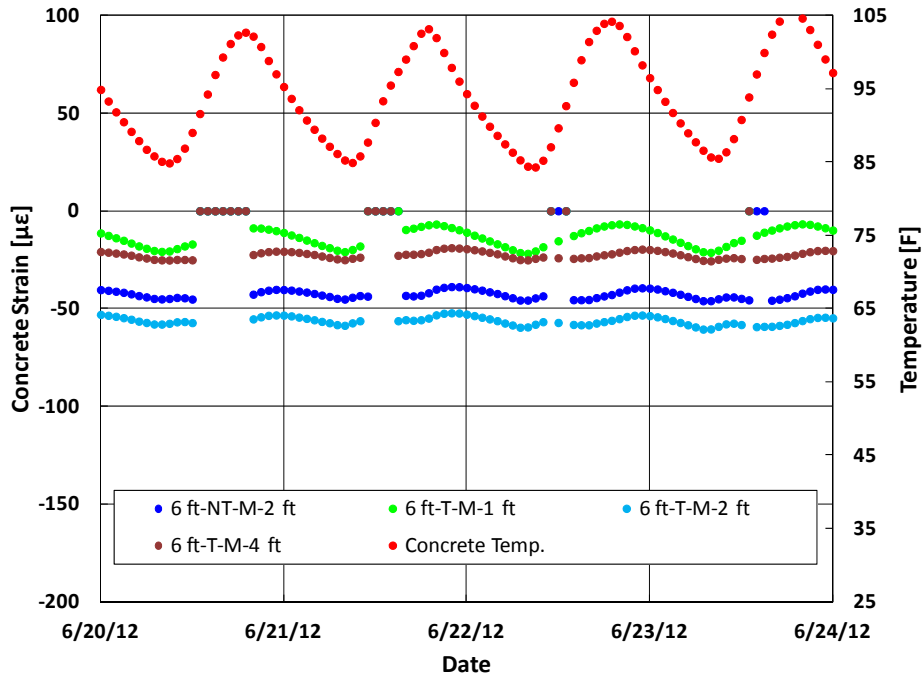


Figure 3. 23 Concrete Strain Variation at LBB-I in June 2012

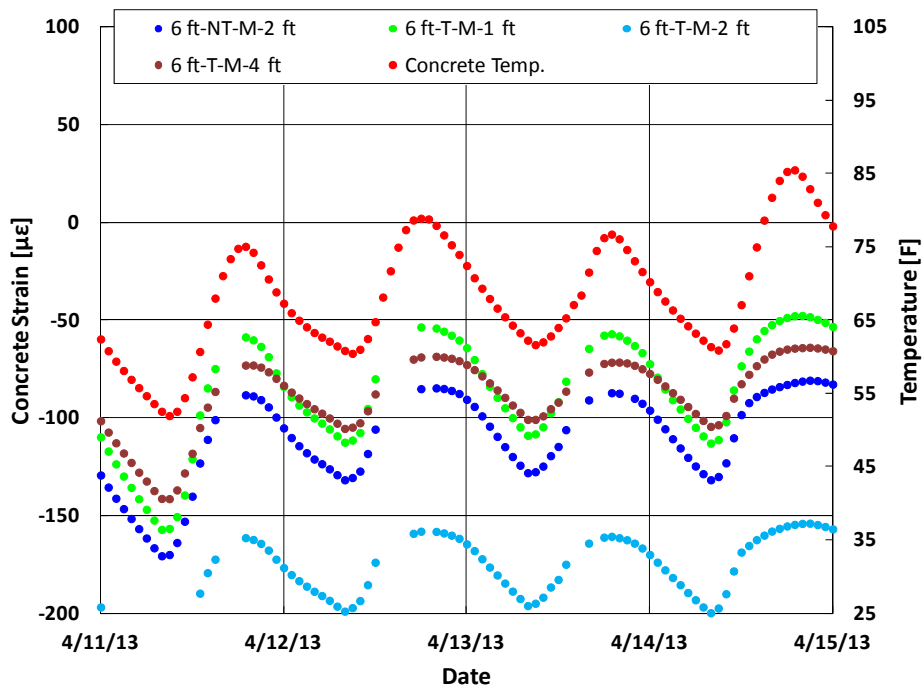


Figure 3. 24 Concrete Strain Variation at LBB-I in April 2013

As discussed in Section 3.2.2, VWSGs were installed on the morning side of construction at the LBB-II test section. The different configurations of steel at the transverse construction joint were

aimed to enable comparison between the concrete behavior in lanes with and without additional steel. VWSGs placed at 1 ft., 2ft. and 4 ft. from the transverse construction joint were intended to evaluate the concrete strains near and away from the transverse construction for both the configurations of steel at the transverse construction joint.

Figures 3.25 through 3.27 illustrate the rate of concrete strain change with temperature at a distance of 1 ft., 2 ft. and 4 ft. from the transverse construction joint at LBB-II morning section. In these figures, “NAT” denotes the VWSG location in the no-additional steel lane and “AT” denotes the VWSG location in the lane with 50% additional steel in the form of tie-bars at the transverse construction joint. As mentioned earlier, AT1 is located in the additional steel lane between two longitudinal steel and in line with the additional tie-bar between them. The AT2 location is where there is no tie-bar between the two longitudinal steel. The legend follows the format of “NAT/AT + Distance from the transverse construction joint”.

Figure 3.25 represents the rate of concrete strain change with temperature at 1 ft. from the transverse construction joint for 465 days since construction. The rate of concrete strain change at 1 ft. in the additional steel lane at AT1 and AT2 is 3.0 micro strains per °F and 3.8 micro strains per °F in the non-additional lane. As the temperature increased during summer, the rate of strain change at all the three locations decreased considerably. In the summer, after 200 days from the date of construction, the rate of concrete strain change at AT1 and AT2 is 0.6 micro strains per °F. At the same time, the rate at NAT is 1 micro strain per °F. With increase in temperature as the summer approached the following year, the difference between the rate of concrete strain change with temperature at the non-additional and additional steel locations at 1 ft from the transverse construction joint is much more evident. After 306 days since construction, the rate at AT1 and AT2 is 2.1 and 1.7 micro strains per °F, whereas at the NAT location the rate is 3.5 micro strains per °F. Thus after 306 days since construction, the rate of concrete strain change with temperature at AT1 and AT2 is considerably lower than when the section was constructed. The rate at NAT is similar to the rate right after construction of the section.

Figure 3.26 presents the rate of concrete strain change with temperature at 2 ft. from the transverse construction joint at AT1, AT2 and NAT locations. In the initial phase after concrete

placement, the rate at NAT and AT2 is similar at 3.7 and 3.5 micro strains per °F respectively. Also, similar to the rate at 1 ft. from the TCJ, during summer the rate of concrete strain change at all three locations decreases considerably and increases again in the following winter. At 306 days after placement, the rate at NAT, AT1 and AT2 is 2.5, 2.2 and 3.0 micro strains per °F.

The rate of concrete strain change at 4 ft. from the TCJ and AT1, AT2 and NAT locations is represented in Figure 3.27. Initially, the rate of concrete strain at NAT is higher than AT1 and AT2, but once the temperature goes down the rate of concrete strain change at all the three locations is similar. At 306 days since construction, the rate at NAT and AT2 is similar at 3.2 micro strains per °F and at AT1 it is 2.5 micro strains per °F.

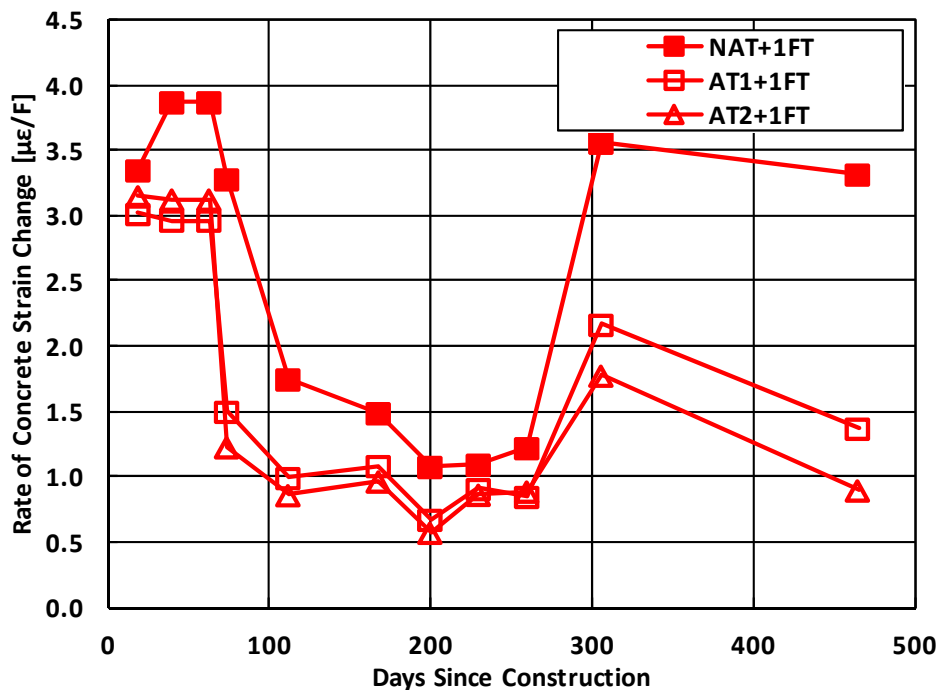


Figure 3. 25 Rate of Concrete Strain Change at 1 ft. From LBB-II Transverse Construction Joint

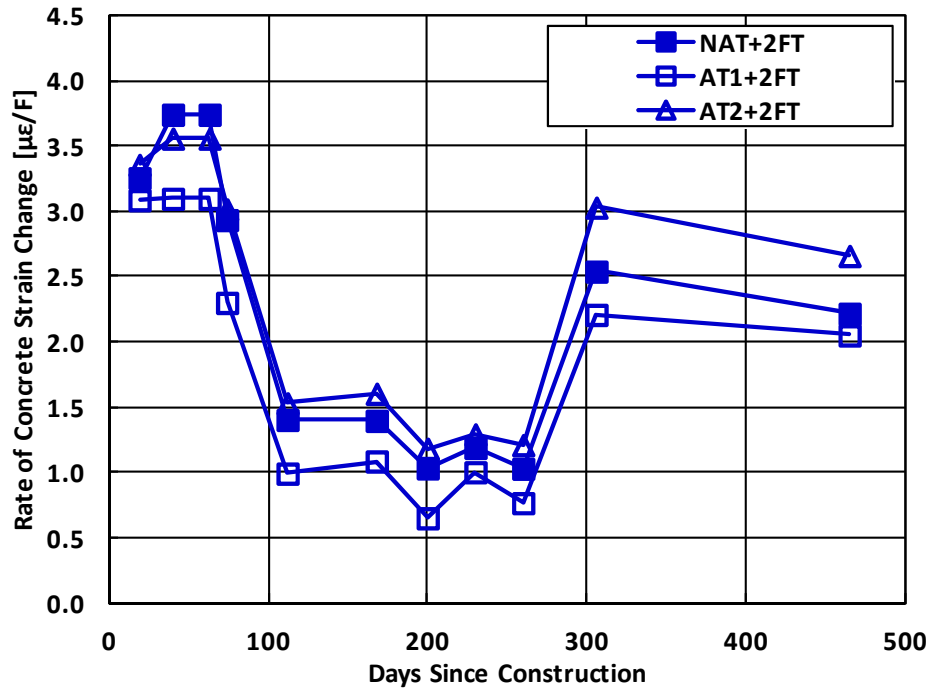


Figure 3. 26 Rate of Concrete Strain Change at 2 ft.
From LBB-II Transverse Construction Joint

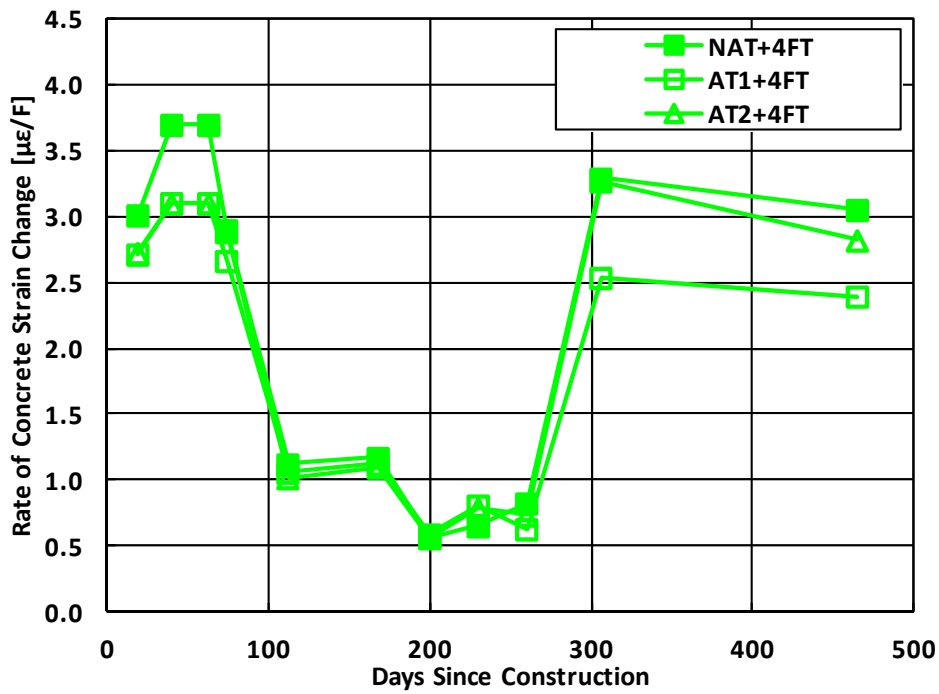


Figure 3. 27 Rate of Concrete Strain Change at 4 ft.
From LBB-II Transverse Construction Joint

3.2.5 Longitudinal Slab Movement at LBB-I TCJ

In order to evaluate the relative as well as independent movement of the existing and newly placed slabs at the TCJ, crackmeters were installed at the LBB-I section as shown in Figure 3.28. Two crackmeters were installed on the existing and newly placed slabs individually. For each crackmeter, one end of the crackmeter was fixed to the slab using concrete anchors and the other end was fixed to an invar bar embedded into the base. The invar bars used in this type of gage setup have minimal temperature co-efficient and thus can help in accurately determining the longitudinal slab movements. A crackmeter was installed across the TCJ with each end attached to either CRCP slab. One end was attached to the existing slab and the other to the newly placed slab. The crackmeter identified as “Across” in Figure 3.28 helped to determine the movement of the TCJ.

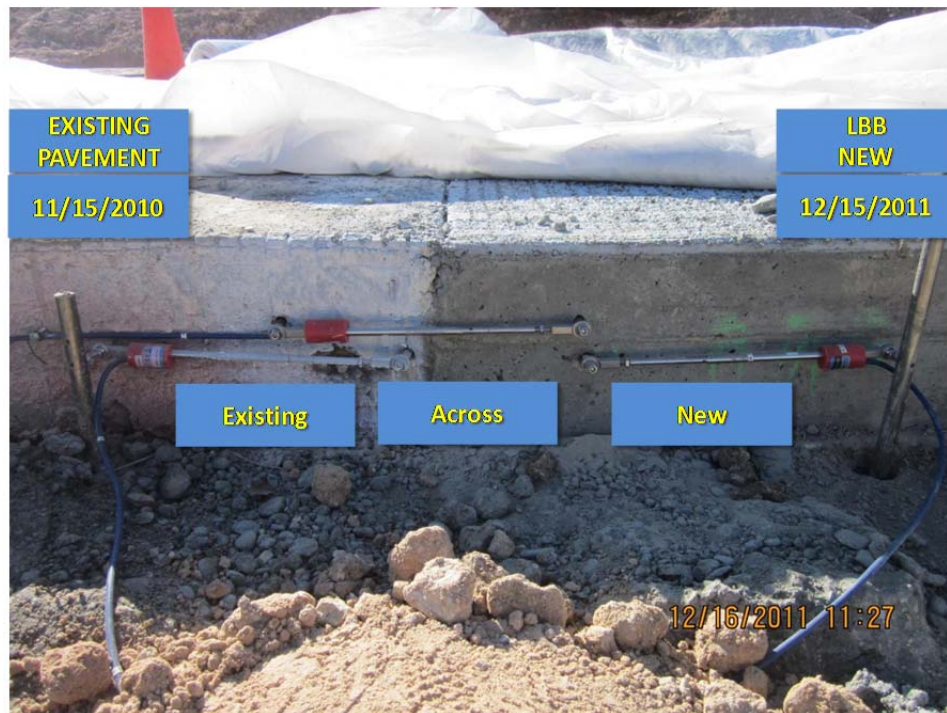


Figure 3. 28 Crackmeter Installation at LBB-I Test Section

Figure 3.29 shows the slab displacements obtained from the crackmeters. As the concrete temperature dropped, the newly placed slab moved towards the right, while the existing slab also

moved to the right. Thus, the newly placed slab was pulling the existing pavement, quite possibly due to the drying shrinkage of concrete. It is to be noted that, even though the modulus of elasticity or stiffness of concrete in the newly placed slab should be lower than that in the existing slab, the difference in stiffness becomes quite small in a few days, and the drying shrinkage of the new slab has a dominant effect. In Figure 3.29, the joint opening, shown in green, is the measured value across the joint and are quite similar to the sum of the other two, indicating the accuracy or quality of the measurement system. As the temperature dropped, the joint width increased.

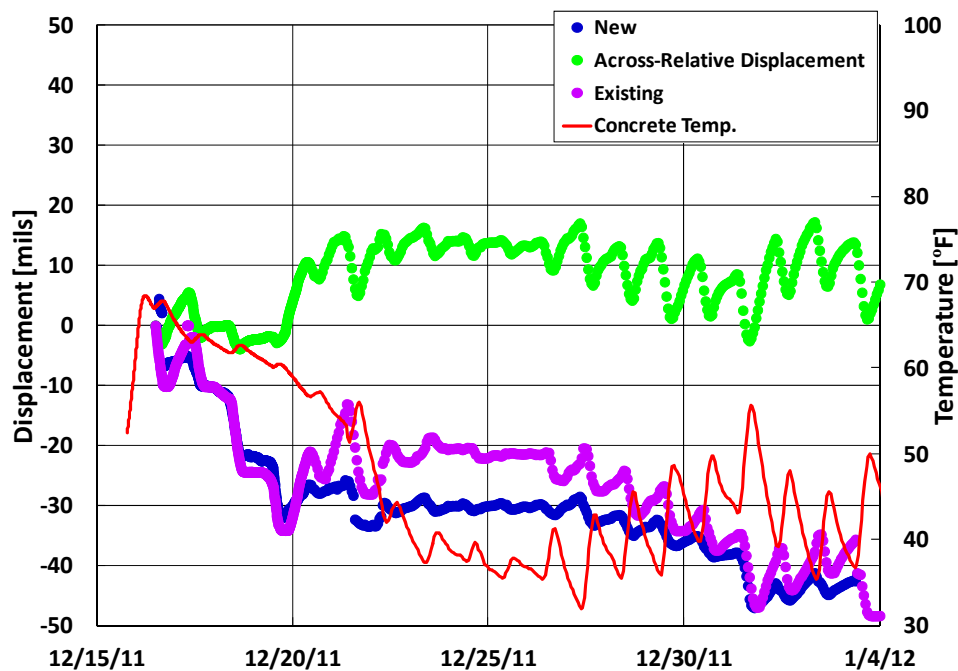


Figure 3. 29 Slab Movement at LBB-I Test Section

3.3 Test Section on IH 20 in Brownwood District

Two test sections denoted as BWD-I and BWD-II were constructed in the Brownwood district on IH 20 west bound near the town of Ranger. Figure 3.30 shows the location of the two sections. The CRCP slab thickness in both of these test sections was 13 in.

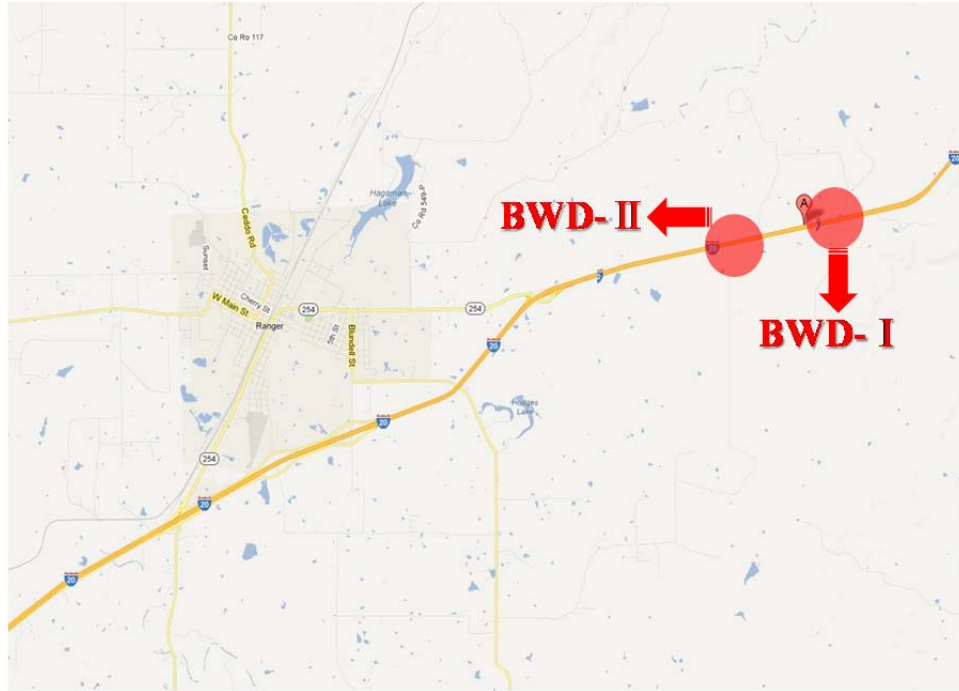


Figure 3. 30 Location Map of Test Sections in Brownwood District

Figure 3.31 depicts the general outlay of BWD-I and BWD-II test sites. Paving was carried out in the west to east direction. The outside lane and outside shoulder were constructed in Phase I and the inside lane and inside shoulder in Phase II as shown. The evening section at BWD-I TCJ was constructed on August 14, 2012 and paving was continued from the morning section on August 16, 2012. VWSGs and SSGs were installed in the inside lane during Phase I. In the evening section at BWD-I the outside shoulder width was 10ft. which transitioned to a 12 ft. wide shoulder on the morning section. Under Phase II of paving, construction stopped at BWD-II TCJ on September 8, 2012 which is depicted as the evening section. Further paving on the other side of the TCJ was initiated in the morning on September 24, 2012. VWSGs were installed in the evening section at BWD-II. The distance between BWD-I and BWD-II sections is 393 ft.

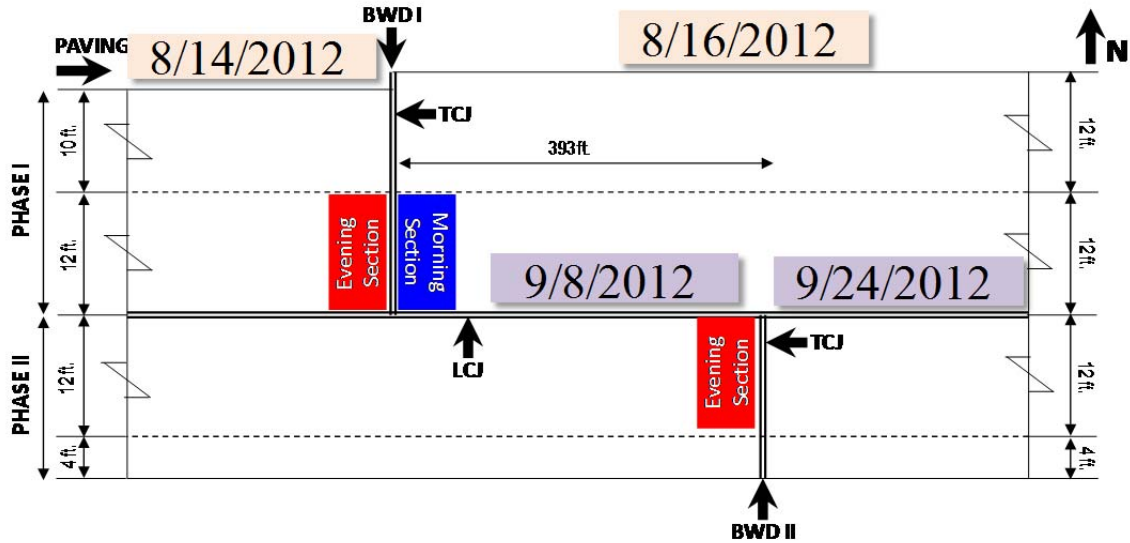


Figure 3.31 Brownwood Test Section Layout

3.3.1 BWD-I Test Section – Testing Plan and Gage Setup

BWD-I test section was constructed in order to compare the concrete strains near and away from the TCJ, with short delay in construction between the evening and morning sides of the TCJ. Also, since the adjacent inside lane was constructed during Phase II, the effect of construction of this additional lane on the concrete strains near the LCJ and TCJ at BWD-I could be determined.

Figure 3.32 shows the gage installation plan for BWD-I section. VWSGs in the transverse direction were installed at a distance of 1 ft. and 4 ft. from the inside LCJ at 1 in. from the top of the slab and 1 in. from the base in both the morning and evening sections. The VWSGs in the transverse direction were at a distance of 4.5 ft. from the TCJ in the evening section and 3.5 ft. from the TCJ in the morning section. Also at 3ft. and 10 ft. from the LCJ and 4.5 ft. from the TCJ, VWSGs in the longitudinal direction were installed in both the morning and evening sections at 1 in. from the top and 1 in. from the bottom. At 6 ft. from the inside LCJ and 1 ft. and 4ft. from the TCJ, VWSGs were installed in the longitudinal direction at 1 in. from the top, mid-depth of the slab and 1 in. from the base in both the morning and evening sections. Six SSGs were also installed in the morning section at BWD-I. Three of these SSGs were installed on the longitudinal steel and the other three on top of additional tie-bars at a distance of 3 ft., 6 ft. and 10 ft. from the inside LCJ.

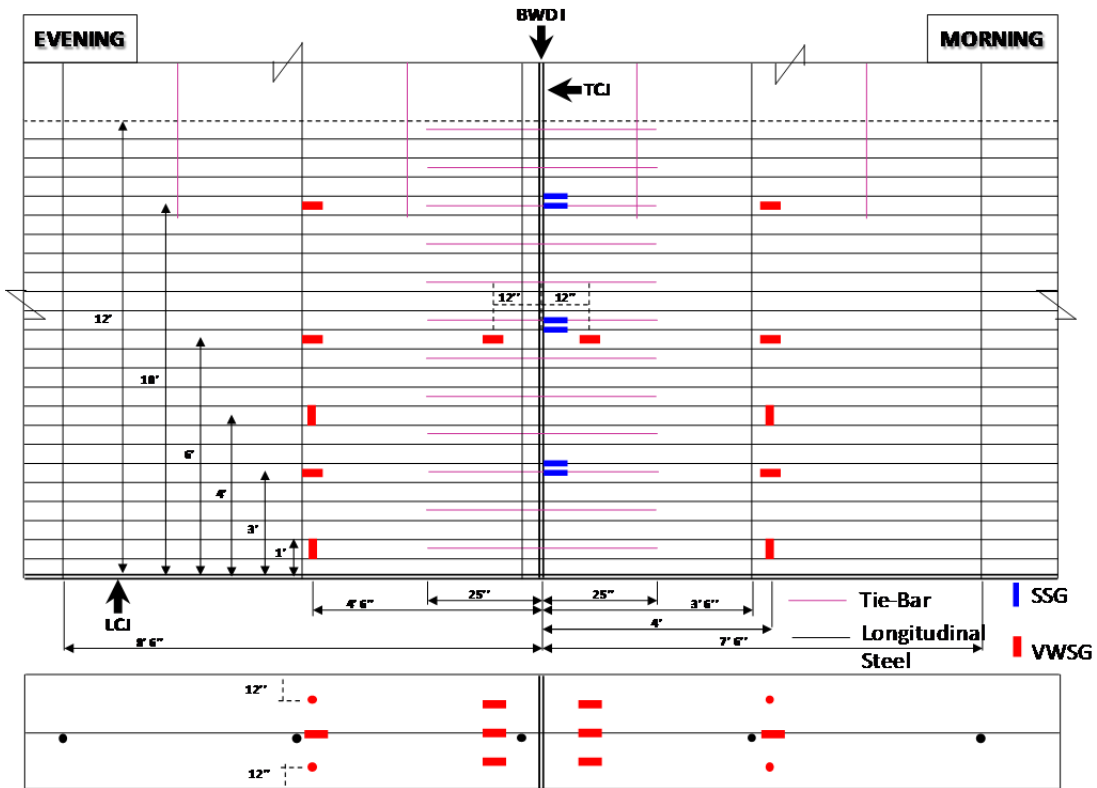


Figure 3.32 Gage Installation Plan at BWD-I Test Location

Figures 3.33 through 3.36 show the construction process at BWD-I TCJ during evening placement on August 14, 2012 and in the morning placement on August 16, 2012. Before concrete was poured around the TCJ, the research team gathered concrete and placed it manually around SSGs and VWSGs to ensure that the gages do not get damaged during the paving and consolidation process using the hand-held vibrator.



Figure 3.33 Concrete Placement at BWD-I Evening Test Section



Figure 3.34 Protecting VWSGs at BWD-I Evening Test Section



Figure 3.35 Concrete Placement at BWD-I Morning Test Section



Figure 3.36 Concrete Finishing at BWD-I Morning Test Section

3.3.2 Steel Strain Behavior near TCJ at BWD-I Test Section

Figures 3.37 and 3.38 illustrate the early and later age behavior of steel strain at BWD-I. As can be seen in Figure 3.37, concrete temperature dropped from 70 °F to 55 °F from October 1, 2012 to November 30, 2012. However, the steel strains in the longitudinal as well as additional tie-bars remained relatively steady, while experiencing daily variations due to daily temperature variations, as observed in the Lubbock test section. As shown in Figure 3.38, the steel strains in the longitudinal steel at 3 ft. and 6 ft. from the LCJ remained steady at around 1,000 micro strains and 500 micro strains in tension, respectively. However, after the temperature increase from March 7, 2012, steel strains in the tie-bar at 6 ft. moved towards compression, as those at the tie-bars at 3 ft. and 10 ft.

On the other hand, strains in the longitudinal steel remained in tension, which indicates that the behavior of longitudinal steel and additional tie bars is quite different. The primary reason for this discrepancy in the behavior is the continuity condition of the bars. When the concrete temperature increases, the volumes of both concrete and steel bars try to increase as well. In general, there is a good bond between longitudinal steel and surrounding concrete, and the concrete and longitudinal steel behaves as a composite material. On the other hand, additional tie bars are not continuous, and there is a discontinuity at the end of the tie bar. When the concrete temperature volume expands due to temperature increase, concrete could push tie bars

longitudinally towards TCJs, causing tie bars in compression and, if excessive, tensile stress in the vertical direction in the concrete near the tie bars, potentially resulting in horizontal cracks at the depth of tie bars. This mechanism of horizontal cracking in concrete slabs has been observed at transverse contraction joints in jointed concrete slabs where dowels cause vertical tensile stresses in concrete when temperature increase is excessive. Based on the available CRCP design standards, TxDOT has been using additional tie bars as early as 1960, and it is difficult to form a logical or technical justification for the use of additional tie bars at TCJs. It could be that an assumption was made at that time that additional tie bars would behave the same way as longitudinal steel and thus complement longitudinal steel at TCJs, reducing the stress level in longitudinal steel at TCJs and improving overall performance. The data from field experimentation indicates that is not the case.

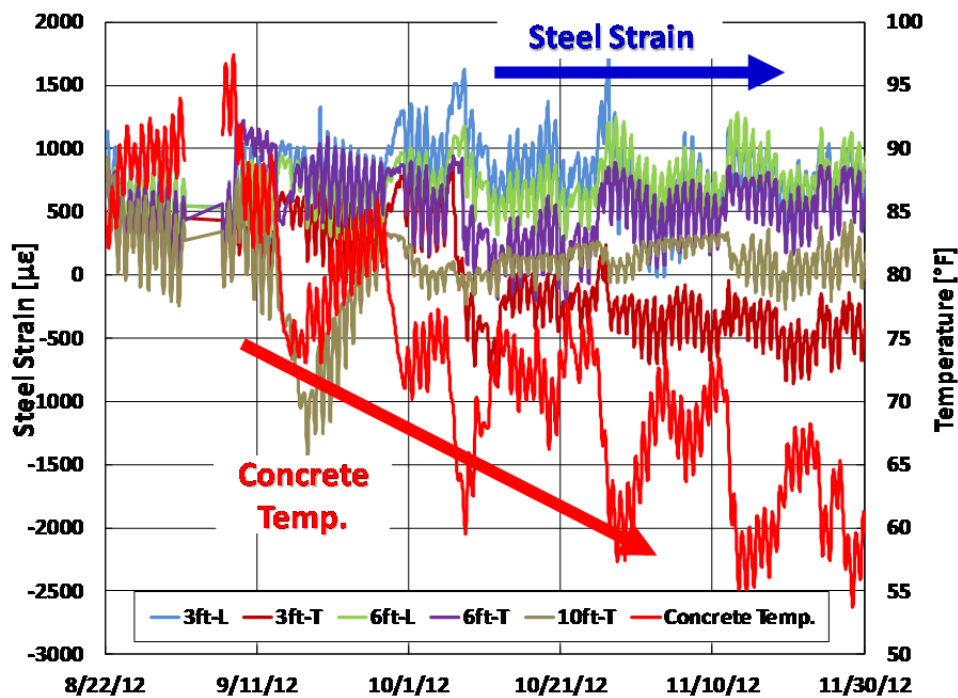


Figure 3. 37 Early Age Steel Strain at BWD-I Test Section

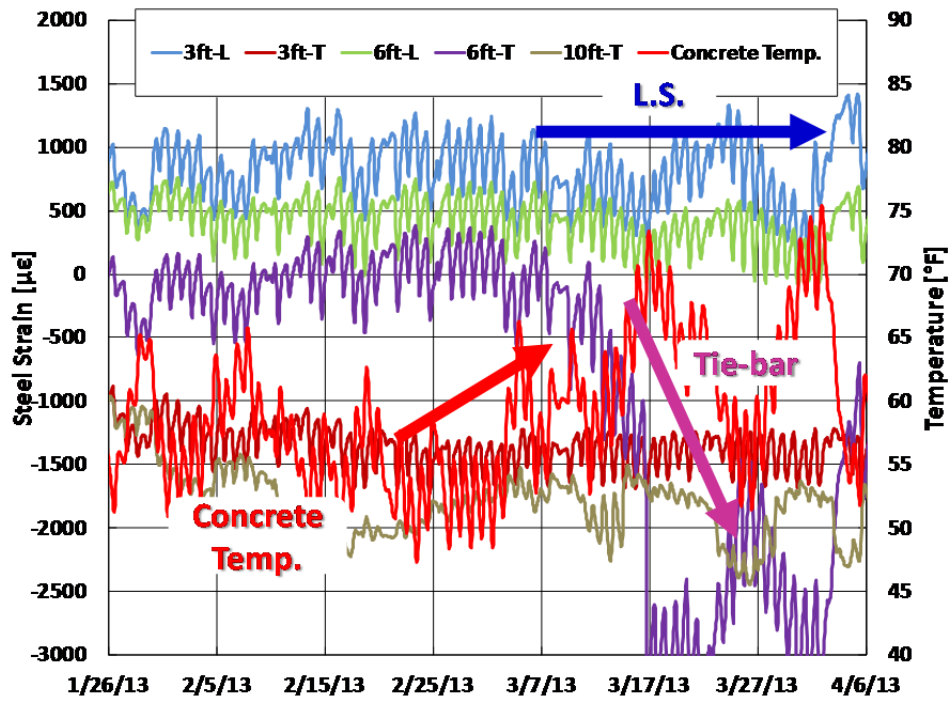


Figure 3. 38 Later Age Steel Strain at BWD-I Test Section

Figures 3.39 through 3.42 provide a more exhaustive display of the steel strains at BWD-I test section from the early age until seven months after construction. They show that the variations in steel strains in longitudinal steel at 3 ft. and 6 ft. from the pavement edge remained relatively small and in tension, whereas the steel strains in tie-bars gradually moved towards compression. This disparity in steel strains between longitudinal steel and additional tie bars provides valuable technical information which should be considered for improved design of TCJs in CRCP.

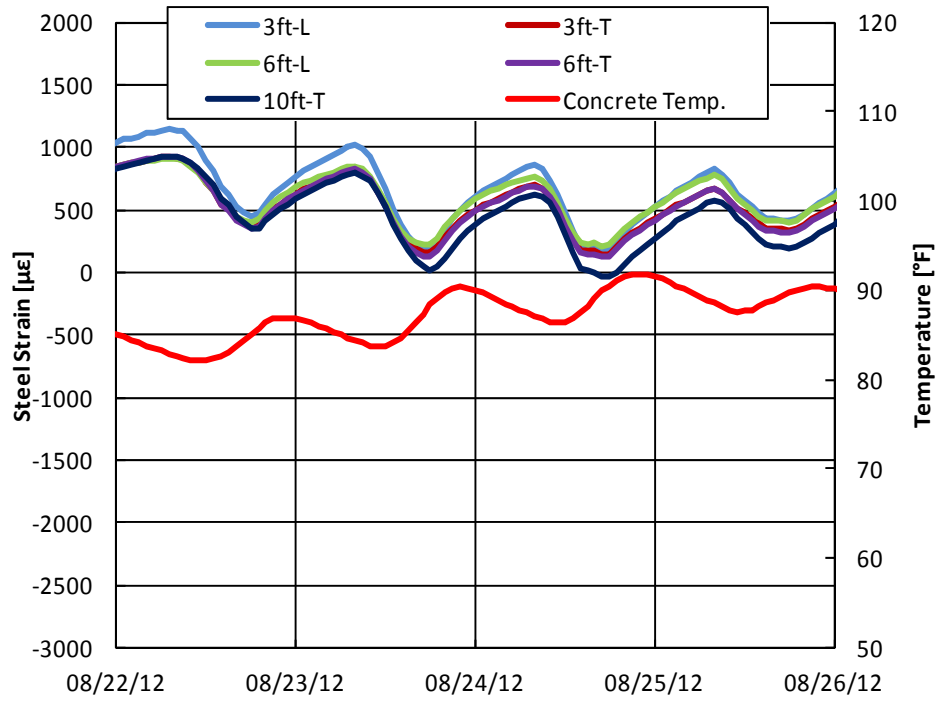


Figure 3. 39 Steel Strain at BWD-I Right After Construction

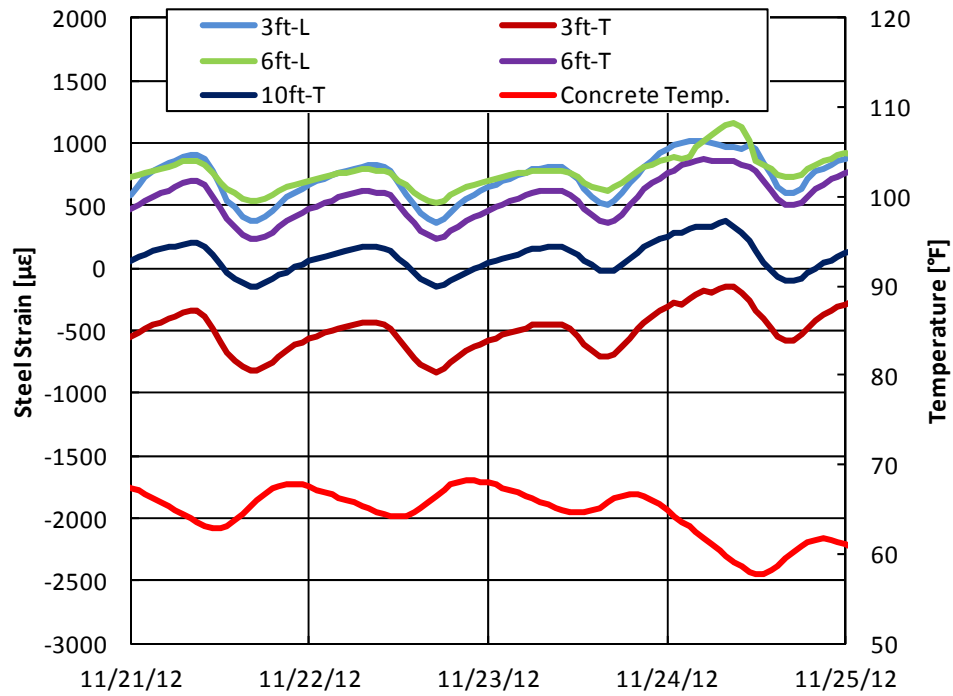


Figure 3. 40 Steel Strain at BWD-I-3 Months After Construction

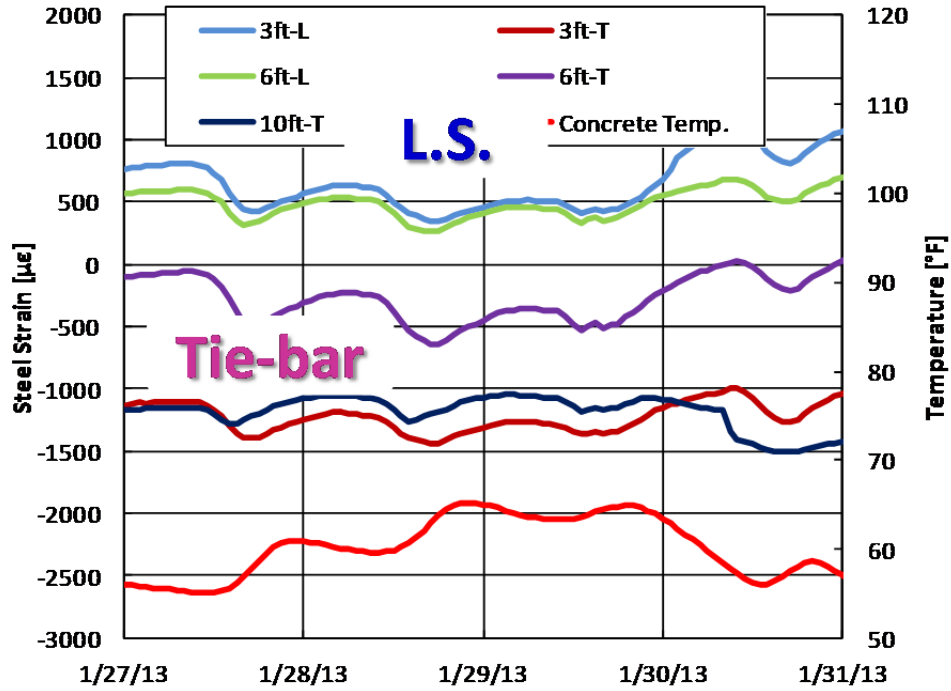


Figure 3. 41 Steel Strain at BWD-I-5 Months After Construction

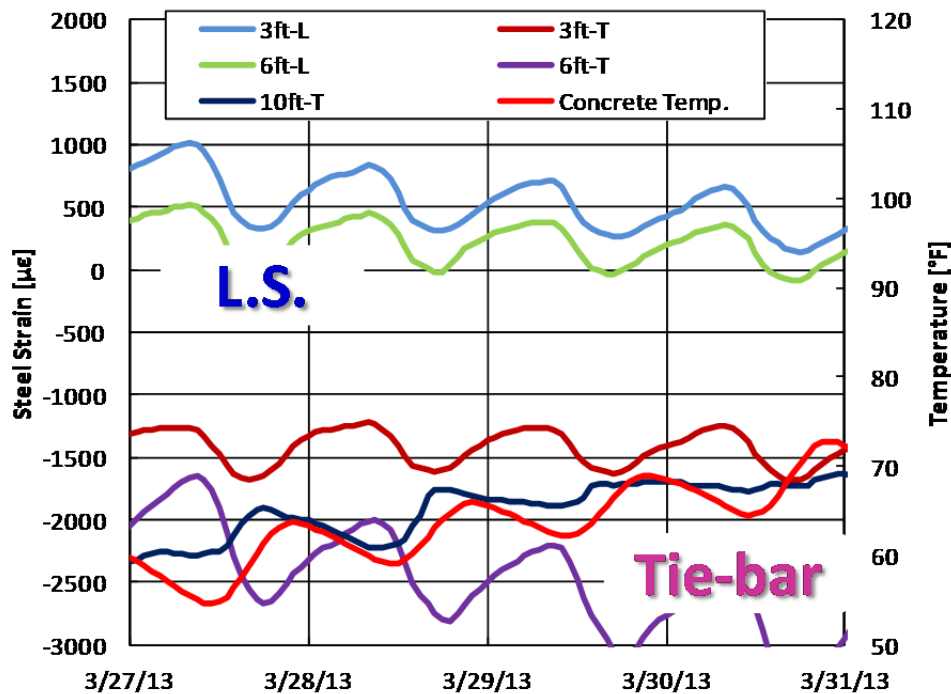


Figure 3. 42 Steel Strain at BWD-I-7 Months After Construction

3.3.3 BWD-II Test Section – Testing Plan and Gage Setup

Figure 3.43 illustrates the gage installation at BWD-II test section. Four VWSGs were installed in the evening section at this location. The VWSGs were installed at mid-depth of the slab and in the longitudinal direction. VWSG-1 and VWSG-3 were installed at a distance of 6 in. from the LCJ and at 1 ft. and 4 ft. from the TCJ respectively. VWSG-2 and VWSG-4 were installed at 4 ft. from the LCJ and 1 ft. and 4 ft. from the TCJ, respectively.

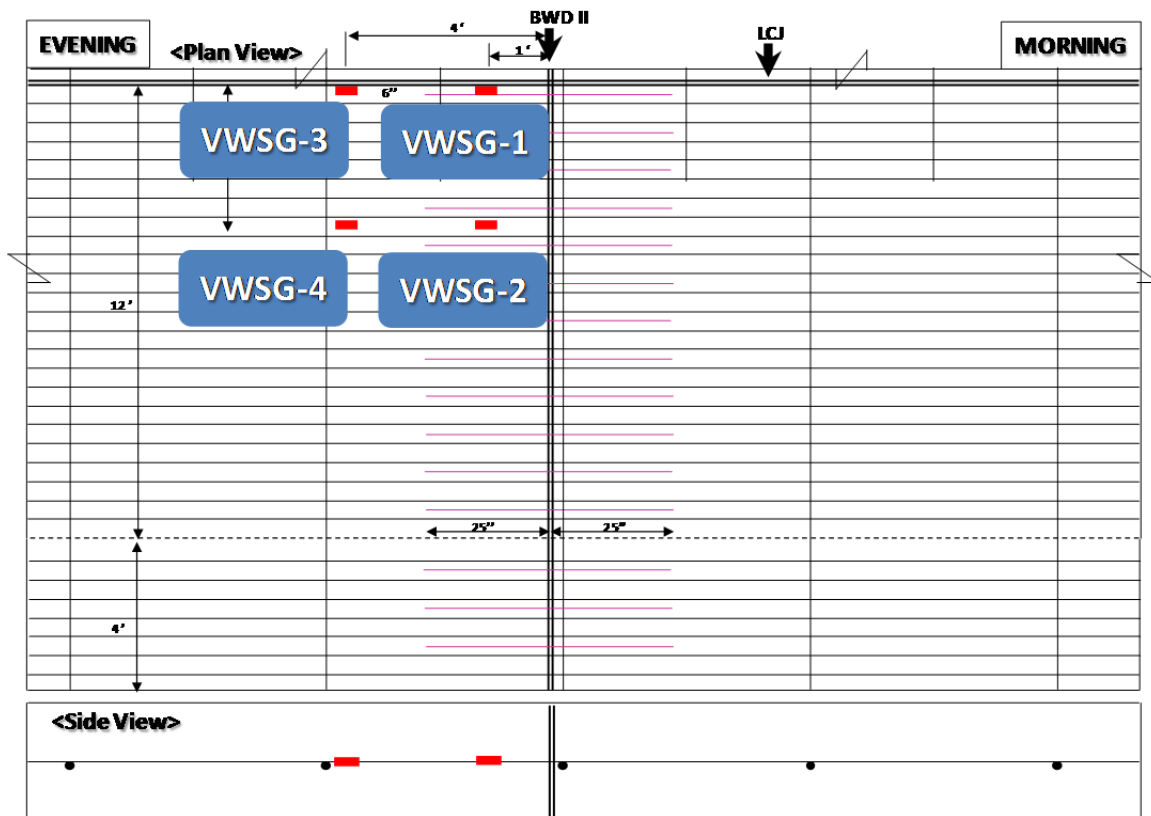


Figure 3. 43 Gage Installation Plan at BWD-II Test Location

As shown in Figure 3.44, additional tie-bars from both the TCJ and LCJ in addition to the longitudinal steel can be seen near the installation of VWSG-1. At VWSG-3, tie-bars from the LCJ and longitudinal steel were present. At VWSG-2 tie-bars from the TCJ and longitudinal steel can be observed. At VWSG-4 only longitudinal steel is present due to the location being 4 ft. from the TCJ as well as LCJ. Thus, the highest concentration of restraint in the form of additional and longitudinal steel can be seen at the location of VWSG-1.



Figure 3. 44 VWSG Installation at BWD-II Evening Test Section

Figures 3.45 and 3.46 show the construction process at the BWD-II evening placement side. The construction near the TCJ is carried out manually since the paver cannot pass over the headers placed to construct the TCJ at the end of the day’s paving. The concrete used for paving near the evening section at TCJ is usually the last batch of concrete and its quality may vary from the concrete used in the rest of the pavement. Also, compaction near the TCJ is carried out using hand-held vibrators which may affect the overall consolidation of concrete in this area.



Figure 3. 45 Concrete Placement at BWD-II Evening Section



Figure 3. 46 Finishing at BWD-II Evening Test Section

Once the concrete on the evening side had set and gained sufficient initial strength, the headers at the TCJ were removed on September 9, 2012. In order to evaluate the longitudinal and vertical slab movement at the TCJ when concrete is not yet placed on the morning side, crackmeters were installed. The crackmeters were installed using an L-shaped concrete embedment anchor. One arm of the L-shaped anchor was embedded into the face of the TCJ longitudinally at mid-depth of the slab as shown in Figure 3.48. The other arm of the anchor was attached to one end of the crackmeter and the other end of the crackmeter was affixed to an invar bar drilled into the base. Crackmeters in the longitudinal direction were installed at 1.5 in., 1.6 ft., 3.3 ft., 6.5 ft. and 15.5 ft. from the LCJ as shown in Figure 3.47. The longitudinal crackmeter at 6.5 ft. from the LCJ was also connected to another crackmeter and a corresponding invar. This second crackmeter connected to the 6.5 ft crackmeter acted as reference to determine the movement in the invar-bars due to the expansion/contraction of the sub base with temperature. Also, at the free corner of the slab at 16 ft. from the LCJ, a vertical crackmeter was installed as shown in Figure 3.48 to determine the vertical movement of the free slab edge.

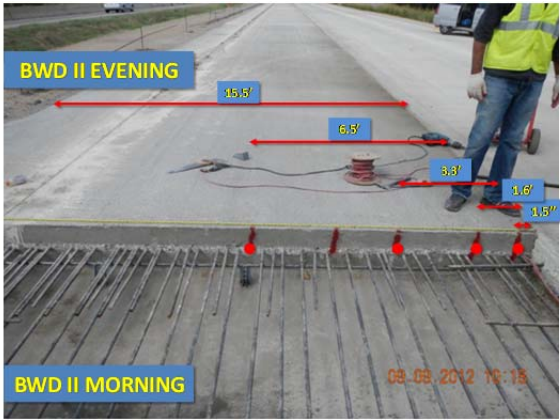


Figure 3. 47 Crackmeter Installation Locations at BWD-II Test Section



Figure 3. 48 Crackmeters Installed to Measure Longitudinal Slab Movement at BWD-II Test Section



Figure 3. 49 Vertical Crackmeter Installed at the Free Slab Edge at BWD-II Test Section



Figure 3. 50 Reference Crackmeter Attached to Measure Invar Movement at BWD-II Test Section

3.3.4 Concrete Strain at Junction of Transverse Construction Joint and Longitudinal Construction Joint – BWD-II TCJ

As discussed in Chapter 2, a lot of premature distresses are observed near the longitudinal construction joint when the transverse construction joint is not continuous in two adjacent lanes, i.e. when two adjacent lanes are not constructed at the same time and hence TCJs are not aligned. In order to investigate such distresses at the intersection of TCJ and LCJ with the adjacent lane being continuous, the BWD-II section in the inside lane was constructed. The outside lanes had already been constructed three weeks prior. At the TCJ location in the BWD-II section, the TCJ is not present at the same location as in the previously constructed outside lane, but is 393 ft. east of it.

On the evening construction side of the section, four VWSGs were placed at mid-depth of the slab. VWSG 1 and VWSG 3 were at a distance of 0.5 ft. from the longitudinal construction joint and 1 ft. and 4ft. from the transverse construction joint, respectively. VWSG 2 and VWSG 4 were at a distance of 4 ft. from the longitudinal construction joint and 1 ft. and 4 ft. from the transverse construction joint respectively.

Figure 3.51 shows the daily concrete strain variation with temperature at the BWD-II section. The evening side of the TCJ was placed on September 8, 2012 and the morning side on September 24, 2012. The concrete strain varies with daily temperature variation at all four

VWSG locations. However, after September 24, 2012, there is a clear distinction between the concrete strains at the four locations. The highest concrete strain can be seen at the VWSG-4 location, which is at 4 ft. from the LCJ and TCJ and the lowest concrete strain is observed at VWSG-1, which is closest to the LCJ and TCJ at a distance of 0.5 ft. from the LCJ and 1 ft. from the TCJ.

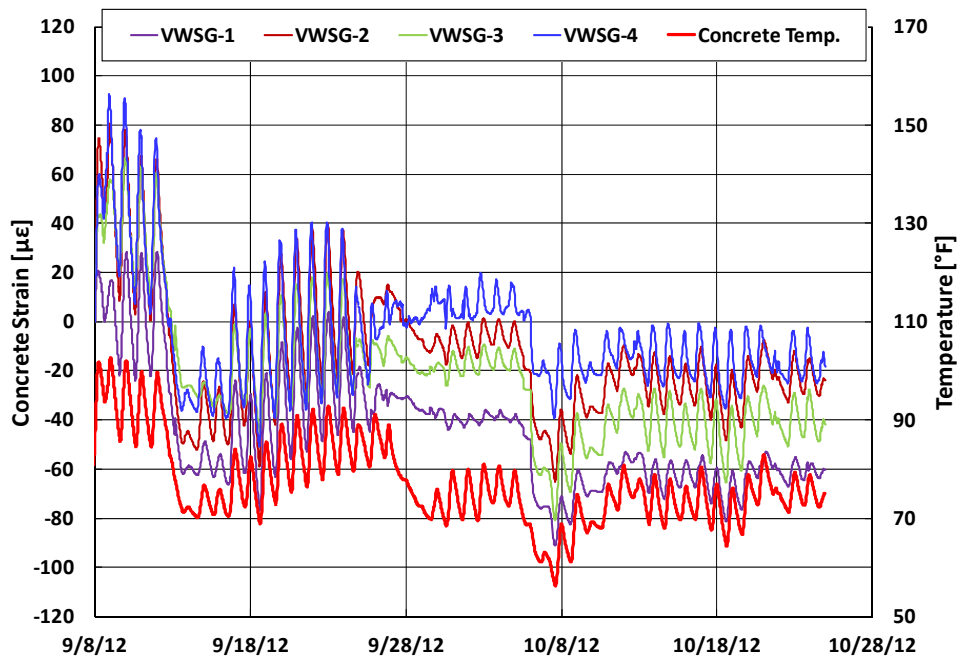


Figure 3. 51 Concrete Strain Variation at BWD-II Test Section

Figures 3.52 and 3.53 represent the concrete strain variation at the four VWSG locations at BWD-II for 4-day intervals, before and after placement of the concrete on the morning side of the TCJ. As shown in Figure 3.52, on September 10, 2012, the daily concrete temperature varied from 85°F to 100 °F. As the temperature varied by 15 °F, the total concrete strain variation at VWSG-1, VWSG-2, VWSG-3 and VWSG-4 was 51.81 με, 54.01 με, 75.14 με and 83.01με respectively. Thus, the highest daily strain variation was experienced at the VWSG-4 location and the lowest at the VWSG-1 location. This can be explained by the presence of additional tie-bars at the junction of TCJ and LCJ where the VWSG-1 is located, leading to high restraint towards movement of concrete and thus exhibiting the lowest daily concrete strain variation. However, VWSG-4 is at a distance of 4 ft. from the LCJ and TCJ. At this location concrete is only restrained by longitudinal steel and hence experiences less restraint and higher total daily

strain variation. Figure 3.53 presents the concrete strain variation from September 24, 2012 to September 27, 2012. As can be seen, the daily total concrete strain variation decreased a lot after concrete was placed on the evening side of the TCJ on September 24, 2012.

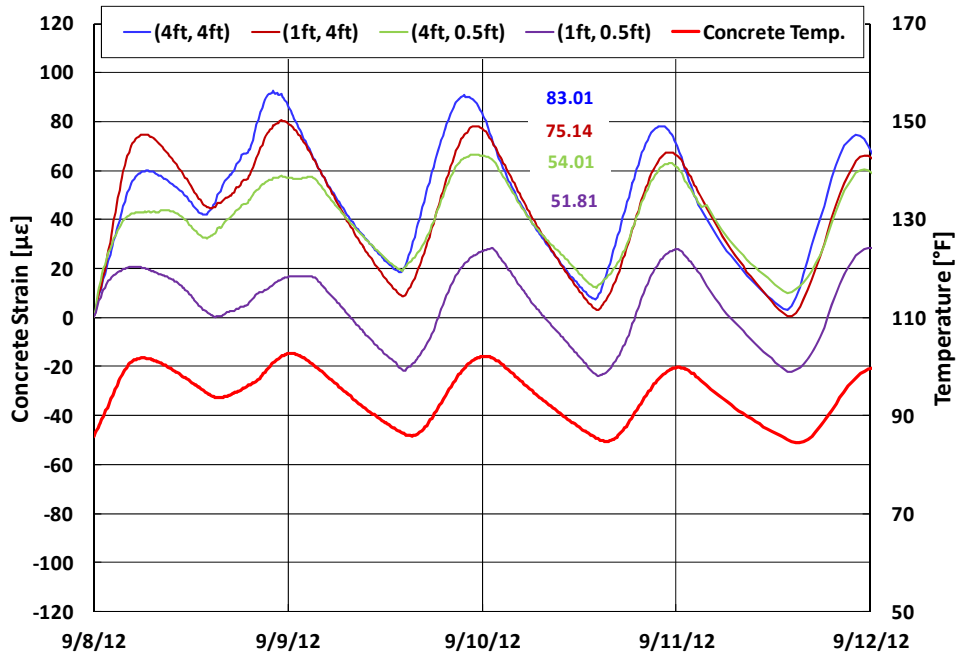


Figure 3. 52 BWD-II Concrete Strain Comparison Before Morning Side Placement

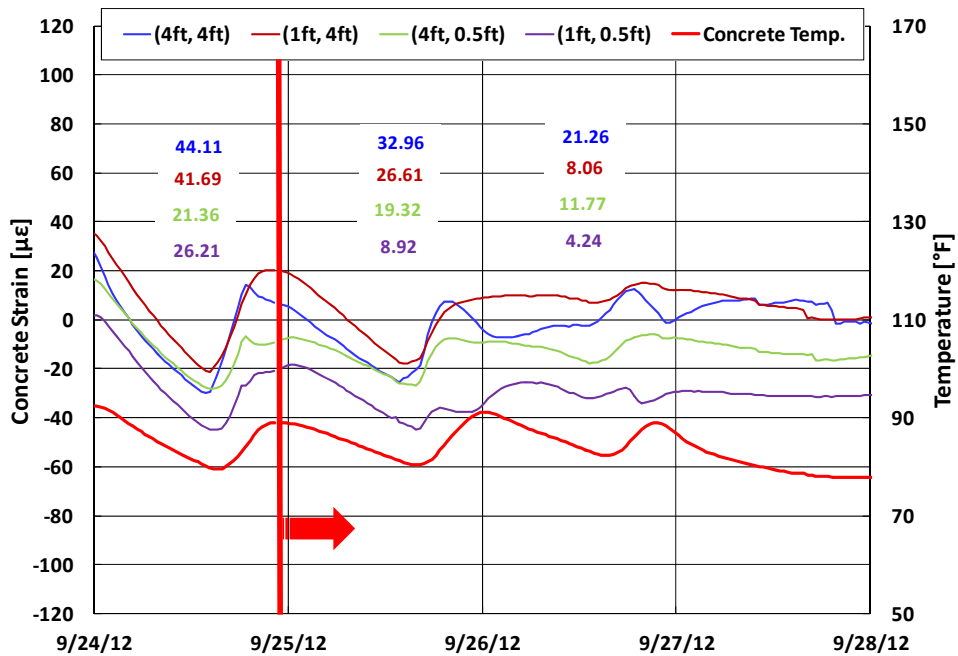


Figure 3. 53 BWD-II Concrete Strain Comparison After Morning Side Placement

Table 3.3 enlists the daily strain variation at the four VWSG locations at different ages. The daily strain variations are represented graphically in Figure 3.54.

Table 3.3 Daily Concrete Strain Variation at BWD-II Test Section

Age [Days]	Daily Strain Variation [$\mu\epsilon$]			
	VWSG-1	VWSG-2	VWSG-3	VWSG-4
2	51.8	75.1	54	83
14	51	64.3	49.6	73.4
16	26.2	41.7	21.4	44.1
17	8.9	26.6	19.3	33
18	4.2	8.1	11.8	21.3
26	2.8	10.6	8.9	12.5

As shown in Figure 3.54, the daily strain variation before the construction of the morning side at the TCJ are highest at VWSG-4, followed by VWSG-2. Both these locations are at a distance of 4 ft. from the LCJ. At 0.5 ft. from the LCJ, VWSG-1 and WSG-3 locations show similar daily strain variation characteristics. On Day 16, after the construction of the morning side, the daily strain variations at all VWSGs dropped drastically. However, the highest drop in daily concrete strain variation can be seen at the VWSG-1 location, where the daily strain variation dropped by 70% from 26 micro strains to 8.9 micro strains on Day 17. Further daily strain variation monitoring revealed that at the end of 26 days since construction of the evening section, the lowest daily concrete strain variation was observed at VWSG-1 and the highest at VWSG-4.

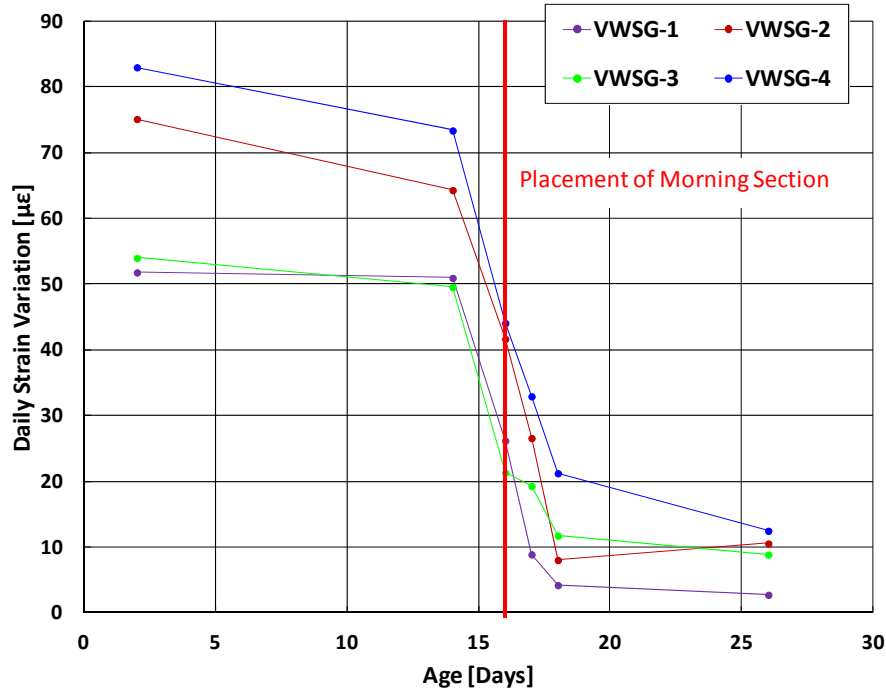


Figure 3. 54 Daily Strain Variation Near and Away From the Longitudinal Construction Joint at BWD-II Test Section

Thus, before the evening side placement at BWD-II, the concrete strain near the junction of the TCJ and LCJ experienced the lowest strain. After construction of the evening side, the concrete strain variation near the junction dropped drastically. As a result, the concrete stress at the junction of the TCJ and LCJ would be higher than the rest of the pavement when the adjacent lane is already constructed and the TCJ is not continuous along the two lanes. Also, when the evening side at such a TCJ is constructed after a delay of more than two weeks, a sudden drop in daily strain variation and a resulting increase in concrete stress is experienced by the concrete closest to the TCJ and LCJ.

3.3.5 Slab Movement at Free Edge at BWD-II Test Section

As discussed earlier, crackmeters were installed longitudinally at the face of the TCJ at the BWD-II test section after concrete had gained enough strength on the evening placement side. Crackmeters were installed at a distance of 1.5 in., 1.6 ft., 3.3 ft., 6.5 ft., 12 ft. and 15.5 ft. from the longitudinal construction joint

Figure 3.55 illustrates the daily longitudinal movement of the slab at different distances from the LCJ measured using the crackmeters. As the daily air temperature and consecutively the concrete temperature increases, the crackmeter movement goes into compression. This means that as the temperature increases and the slab expands at the face of the TCJ, the crackmeter goes into compression. Inversely, as the air and temperature decreases, the slab contracts and the crackmeter's movement exhibits tension.

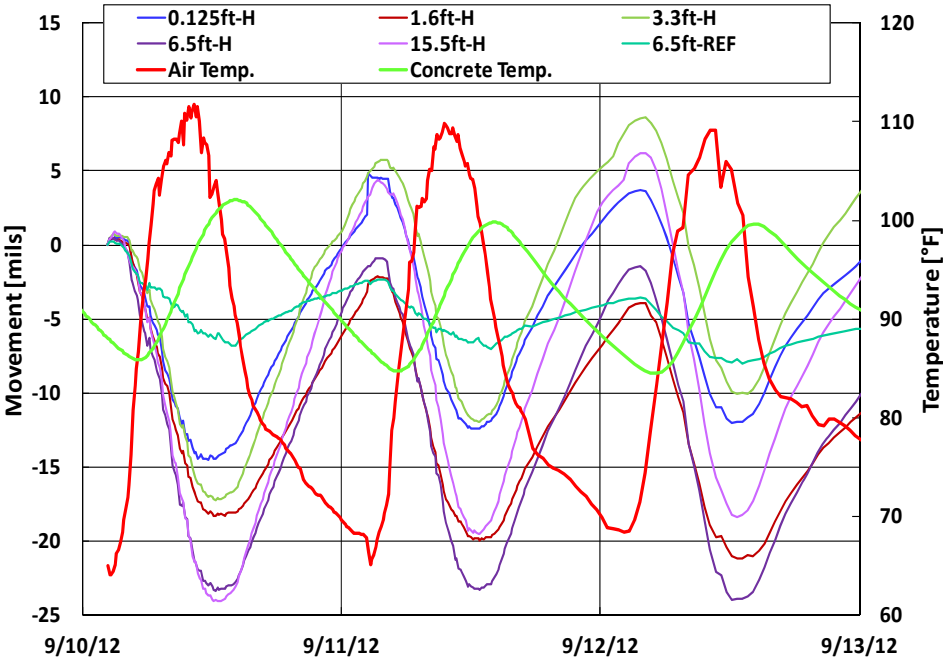


Figure 3. 55 Daily Slab Movement Along the Transverse Construction Joint at BWD-II

For the first 60 hours after the crackmeters were installed, the slab movements at each crackmeter location were evaluated and are presented in Table 3.4. As can be seen in Table 3.4, as the distance between the LCJ and the crackmeter installation location increases, the longitudinal movement of the slab also increases.

Table 3. 4 Slab Movement at Transverse Construction Joint

	Slab Movement [mils]				
	0.125 ft.	1.6 ft.	3.3 ft.	6.5 ft.	15.5 ft.
12 hr.	15	18.7	17.9	23.8	24.9
24 hr.	19.3	16.2	23	22.5	28.4
36 hr.	17.2	17.8	17.7	22.4	23.9
48 hr.	16.1	16	20.6	21.3	25.8
60 hr.	15.7	17.2	18.6	22	24.6
Average	16.7	17.2	19.6	22.4	25.5

The average longitudinal movement of the slab over five days is illustrated in Figure 3.56. The displacement at the location closest to the LCJ at 0.125 ft. is 16.7 mils and the displacement at the free edge of the slab, 15.5 in. from the LCJ is 25.5 mils. This difference quantifies into a difference of 8.9 mils between the two terminals of the slab along its width. Thus, when concrete is not placed on the morning side of a TCJ, the slab exhibits large movement as we move away from the longitudinal construction joint.

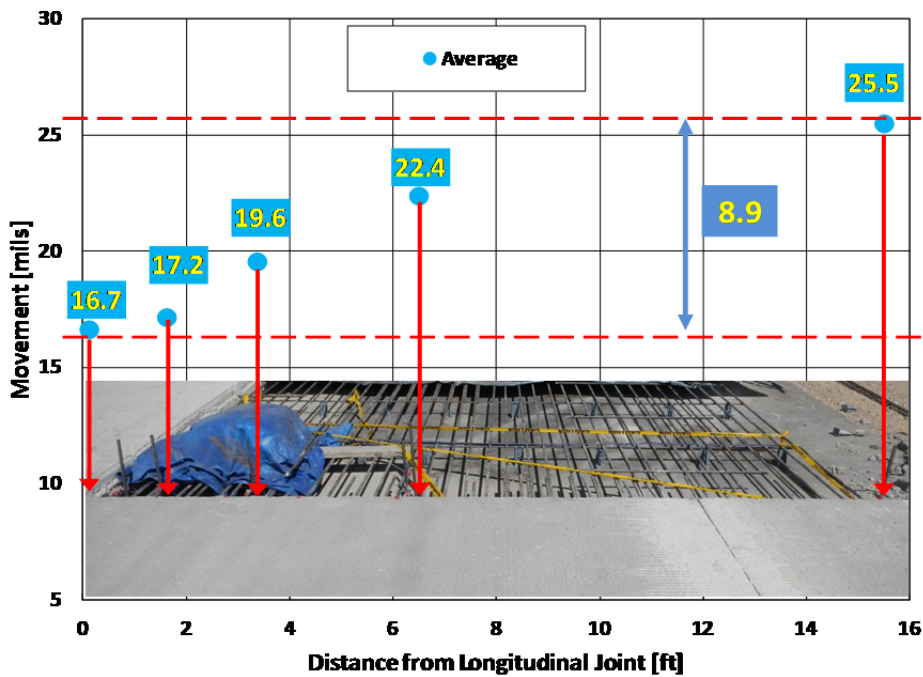


Figure 3. 56 Average Longitudinal Movement of the Slab Along the Transverse Construction Joint

3.3.6 Relationship Between Crackmeter Movement and Concrete Strain Change

Since VWSGs had been installed inside the concrete in the evening side of the slab where crackmeters were installed at the face of the TCJ at BWD-II test section, a good relationship between the longitudinal movement of the concrete slab near the TCJ and the concrete strains evaluated using the VWSGs can be determined. Figure 3.57 presents the longitudinal movement of the slab at a distance of 0.125 ft. from the LCJ and the concrete strain movement at VWSG-1 and VWSG-3 locations that are at a distance of 0.5 ft. from the LCJ and 1 ft. and 4ft. from the TCJ respectively. On September 11, 2012, as the temperature dropped during the night, the slab contracted, the crackmeter was in tension whereas the concrete strain was in compression. As temperature increases during the day and the slab expands, the crackmeter moves from 5 mils in tension to 12 mils in compression and the VWSG-1 moves from 25 microstrain in compression to 25 microstrain in tension. Figure 3.58 shows the relationship between crackmeter movement at 3.3 ft. from the LCJ and concrete strain variation at VWSG-2 and VWSG-4. Similar behavior of crackmeter movement and daily variation in concrete strain can be observed at this location.

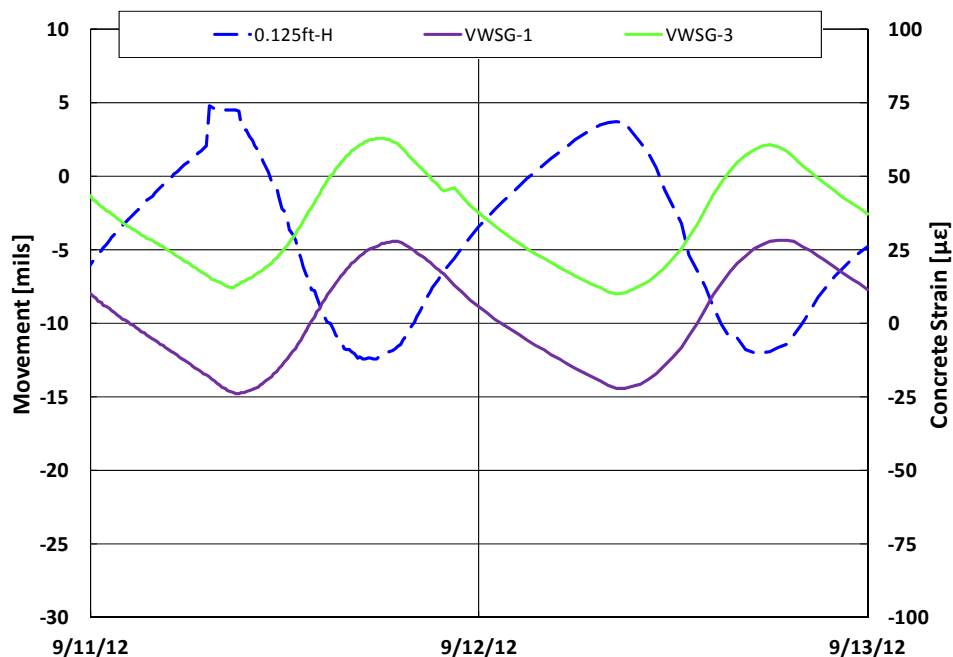


Figure 3. 57 Slab Movement and Concrete Strain Variation Near the Junction of LCJ and TCJ

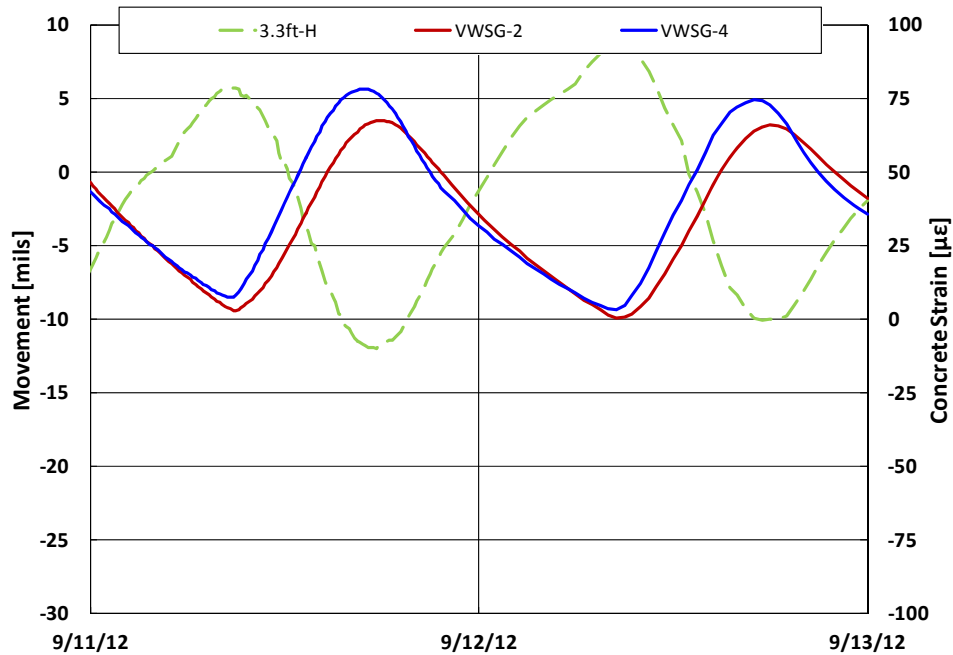


Figure 3. 58 Slab Movement and Concrete Strain Variation Away from the Junction of LCJ and TCJ

3.3.7 Vertical Slab Movement at BWD-II TCJ

A vertical crackmeter was installed at the free edge of the BWD-II test section before concrete was placed on the evening side to determine the vertical movement of the slab with temperature variations in concrete. Figure 3.59 illustrates the vertical movement at 15.5 ft. from the longitudinal construction joint, at the free edge of the slab. The air temperature and concrete temperature during the period of monitoring from September 10, 2012 to September 29, 2012 are also represented in Figure 3.59. As the concrete temperature increases, the vertical movement goes into compression; that is, the slab curls down and with the decrease in concrete temperature, the vertical movement goes into tension, causing the slab to curl up. During the period between September 10, 2012 and September 12, 2012 when the concrete temperature varied between 84 F and 98 F, the vertical movement experienced by the slab was 26 mils. Also, when it rained on September 13, 2012 and the concrete temperature kept going down overnight on September 14, 2012, the crackmeter movement experienced compression. From September 19, 2012 to September 24, 2012 as the concrete temperature started increasing from 83 F to 93 F, a vertical movement of 30 mils was recorded.

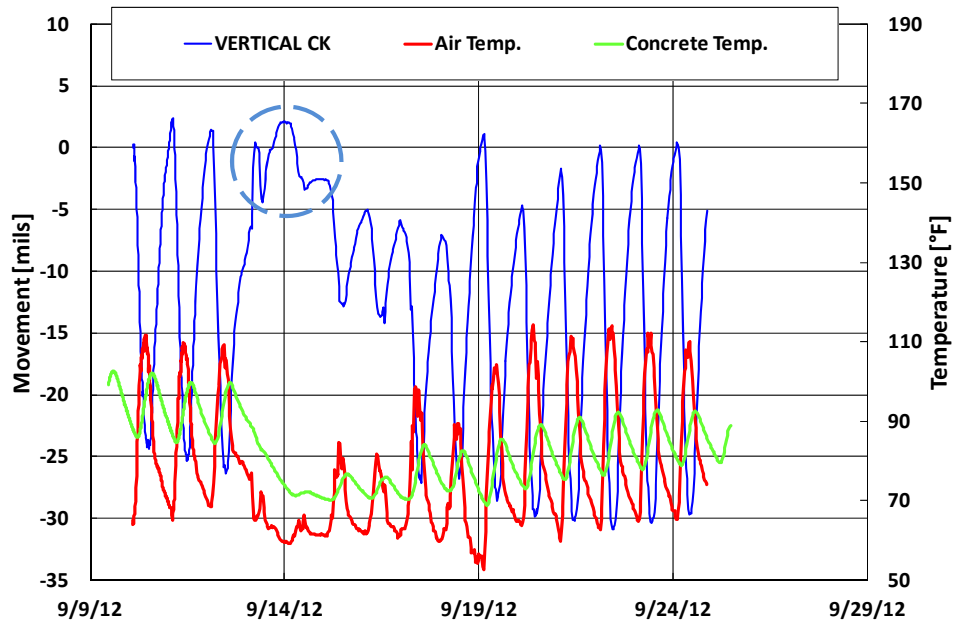


Figure 3. 59 Vertical Slab Movement at the Free Edge of the Slab

3.4 Effect of Construction Season on Concrete Strain near Transverse Construction Joint

Behavior of concrete strain variation derived from VWSGs installed in LBB-I test section is shown in Figure 3.60. Figure 3.60 illustrates the rate of concrete strain variations with temperature until 500 days from the day of construction at LBB I section. Right after construction, during the winter season, the rate of concrete strain change was between $3.5 \mu\epsilon/^\circ\text{F}$ and $4.0 \mu\epsilon/^\circ\text{F}$. As the concrete temperature increased during summer, the rate of strain change dropped to between $1.5 \mu\epsilon/^\circ\text{F}$ and $2.0 \mu\epsilon/^\circ\text{F}$. In the following winter, rate of concrete strain change increased again to between $4.0 \mu\epsilon/^\circ\text{F}$ and $5.0 \mu\epsilon/^\circ\text{F}$. With increase in temperature during the summer, more than 400 days after construction, the rate of concrete strain change again start drops. LBB I section was constructed in the winter, when the rate of concrete strain variations are high; as temperature increases in summer, the rate of concrete strain changes reduced substantially. The rate increased again in the winter season in the following year and it seems to follow the same pattern of reduction in strain changes as the summer sets in the following cycle. This pattern of reduction in the rate of concrete strain changes during summer can be explained by insufficient space for concrete to expand at the TCJ, for TCJs placed during the winter.

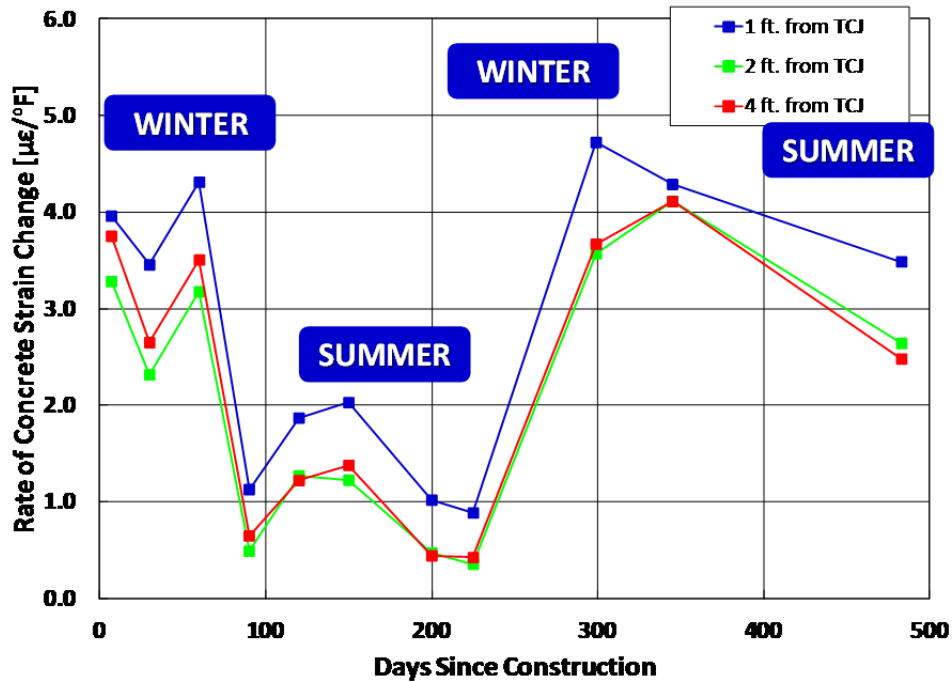


Figure 3. 60 Rate of Concrete Strain Change at TCJ – LBB-I Test Section

Figures 3.61 and 3.62 display the variations in the rate of concrete strain overtime at TCJs constructed in the winter (LBB II) and summer (BWD I) respectively. Figure 3.61 shows that the rate of concrete strain change at 1 ft, 2 ft and 4 ft from the TCJ was high in winter and low in summer. The initial rate of concrete strain change during the winter season was between 2.7 $\mu\epsilon/^\circ\text{F}$. Once temperature increased during the summer, the rate dropped to 0.5 $\mu\epsilon/^\circ\text{F}$. Again, as temperature dropped during the following winter, the rate increased to 2.5 $\mu\epsilon/^\circ\text{F}$.

In the summer construction section at BWD I, the data available until now, shown in Figure 3.62, shows a similar pattern of low concrete strain change rate initially in the summer but the rate increased as winter approached. These concrete strain rate changes were at a distance of 1 ft. and 4 ft from the TCJ in the evening and morning sections at BWD-I. The rate of concrete strain change right after construction of the BWD-I test section in summer 2012, was between 0.3 $\mu\epsilon/^\circ\text{F}$ and 1.5 $\mu\epsilon/^\circ\text{F}$. As the temperature dropped in winter, around 100 days after construction, the rate of strain change increased to between 2.0 $\mu\epsilon/^\circ\text{F}$ and 3.0 $\mu\epsilon/^\circ\text{F}$.

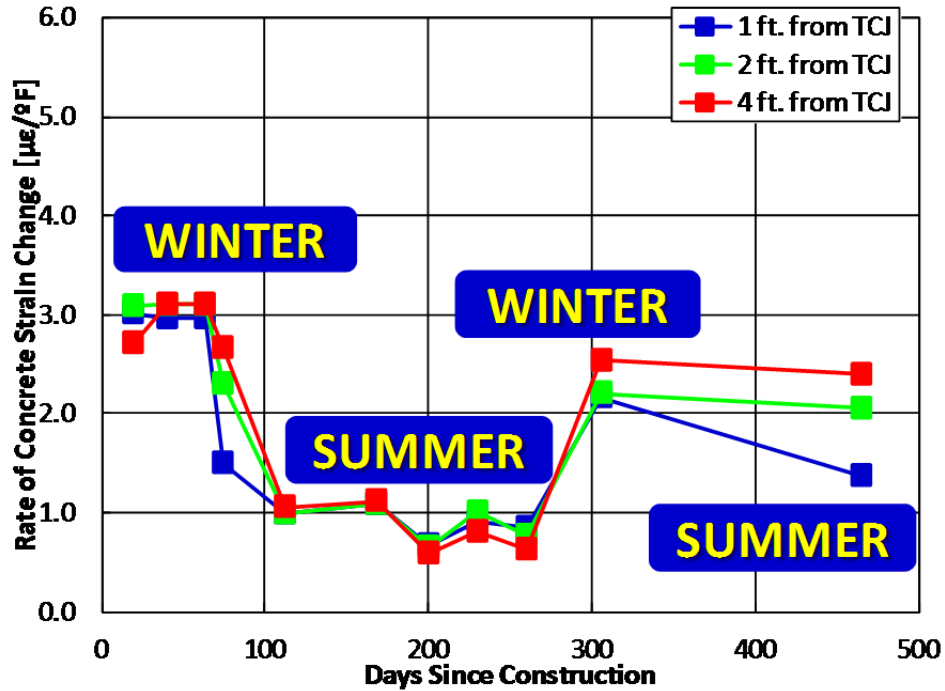


Figure 3. 61 Rate of Concrete Strain Change at LBB II TCJ - Winter Construction

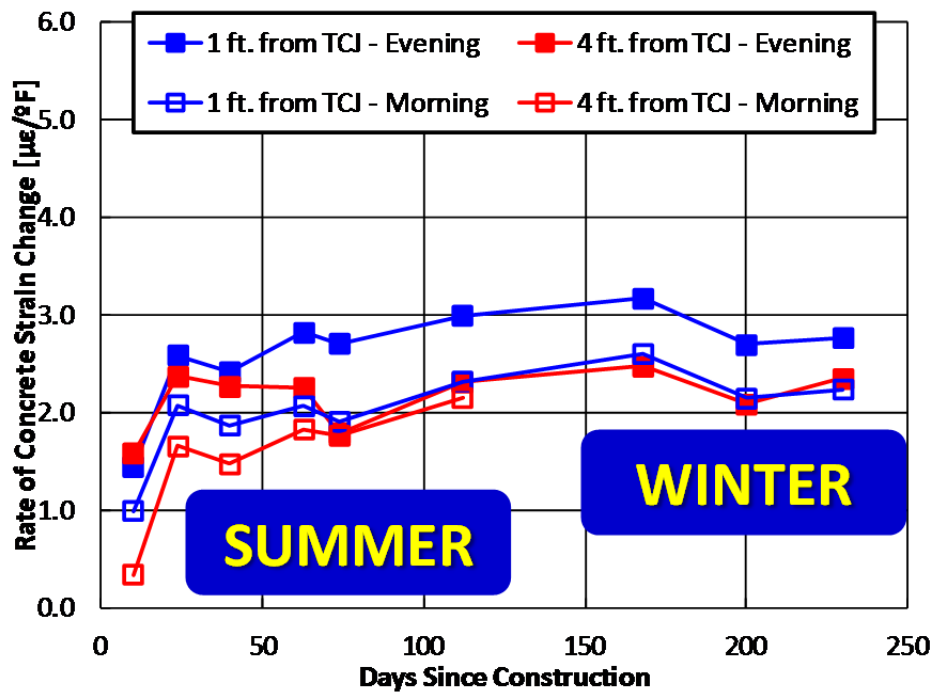


Figure 3. 62 Rate of Concrete Strain Change at BWD I TCJ - Summer Construction

It is postulated that when the concrete is placed at the TCJ during winter construction, the concrete setting temperature is low, and as the concrete temperature increases in the summer,

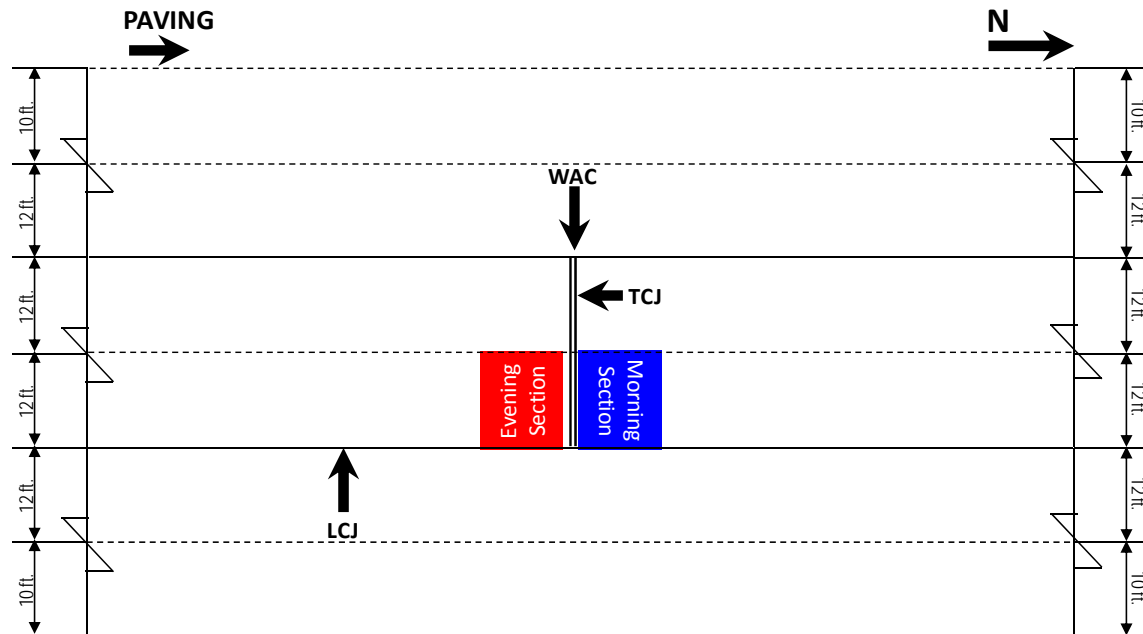


Figure 3.64 Waco Test Section Layout

SSGs at different distances from the LCJ were installed at the WAC test section. The focus of this test setup was to accurately estimate the steel strain in additional and longitudinal steel at the TCJ. Hence, a large number of SSGs were installed at different distances from the LCJ.

A total of 16 SSGs were installed at the WAC test section. Figure 3.65 provides an illustration of the test section and the SSG locations. SSGs on top of tie-bars were installed at 8 in., 34 in., 77 in., 110 in. and 132 in. from the free edge as shown in Figure 3.65. On top of longitudinal steel, SSGs were installed at 8 in., 12 in., 34 in., 77 in., 110 in. and 132 in. from the LCJ. At 8 in., 34 in., 77 in., 110 in., and 132 in. from the LCJ, SSGs were installed at two longitudinal steel on either side of the tie-bars, as shown in Figure 3.65. The SSGs towards the outside LCJ are referred to as L1, and the ones on the other side of the tie-bar are referred to as L2. The SSGs installed on top of the tie-bars at each location are denoted by the distance from the LCJ and the letter “T”.

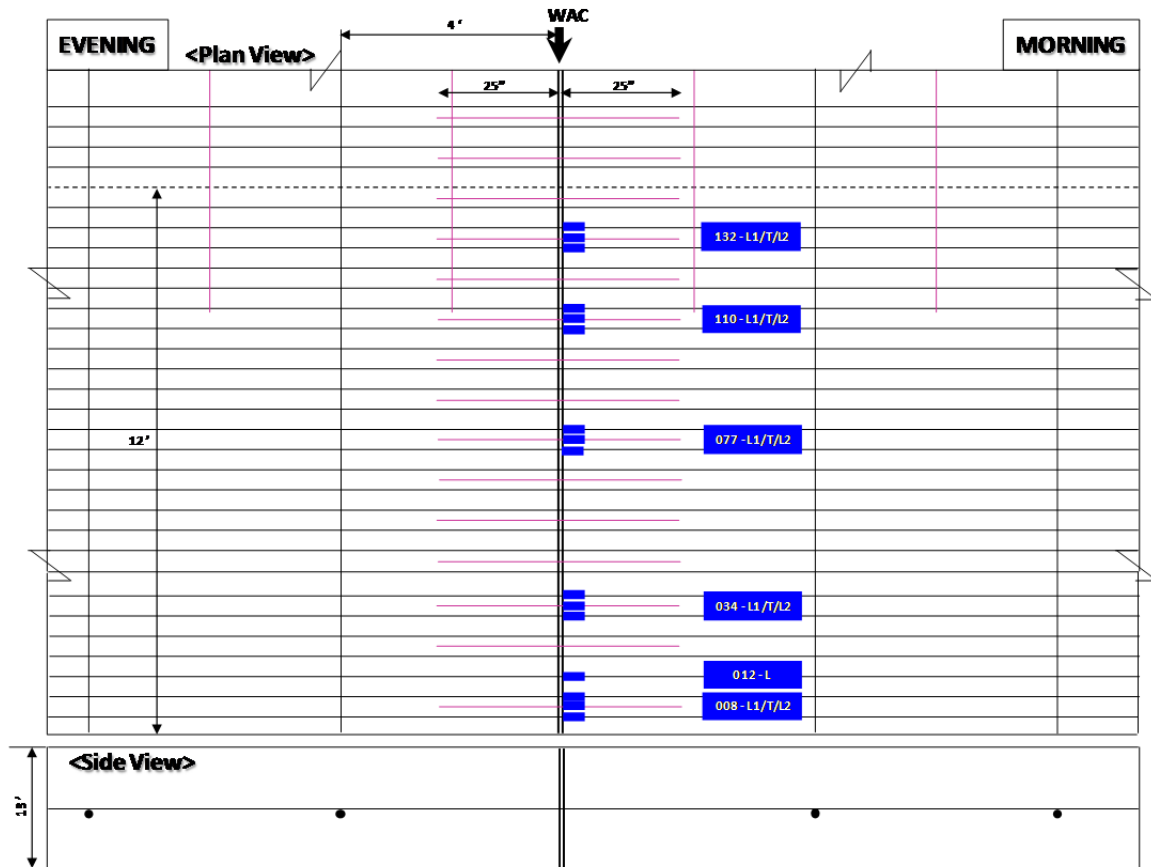


Figure 3. 65 Steel Strain Gage Installation Plan at Waco Test Location

Figure 3.66 shows the SSG installation at the WAC test section. As can be seen in Figure 3.66, SSGs were installed on top of additional and longitudinal steel right at the face of the TCJ. Also, it was noticed that the additional tie-bar diameter was smaller than the longitudinal steel diameter at this test section, as illustrated in Figure 3.67. Since the center two lanes were paved first, the SSG lead wires had to be run through the outside two lanes into the datalogger. Hence, the SSGs lead wires were run through PVC pipes and embedded into the asphalt base in the outside lanes, as shown in Figures 3.68 and 3.69.



Figure 3.66 Steel Strain Gage Installation Near Transverse Construction Joint



Figure 3.67 Tie-Bar Diameter Smaller than Longitudinal Steel



Figure 3.68 Steel Strain Gage Lead Wire Protected by PVC Pipes and Embedded in the Asphalt Base



Figure 3.69 Embedded PVC Pipes Carrying SSG Lead Wires Covered With Cold-Mix Asphalt

3.5.1 Steel Strain Behavior near TCJ in Waco District

Figures 3.70 through 3.73 provide the steel strains at 34 in., 77 in., 110 in. and 132 in. from the longitudinal construction joint [LCJ] or free edge at the time of SSG installations at this location. At each location, SSGs were installed on two adjacent longitudinal steel rebar and the additional tie-bar between them. The longitudinal steel nearer to the LCJ at each location was denoted as L1 and the longitudinal steel on the other side of the tie-bar as L2. The tie-bars were denoted by the suffix “T”.

Figures 3.70, 3.71, 3.72 and 3.73 represents steel strain variation at 34 in., 77 in., 110 in. and 132 in. from the LCJ, respectively, from May 4, 2013 to May 16, 2013. The maximum air temperature during this period varied between 79 °F and 87 °F.

As shown in Figure 3.70, the daily steel strain variation due to temperature from May 4, 2013 to May 8, 2013 at L1 and T (i.e. one longitudinal steel bar towards the longitudinal construction joint and tie-bar) at this location was limited, although the maximum air temperature went up by 10 °F, from 79 °F to 89 °F. However, during the same duration, the steel strain in the other longitudinal steel bar experienced variation with the change in temperature. During this period, the maximum steel strain at location L2 also went from tension into compression as the air temperature increased. From May 10, 2013 to May 16, 2013, the maximum air temperature increased from 81 °F to 87 °F. During this duration, the steel strains at both the longitudinal steel and additional tie-bar experienced daily strain variation with temperature. Overall the behavior of longitudinal steel L1 and tie-bar was similar but differentiated from the behavior of longitudinal steel L2. The maximum steel strain at L1, T and L2 during this analysis period was 1500 micro strains, 1200 micro strains and 750 micro strains, respectively. Thus overall the steel strain at L2 was almost 50% lower than the steel strains in the longitudinal steel at L1 and in the tie-bar.

Figure 3.71 illustrates the steel strain variation at 77 in. from the LCJ between May 4, 2013 and May 16, 2013. At this location, overall the daily strain variation of steel strain seems to be in tandem with the daily air temperature variation at all three SSG locations i.e. L1, T and L2. Also, even as the air temperature increased from 80 °F to 87 °F, the overall maximum steel strain at all three locations remained steady in tension. The maximum steel strain at L1, T and L2 recorded during this period was 1500, 1200 and 1300 micro strains. Thus, the behavior of longitudinal steel at 77 in. from the LCJ seems to be similar in terms of daily steel strain variation as well as maximum total steel strain.

Figure 3.72 shows the steel strain behavior at 110 in. from the LCJ. The variation of the steel strain in the tie-bar at this location was the least, as can be seen in Figure 3.72. The longitudinal steel at L2 experienced minimal daily strain change as well as tensile strain until May 10, 2013.

Henceforth, the steel strain at L2 went into constant compression with the air temperature increasing from 79 °F to 88 °F. The steel strain at longitudinal steel L1 went into compression from May 6, 2013 and then maintained almost constant daily strain. During this duration, maximum steel strain at L1 dropped from 220 micro strains in tension to 260 micro strains in compression. At location L2 the maximum steel strain dropped from 636 micro strains in tension to 72 micro strains in compression. At location T, the maximum steel strain varied between 680 micro strains in tension to 140 micro strains in tension. Thus, the highest drop in maximum steel strain at this location was experienced by longitudinal steel at L2.

Figure 3.73 represents the steel strain at 132 in. from the LCJ. This location is closest to the warping joint. As can be seen, the steel strains at longitudinal steel L1 and tie-bar were higher than the steel strains noticed at 34 in., 77 in. and 110 in. from the LCJ. Also, there was considerable difference between the maximum total strain of longitudinal steel at L1 and L2. The steel strain at L2 moved towards the compression side as temperature increased after May 7, 2013 and showed daily strain variation in the compressive side. However, steel strains in the longitudinal steel at L1 and in the tie-bar T were tensile side throughout. The maximum steel strain at L1 and T were 2500 and 2200 respectively. At longitudinal steel location L2, the maximum steel strain was 300 micro strains in the tensile direction and 1600 micro strains in the compressive direction.

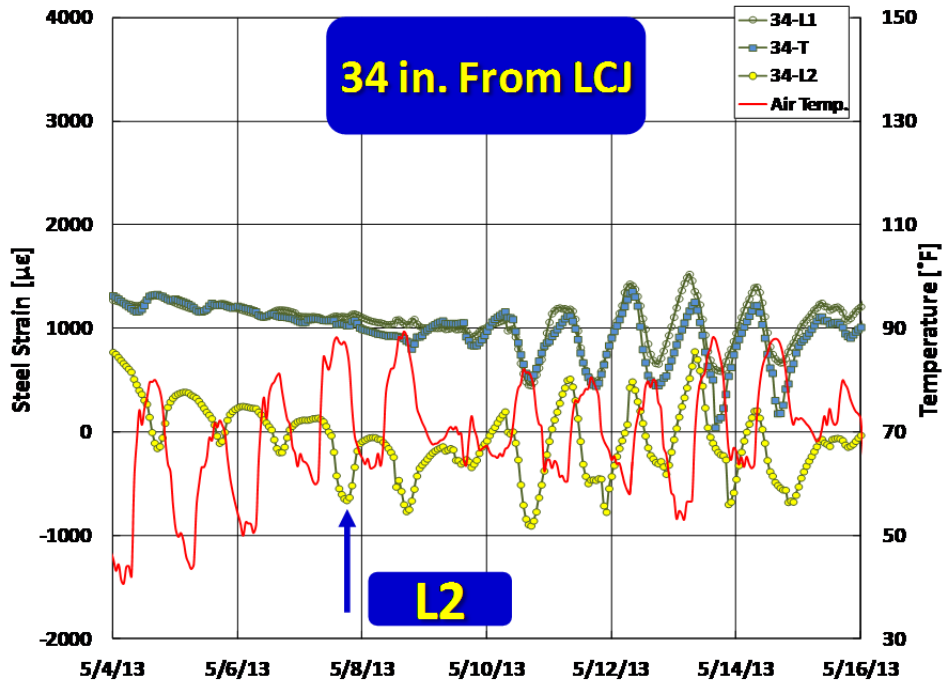


Figure 3. 70 Steel Strain at 34 in. From Longitudinal Construction Joint

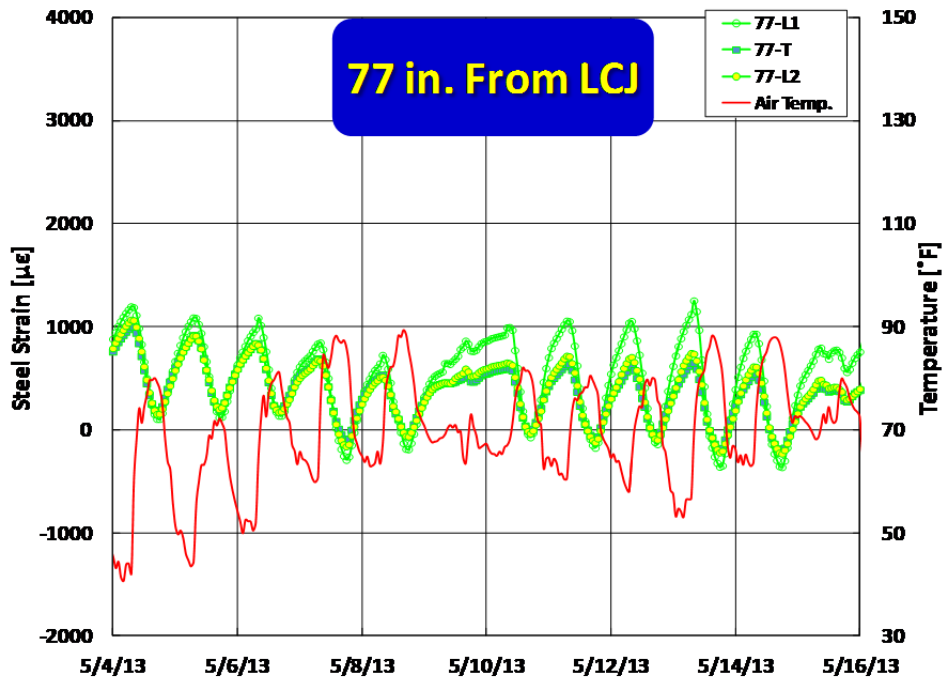


Figure 3. 71 Steel Strain at 77 in. From Longitudinal Construction Joint

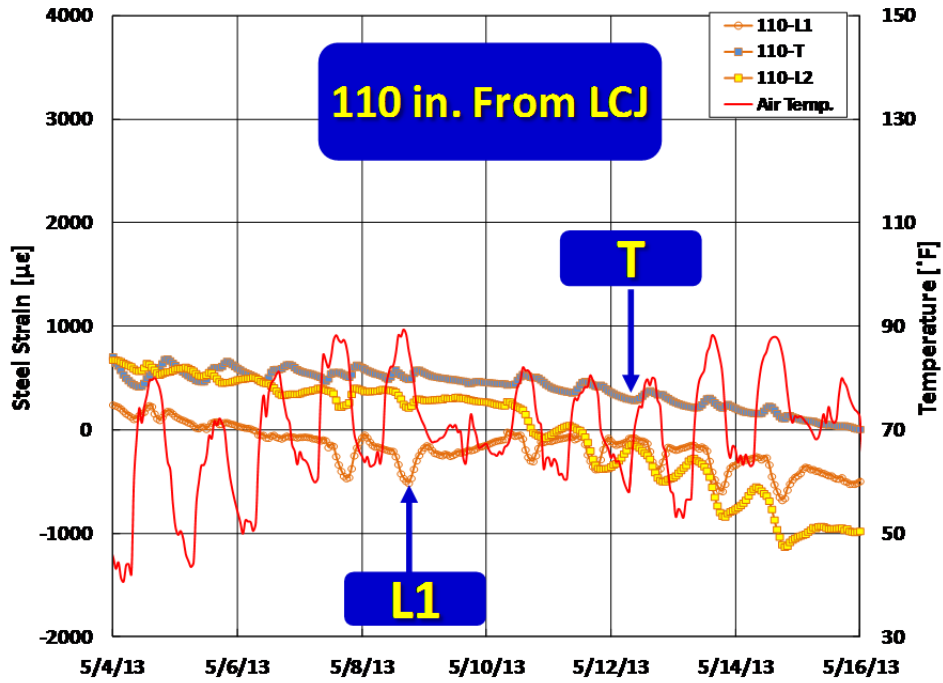


Figure 3. 72 Steel Strain at 110 in. From Longitudinal Construction Joint

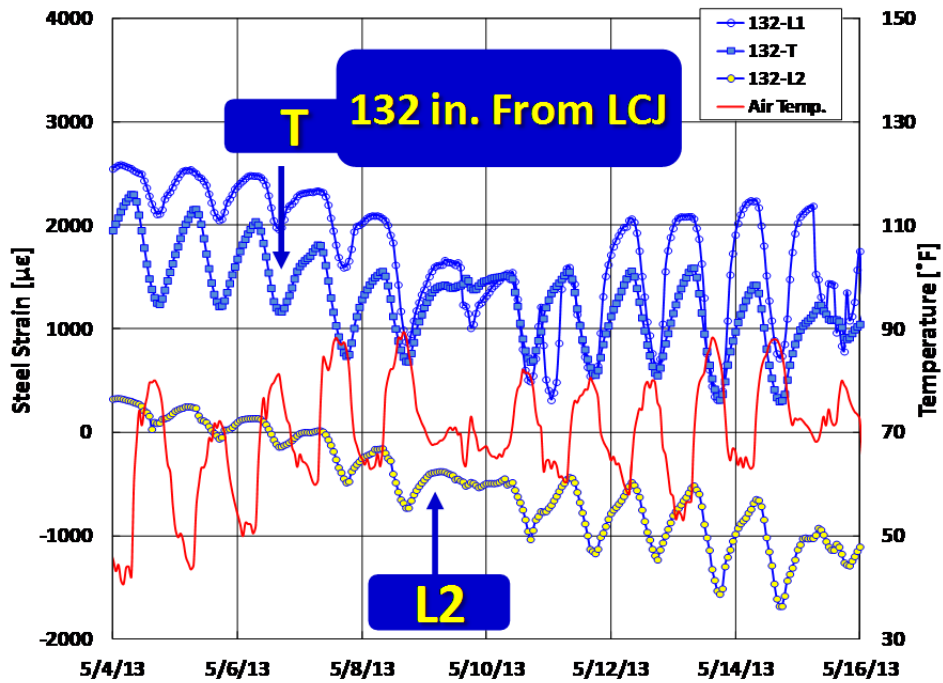


Figure 3. 73 Steel Strain at 132 in. From Longitudinal Construction Joint

From the steel strain data discussed above, it appears that the behavior of longitudinal steel and tie-bars along the width of the slab at the transverse construction joint is not uniform. Also, at a

particular location the behavior of longitudinal steel rebar at fixed spacing is not similar. Thus, the behavior of each rebar at the transverse construction joint appears to be localized and independent from the above steel strain data. Further data collection from the Waco test section will provide better understanding of the behavior of longitudinal and additional steel at the transverse construction joint.

Chapter 4 Identification of Premature Distress Mechanisms at Transverse Construction Joint in Existing CRCP

4.1 Large Joint Width Section on IH 10 in the El Paso District

Wide joint widths due to insufficient bond between steel and concrete were discussed in Chapter 2. In order to quantify the movement at the joint width, two test sections were selected in El Paso and Wichita Falls districts, and crackmeters were installed at each location.

During field surveys, two transverse construction joints on IH 10 west bound in the El Paso district near Milepost 45 were identified. These sections are denoted as ELP-I and ELP-II as shown in Figure 4.1. The distance between the two sections is 780 ft. as shown in Figure 4.2. ELP-I and ELP-II are successive TCJs, as no other TCJ was found between them. This section was built in 1995 and the slab thickness is 13 in.



Figure 4. 1 Location Map of Test Sections in El Paso District

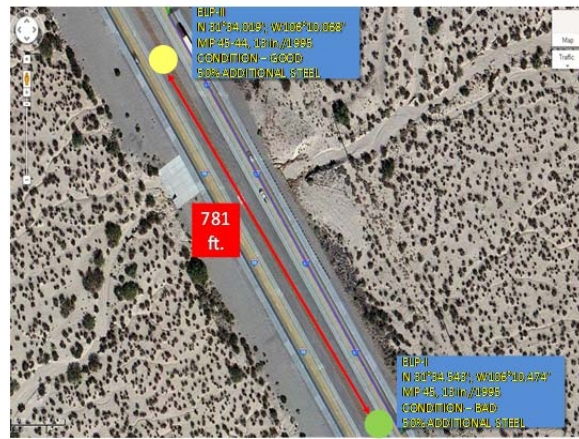


Figure 4. 2 Distance Between Consecutive Transverse Construction Joints in El Paso District

Field conditions of ELP-I and ELP-II transverse construction joints were not similar, although being successively located. As shown in Figure 4.3, at ELP-I distress had occurred at the TCJ and had been repaired by Portland cement concrete (PCP) patching. The joint width at the ELP-I TCJ was around 2 in. as shown in Figure 4.4. Contrastingly, at the ELP-II section the pavement near the TCJ was in good condition without sign of any distresses as shown in Figure 4.5. Also, the joint width at ELP-II was around 3/8 in. as illustrated in Figure 4.6.



Figure 4. 3 Distresses at ELP-I Test Section



Figure 4. 4 Wide Transverse Construction Joint Width at ELP-I Test Section



Figure 4. 5 Transverse Construction Joint Condition at ELP-II Test Section



Figure 4. 6 Narrow Transverse Construction Joint Width at ELP-II Test Section

4.1.1 ELP-I and ELP-II Test Section – Testing Plan and Gage Setup

In order to determine the difference in slab movements at ELP-I and ELP-II, crackmeters were installed at each location. A ditch was dug out near the outside shoulder of both ELP-I and ELP-II test sections and crackmeters were installed to measure the longitudinal slab movements individually. Also, a crackmeter was installed across the TCJ to measure the movement of the joint as shown in Figures 4.7 and 4.8.

For the crackmeters to measure longitudinal displacement of the individual slabs on the two sides of the TCJ, one end of the crackmeters was attached to anchors embedded into the concrete and the other end was connected to an invar bar with low temperature sensitivity. For the crackmeter across the joints, the ends of the crackmeter were connected to slabs on either side with the use of anchors embedded into the slab as shown in Figures 4.7 and 4.8.



Figure 4. 7 Crackmeter Installation Across Transverse Construction Joint at ELP-I Test Section

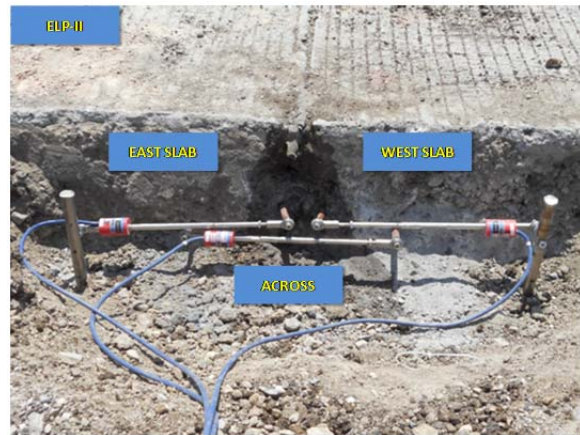


Figure 4. 8 Crackmeter Installation Across Transverse Construction Joint at ELP-II Test Section

4.1.2 Crackmeter Data from IH 10 in the El Paso District

Figures 4.9 and 4.10 represent the movement of the transverse construction joint on the day of placement of crackmeters and seven days later, respectively, for ELP-I TCJ described as the Bad Section. Similarly, Figures 4.11 and 4.12 represent the transverse construction joint movement at ELP-II TCJ mentioned as the Good Section in this discussion, over the same period of time.

As shown in Figure 4.9, the air temperature dropped from 85 °F to 75 °F from 11:30 p.m. on July 12, 2012 to 9:00 a.m. on July 13, 2012. During this period, the movement of the joint recorded by the crackmeter was 25 mils, which implies that with the decrease in temperature of 10 °F, the joint width increased by 25 mils. Similarly, Figure 4.10 depicts the movement of the transverse construction joint seven days after installation of the gages. The temperature dropped from 95 °F at 6:45 p.m. on July 19 to 75 °F at 9:07 a.m. on July 20, 2012. During this phase of 20 °F drop in air temperature, the joint width experienced a movement of 28 mils. Thus the average movement of the joint at ELP-I was 1.95 mils per °F. During the same duration, the movement of the TCJ at

ELP-II without distresses and narrow joint width is depicted in Figures 4.11 and 4.12. According to the data available, the average joint movement at the ELP-II location is 0.075 mils per °F.

Thus from the crackmeter data available it can be determined that the movement at the ELP-I transverse construction joint was 25 times more than the movement of the ELP-II joint. These two construction joints being at successive locations were built around the same period of time. However, large movement of the joint at one section indicates absence of a good bond between the longitudinal steel and concrete at this joint. The successive large scale movements of the individual slabs due to temperature variation, on either side of the joint could have led to the occurrence of distresses at the ELP-I transverse construction joint.

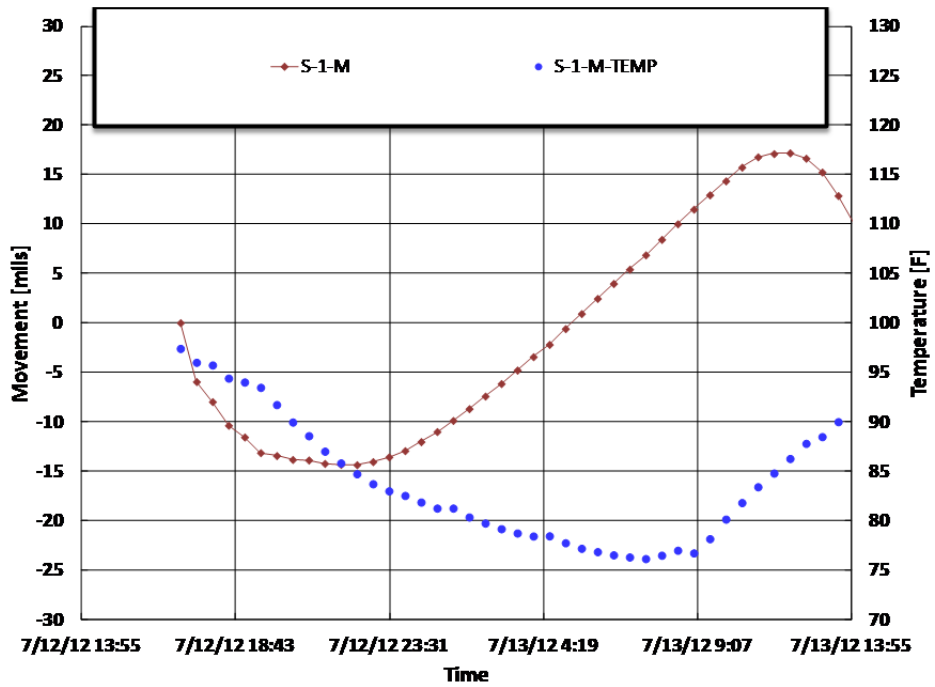


Figure 4. 9 Movement of Bad Transverse Construction Joint on IH 10 in El Paso – Day 1

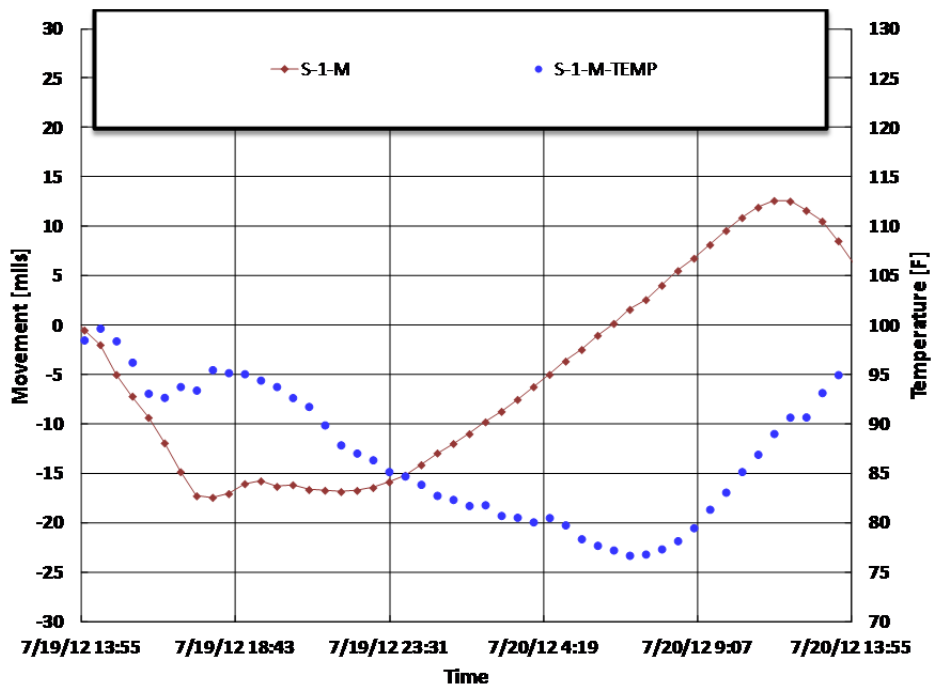


Figure 4. 10 Movement of Bad Transverse Construction Joint on IH 10 in El Paso – Day 7

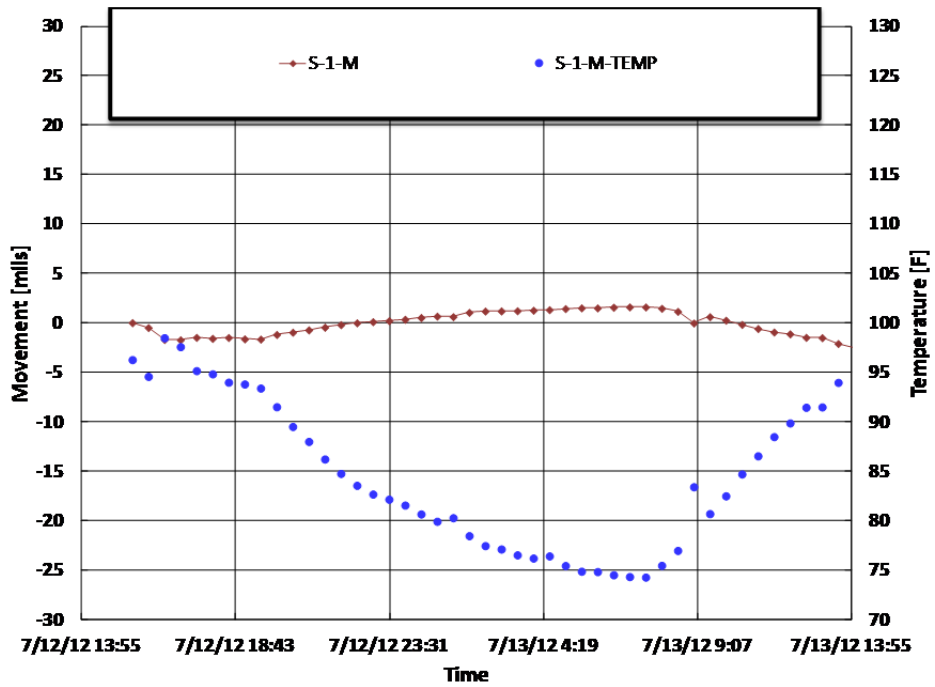


Figure 4. 11 Movement of Good Transverse Construction Joint on IH 10 in El Paso – Day 1

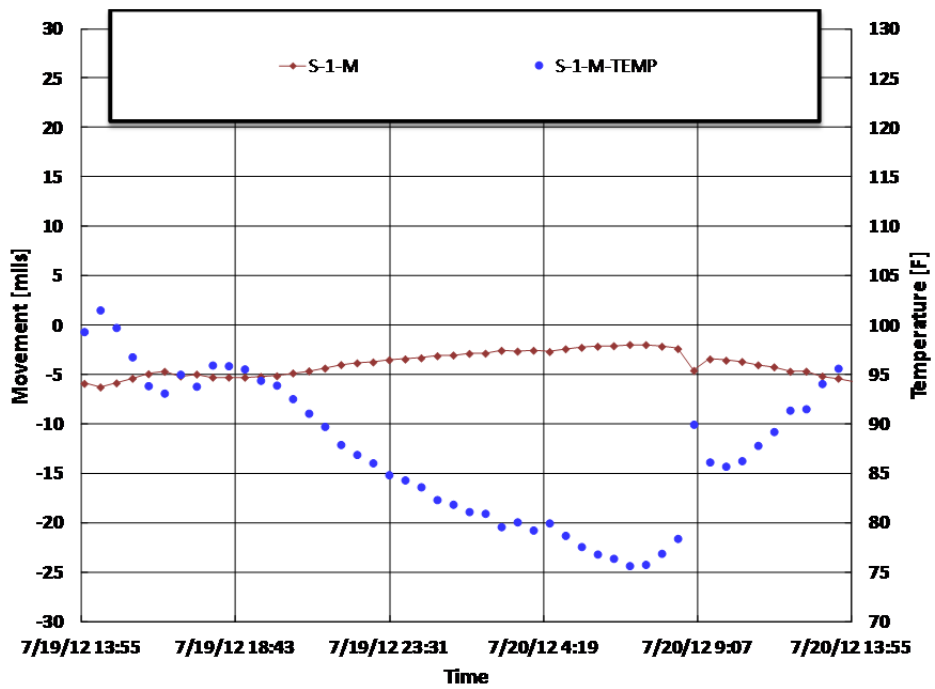


Figure 4. 12 Movement of Good Transverse Construction Joint on IH 10 in El Paso – Day 7

4.2 Large Joint Width Section on IH 40 in Childress District

Debonding between steel and concrete at the transverse construction joint and wide joint movement due to temperature variation were observed on IH 40, MP 163, west bound near Shamrock in the Childress district. The location of the test section is shown in Figure 4.13 and this section is referred as the CHS test section. The CRCP slab thickness at this section is 12 in., as shown in Figure 4.14.



Figure 4. 13 Location Map of Test Section in the Childress District



Figure 4. 14 Concrete Disintegration Near Transverse Construction Joint at Childress District Test Section

The test section on IH 40 in the Childress district exhibits severe distresses near the transverse construction joints, as shown in Figures 4.15 and 4.16. As discussed earlier, CRCP segments in this area were removed due to the expansion of lime-stabilization of gypsum bearing soil. The distresses observed seem to be more concentrated at the junction of the transverse and longitudinal joint in both the inside and outside lanes. Also, both the lanes seem to be constructed at the same time since the transverse construction joint runs through both the lanes at the same location.



Figure 4. 15 Distresses Near Transverse and Longitudinal Construction Joint Intersection at Childress Test Section



Figure 4. 16 Distresses near Longitudinal Construction Joint at Childress Test Section

The crack spacing at the transverse construction joint were measured at this location in the morning and evening on November 2, 2012, as shown in Figures 4.17 and 4.18. In the morning the joint width was $\frac{1}{2}$ in. and in the evening the joint width decreased to $\frac{3}{8}$ in. This implies that during the day when ambient temperature, and consequently the concrete temperature, increased, the slabs on both the sides of the TCJ expanded, resulting in reduced joint width. With decrease in temperature during the night, the joint width again increased to $\frac{1}{2}$ in. for the same temperature variation. Also, the joint spacing at this TCJ was noted in February 2011 as 1 in. and again in March 2013 as $\frac{7}{8}$ in., as shown in Figures 4.19 and 4.20, respectively. This considerable variation in longitudinal movement of individual slabs at the TCJ needed to be investigated.



Figure 4.17 Transverse Construction Joint Width in the Morning at Childress Test Section

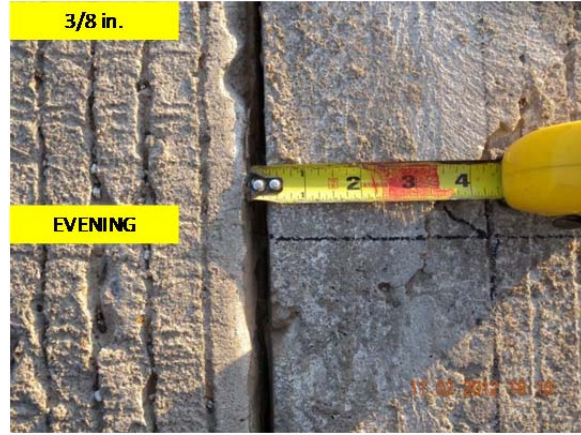


Figure 4.18 Transverse Construction Joint Width in the Evening at Childress Test Section



Figure 4.19 Transverse Construction Joint Width at Childress Test Section in February 2011

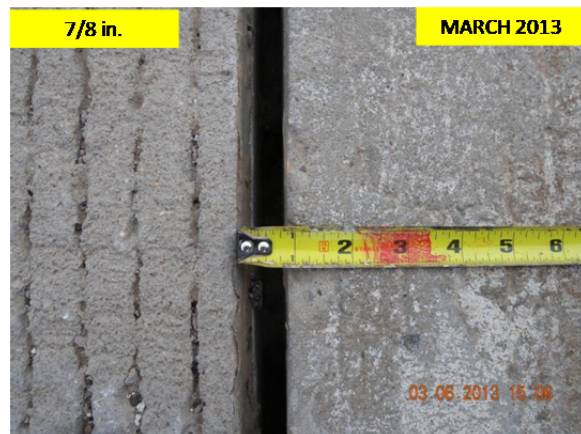


Figure 4.20 Transverse Construction Joint Width at Childress Test Section in March 2013

On removing the soil from the outside shoulder (North Side) and inside shoulder (South Side), concrete deterioration near the transverse construction joint was observed as shown in Figure 4.21 and 4.22.

Also, while closely observing the longitudinal and additional steel through the depth of the transverse construction joint, concrete was found to be protruding from the face of the slab at the transverse construction joint as shown in Figure 4.23.



Figure 4. 21 Concrete Deterioration at Inside Shoulder of TCJ – Childress Test Section



Figure 4. 22 Concrete Deterioration at Outside Shoulder of TCJ – Childress Test Section



Figure 4. 23 Steel Slipping Out of Concrete at Transverse Construction Joint

4.2.1 IH-40 Test Section in Childress – Testing Plan and Gage Setup

Crackmeters were installed at the mid-depth of the slab on the north side and south side of the transverse construction joint at the CHS test section. At each location, crackmeters were installed individually to the two slabs at the transverse construction joint and one crackmeter was installed across the joint. The anchors embedded into the concrete to attach the two ends of the crackmeter installed across the joint were also used to attach one end of the crackmeters connected to the individual slab on each side, as shown in Figures 4.24 and 4.25. This setup of gage installation ensures that the movement of the individual slabs is manifested into the movement at the transverse construction joint recorded by the crackmeter.



Figure 4. 24 Crackmeter Installation at Outside Shoulder – Childress Test Section



Figure 4. 25 Crackmeter Installation at Inside Shoulder – Childress Test Section

4.2.2 Crackmeter Data from IH 40 in Childress District

MIRA 3-D scanning was conducted at this location as depicted in Figure 4.26, which revealed delamination under the longitudinal steel. However, this delamination was observed only near the transverse construction joint and did not extend longitudinally through the entire length of the pavement, as shown in Figure 4.27.



Figure 4. 26 Location of MIRA 3-D Section At TCJ on IH 40 in Childress

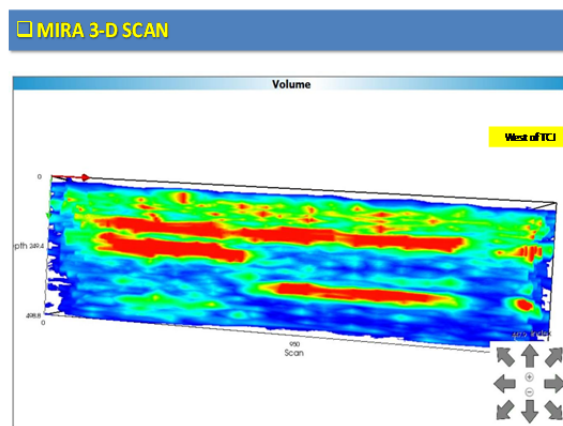


Figure 4. 27 Delamination Near Transverse Construction Joint on IH 40 in Childress

Figure 4.28 represents the movement of the individual slabs denoted as “EAST-1” and “WEST-1” at the outside shoulder location. The movement of the joint itself at the inside shoulder location is denoted as “MID-1”. The air temperature at this location is denoted as “EAST-T-1”.

The slab movement data was collected from November 2, 2012 to January 1, 2013. As can be seen, with decrease in the overall air temperature, the “EAST-1” and “WEST-1” slabs go into compression. Also, the “MID-1” movement goes into tension which means that as the temperature decreases and individual slabs go into compression, the transverse construction joint between them opens up and the joint width increases. The rate of individual slab movements with temperature at this location is 5.4 mils per °F for “EAST-1” slab and 6.4 mils per °F for “WEST-1” slab. The movement across the joint during this period was 14.4 mils per °F.

Figure 4.29 depicts the longitudinal slab movement at the transverse construction joint at the inside shoulder location. The overall longitudinal slab movement followed the same behavior as the transverse construction joint on the outside shoulder described above. The individual slab movement measured on this side for the “EAST-2” and “WEST-2” slabs was 6.2 mils per °F and 7.2 mils per °F respectively. The rate of movement across the transverse joint at this location was 14.8 mils per °F.

The crackmeter movement data discussed above provided good correlation between the individual longitudinal slab movements and movement across the transverse construction joint. The average joint movement at this location from the gages installed on the inside and outside shoulder can be computed as 14.6 mils per °F, which is quite high.

In the presence of such large longitudinal movement at the transverse construction, the occurrence of distresses near the longitudinal and transverse construction joint with relative movement of slab due to temperature variations is unavoidable.

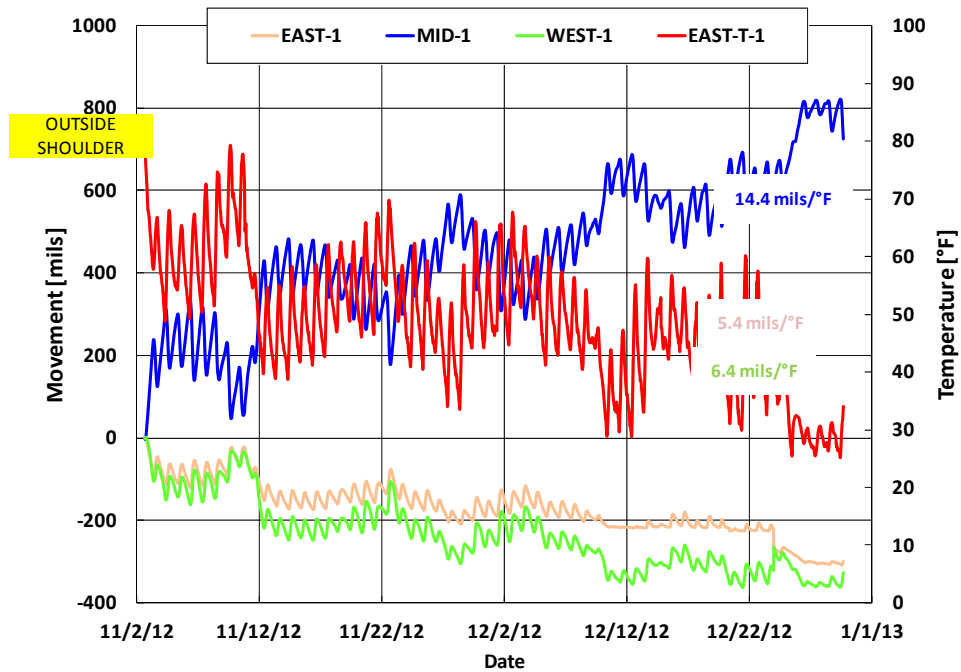


Figure 4. 28 Slab and Joint Movement at Transverse Construction Joint on IH 40 in Childress – Outside Shoulder

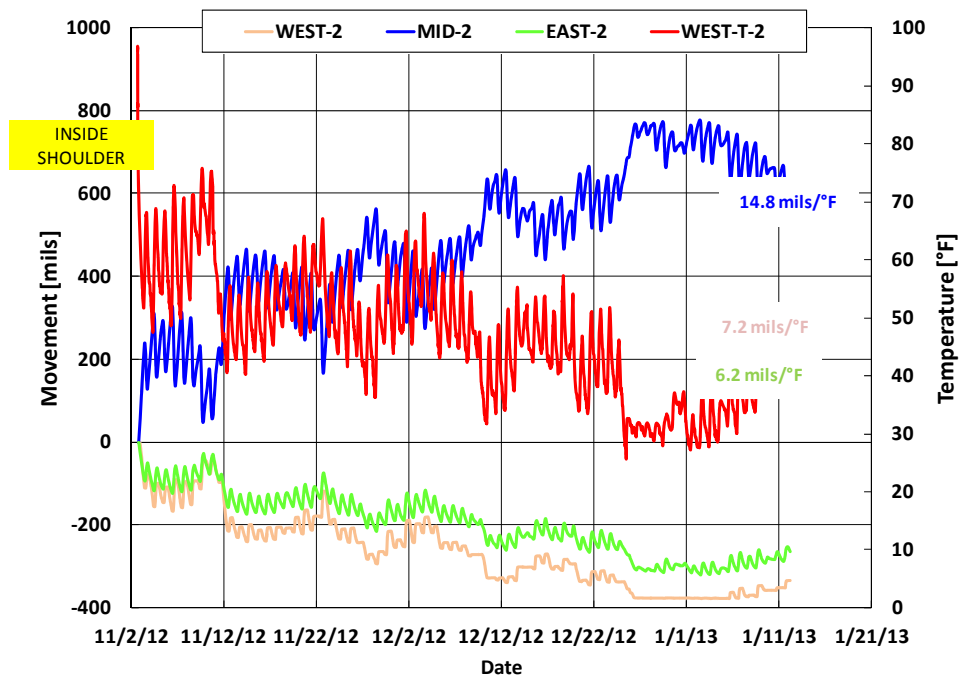


Figure 4. 29 Slab and Joint Movement at Transverse Construction Joint on IH 40 in Childress – Inside Shoulder

4.3 Construction and Material Issue at Transverse Construction Joint

As discussed in Chapter 2, a majority of the distresses in CRCP are due to construction or material related issues. Also, the construction of TCJs is different than usual CRCP construction. Since construction near the TCJ is not possible with the paving machine, concrete placement is carried out manually. Compaction is also carried out using hand-held vibrators in this region. Hence, understanding the effect of manual placement and hand compaction on the concrete near the TCJ would give a better understanding of whether the distresses occurring in this area are related to construction practices. Since the concrete near the TCJ is usually the first or last batch of the day, there could be a difference in the concrete quality at the TCJ as compared to the rest of the pavement. Also, at locations where concrete is placed at high temperatures, de-bonding of concrete and longitudinal steel at the TCJ could lead to problems at the TCJ. In order to understand the above mentioned mechanisms of premature distresses related to construction and/or material issues, field and laboratory testing conducted and results inferred are discussed below.

4.3.1 Construction Practice at Transverse Construction Joint

Figures 4.30 through 4.35 shows various stages of construction at the BWD-I transverse construction joint, in the morning section on IH 20 in the Brownwood district. As can be seen in the pictures, the first concrete truck arrived at 9. 30 a.m. on August 16, 2012. Concrete was placed using shovels in the area near TCJ, and a hand-held vibrator was used for compaction. How far the vibrator is effective in compaction in this area due to the presence of additional steel, cannot be stated. Construction in this area lasted more than one and a half hours, and the concrete started to harden; this hardening caused the auto-float used for finishing to get stuck in the concrete, as can be seen in Figure 4.32. Also, in the absence of any formwork on the sides, pavement on the inside edge looks uneven compared to the rest of the pavement.



Figure 4. 30 First Truck of Concrete Arrives at BWD-I Test Section



Figure 4. 31 Manual Placement of Concrete At the Transverse Construction Joint – Morning



Figure 4. 32 Auto-Float Stuck in Concrete Due to Mis-alignment of Paver



Figure 4. 33 Manual Finishing of Concrete at BWD-I Test Section



Figure 4. 34 Finishing Process Becomes Difficult as Concrete Hardens



Figure 4. 35 Uneven Slab Edge

4.3.2 Concrete Properties near the Transverse Construction Joint

In order to evaluate the difference between the concrete near the transverse construction joint, which is constructed manually, and the rest of the pavement, concrete cores were taken at test sections. Two test sections, one each in Brownwood and Wichita Falls districts were selected to determine the concrete properties by comparing the unit weight and modulus of elasticity of concrete samples near and away from the transverse construction joint. The section on IH 20 in Brownwood was a relatively recently constructed section (2012) as compared to the section on US 287 in Wichita Falls, which was constructed in 1970.

4.3.2.1 Coring on IH 20 in the Brownwood District

To identify the difference between the quality of concrete near and away from the transverse construction joint or the presence of voids in concrete at TCJ due to insufficient compaction, coring was undertaken at the TCJ on the BWD-II section. The cores were taken at two locations near the TCJ and one location away from the TCJ, as shown in Figure 4.36.

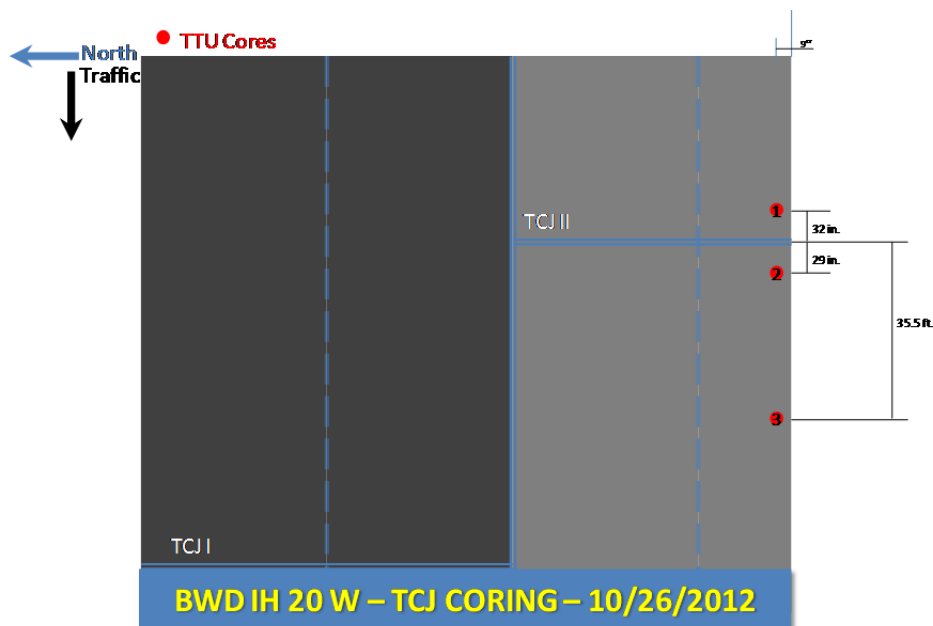


Figure 4. 36 Coring Locations at BWD-II Transverse Construction Joint

Before coring, the MIRA Tomographer was used to estimate the location of the steel in concrete. Figure 4.37 presents the scan from the MIRA Tomographer at Location 1 on the morning construction side on IH 20 in Brownwood. This location is at 32 in. from the TCJ. In addition to the red areas representing the longitudinal steel, certain voids appear in the top 4 in. of the concrete slab at this location. Similarly, the MIRA Tomographer was used to scan the pavement at 29 in. from the TCJ in the evening construction section at BWD-II. Again, the presence of voids on the top 4 in. was observed at this location, as shown in Figure 4.38. MIRA Tomographer was used again at 35.5 ft. from the TCJ on the evening construction side of BWD-II. The MIRA scan is shown in Figure 4.39. The concrete appears to be free of any voids. Also, while coring at location 1 and 2 near the TCJ, the coring team was able to remove cores right off after coring to the base. However, at Location 3, as shown in Figure 4.39, after coring through the depth of the slab, the core had a good bond with the asphalt base below and hence had to be struck with a hammer to remove the core.

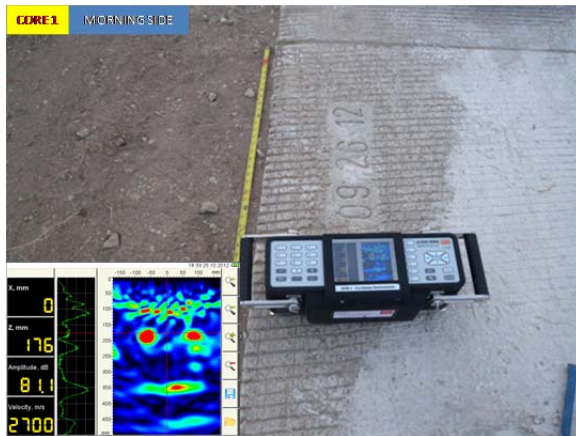


Figure 4. 37 BWD-II Coring Location 1 and MIRA Scan

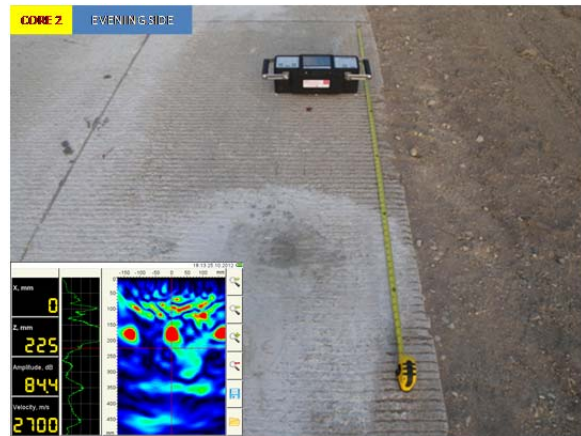


Figure 4. 38 BWD-II Coring Location 2 and MIRA Scan

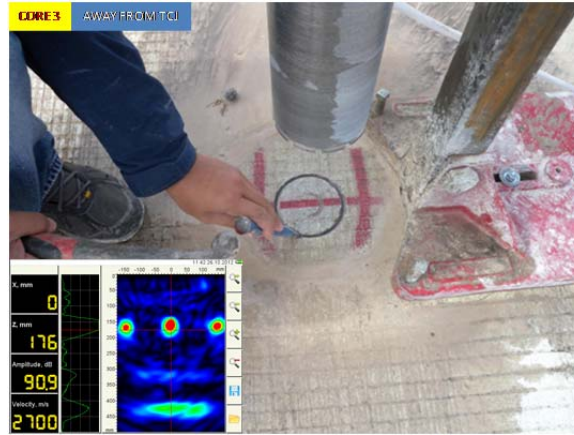


Figure 4.39 BWD-II Coring Location 3 and MIRA Scan

Coring was conducted at these three locations on October 26, 2012 and the unit weight of the cores was evaluated. The dynamic modulus of the cores was evaluated using Free-Free Resonance Core Tester. As can be seen in Figure 4.40, the unit weight of cores near the construction joint in both the evening and morning construction sections are lower by more than 1% compared to the core away from the TCJ. Figure 4.41 shows the Dynamic Young's Modulus of the three cores. The Dynamic Modulus of the core in the morning construction section is almost 9% less and of the evening construction section is around 5% less than the core taken away from the TCJ. It should be noted that there is a significant difference in the Dynamic Young's modulus of cores in the evening area near the TCJ and 35.5 ft. from the TCJ, even though concrete placement at both these locations took place on the same day.

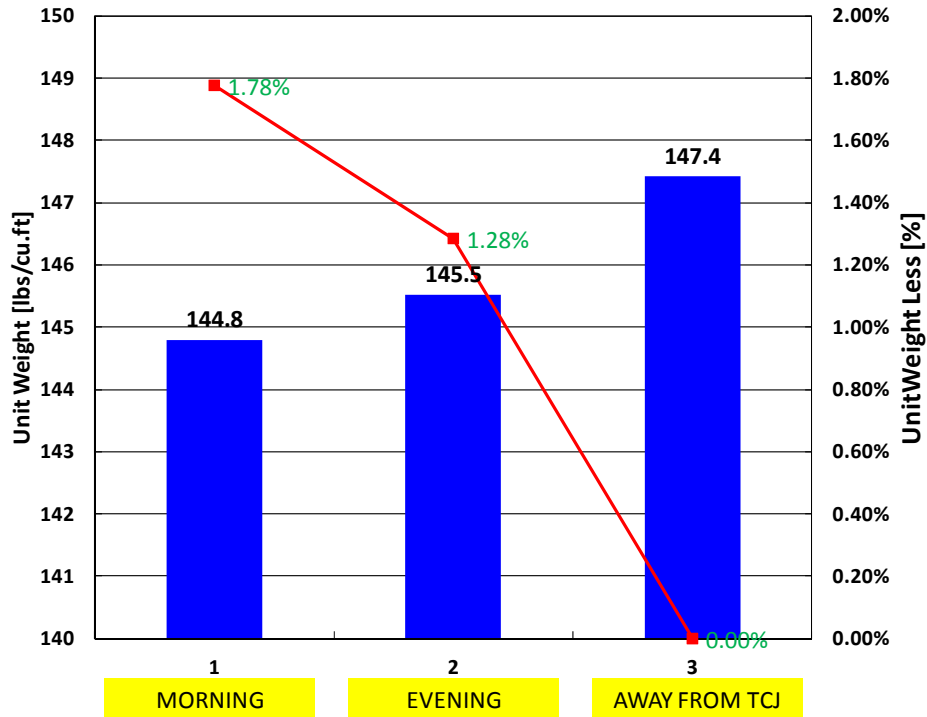


Figure 4.40 Unit Weight of Cores Taken at BWD-II Section

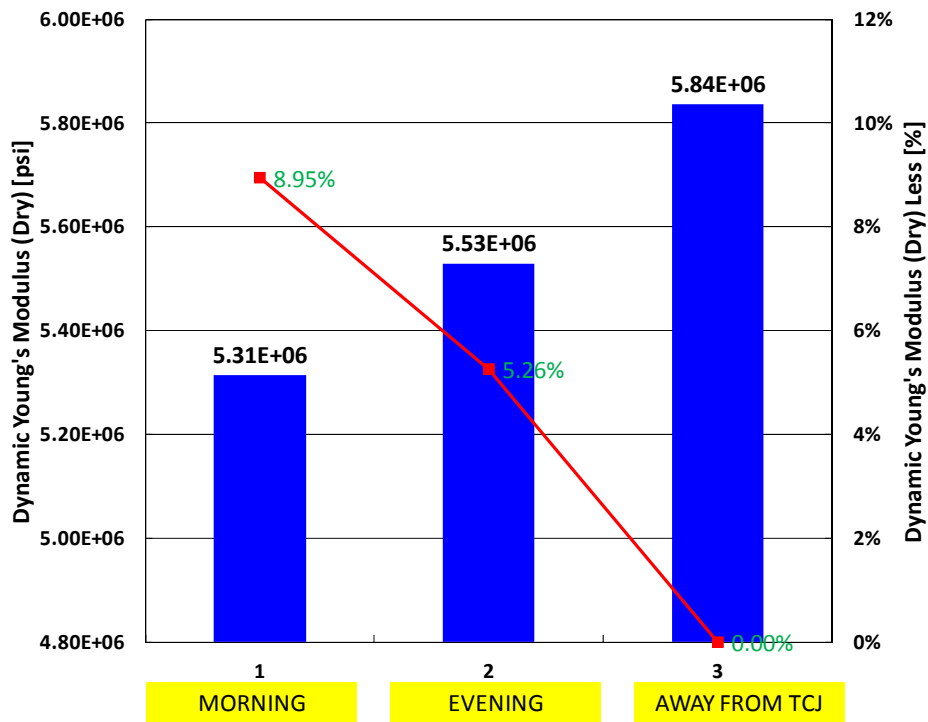


Figure 4.41 Dynamic Young's Modulus (Dry) of Cores Taken at BWD-II Section

4.3.2.2 Coring on US 287 in Wichita Falls District

As shown in Figure 4.42, coring was conducted at three locations on US 287 in the Wichita Falls district on November 14, 2012. A number of voids were observed on the concrete pavement surface. Figures 4.43 through 4.45 represent the MIRA Tomographic scans and the cores taken from two bad sections and one good section at this location. Voids that appear in the MIRA Tomographic scans as red areas can also be seen in the cores as represented for the sections B1 and B2 in Figures 4.43 and 4.44, respectively. Figure 4.45 represents the MIRA scan and core taken at the location with no voids.

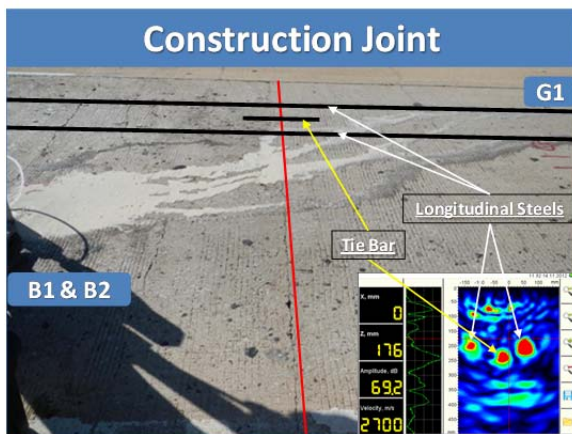


Figure 4.42 Surface Condition of Coring Location on US 287 in Wichita Falls

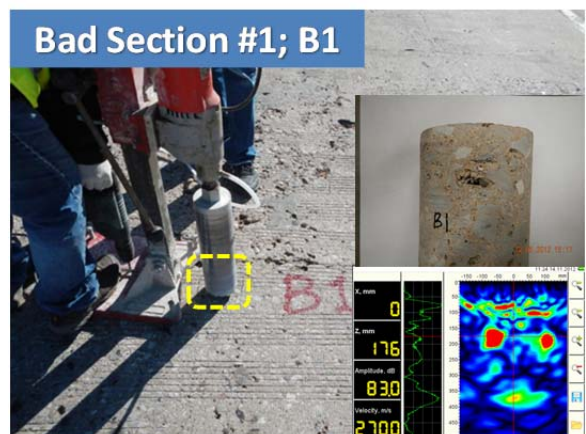


Figure 4.43 Core Taken at Location B1 on US 287 in Wichita Falls

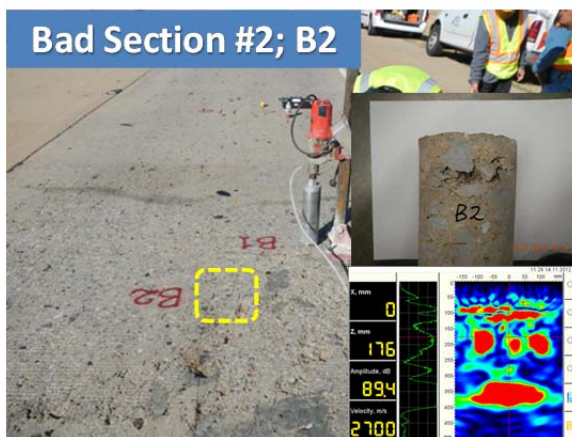


Figure 4.44 Core Taken at Location B2 on US 287 in Wichita Falls



Figure 4.45 Core Taken at Location G1 on US 287 in Wichita Falls

The results for Unit Weight and Young’s Modulus testing carried out at the three locations on US 287 in Wichita Falls district are presented in Figures 4.46 and 4.47 respectively. As shown in Figure 4.46, the unit weights of cores at B1, B2 and G1 location are 143 lbs./cu. ft., 141 lbs./cu. ft. and 147 lbs./cu. ft. respectively. The unit weight of core B1 is 2.80% lower and of B2 is 3.56% lower than the core from the good location G1 with no voids. The difference in Dynamic Young’s Modulus of Elasticity between the locations with and without voids in the cores is significant, as shown in Figure 4.47. The Dynamic Young’s Modulus of cores B1, B2 and G1 are 5.2 million psi, 3.08 million psi and 5.4 million psi respectively. The Dynamic Young’s modulus of the core B2 with voids is 43.75 lower than that of the core G1, which had no voids.

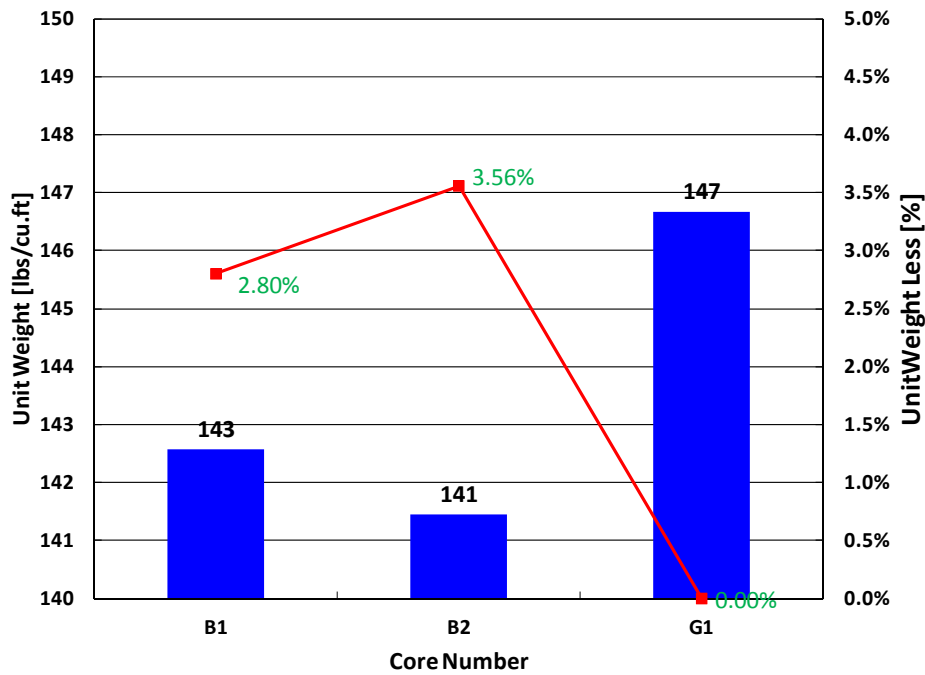


Figure 4. 46 Unit Weight of Cores Taken on US 287 in Wichita Falls

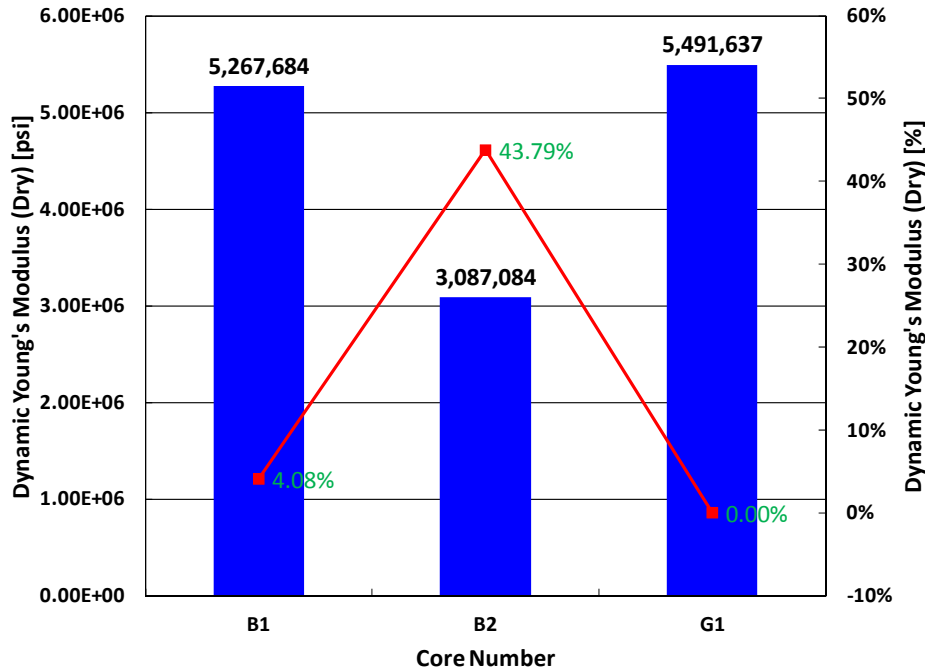


Figure 4. 47 Dynamic Young's Modulus (Dry) of Cores Taken on US 287 in Wichita Falls

From the investigations conducted at the sections in Brownwood and Wichita Falls discussed above, it can be stated that there is considerable difference between the concrete quality at the transverse construction joint and the concrete away from the slab. The presence of voids above the depth of the steel in Brownwood and on the surface of the slab in the Wichita Falls district as depicted in the MIRA tomography scans is a clear indication of insufficient compaction using the hand-held vibrator at the transverse construction joint. The difference in unit weight between the cores in the good and bad sections validates the presence of voids in concrete.

4.4 Coefficient of Thermal Expansion and Dynamic Modulus of Elasticity at Y and Narrow Crack Sections

Figure 4.48 represents Y-cracks observed on US 81 in Montague County in the Wichita Falls District. This CRCP section was built in 1972 with 8-in. slab thickness and 4-in. asphalt stabilized base. As can be seen, although this section is fairly old and well over its design life, the presence of Y-cracks has not led to occurrence of distresses yet. MIRA system was used to scan the Y-cracks on this section. As illustrated in Figure 4.49, the Y-cracks were observed at the

exact location of the transverse steel. Also, the Y-cracks do not appear to be tight and hence could be accounted for as early age Y-cracks. Although these Y-cracks seemed to have occurred at an early age, there are no signs of distresses due to Y-cracks in this section.



Figure 4. 48 Y-cracks on US 287 in the Wichita Falls District



Figure 4. 49 Y-Crack on Top of Transverse Steel on US 287 in the Wichita Falls District

Figures 4.50 and 4.51 illustrate Y-cracks surveyed on IH 35 in the Laredo District. This section was constructed in 2002. The pavement thickness is 10 in. As can be seen in Figure 4.51, the Y-cracks in this section have caused formation of certain distresses that may exhibit increased severity in the near future. The investigation of truck traffic in this section revealed the applications of over-weight trucks, which could have caused those distresses.



Figure 4. 50 Y-Crack on IH 35 in the Laredo District



Figure 4. 51 Distress Due to Y-Crack on IH 35 in the Laredo District

Figures 4.52 and 4.53 represent narrowly spaced transverse cracks on US 287 in the Wichita Falls district. The cracks appear to be later age. There is no evidence of distresses due to the narrowly spaced cracks in this section.



Figure 4. 52 Narrow Cracks on US 287 in the Wichita Falls District



Figure 4. 53 Narrow Cracks on US 287 in the Wichita Falls District

Figures 4.54 and 4.55 represent narrowly spaced cracks on IH 45 in the Dallas district. This section was built in 1975. The pavement thickness is 10-in. The subbase and subgrade for this section comprise of 6-in. cement stabilized base and 6-in. lime treated subgrade respectively.



Figure 4. 54 Distress Due to Narrow Cracks on IH 45 in the Dallas District



Figure 4. 55 Distress Due to Narrow Cracks on IH 45 in the Dallas District

Y and narrow transverse cracks were identified in Amarillo, Laredo, Dallas and Wichita Falls districts. The narrow and Y-cracks were detected to be on top of transverse steel using MIRA

tomography. Also, only Y-cracks in Laredo district on IH 35 and in Dallas district on IH 45 were identified to be showing signs of distress. The Y-crack widths on US 81 in Wichita Falls district were noted to be wide. But there were no signs of any present or potential distresses in this section.

Coring was conducted at Y and Narrow Transverse crack locations in Amarillo, Laredo and Dallas districts. Coefficient of thermal expansion and dynamic modulus of elasticity testing was conducted on the concrete cores and the results are enlisted in Table 4.1. As can be seen in Table 4.1, the coefficient of thermal expansion of concrete in Laredo and Dallas test sections is 3.83 $\mu\epsilon/^\circ\text{F}$ and 4.13 $\mu\epsilon/^\circ\text{F}$ respectively. In spite of having a lower coefficient of thermal expansion, narrow and Y-cracks in these sections were in poor condition and would lead to distress formation in the near future. It also has to be noted the traffic volume on both these sections is high including high volume of truck traffic. As a result, Y-crack and narrow transverse cracks at these two locations that are leading to distresses are more due to increased heavy traffic load.

Table 4. 1 CoTE and Dynamic Modulus of Elasticity at Y and Narrow Transverse Cracks

District	Highway	Crack Type	CoTE [$\mu\epsilon/^\circ\text{F}$]	Dynamic Modulus of Elasticity [psi]
AMARILLO	IH 40	Y-crack	4.83	5,793,270
LAREDO	IH 35	Y-crack & Narrow Crack	3.83	6,350,400
DALLAS	IH 45	Narrow Crack	4.13	6,581,190

4.4.1 Y-Cracks on IH 10 in El Paso District

Y-cracks were also identified on IH 10 near mile post 20 in El Paso district at two locations identified as Location-1 and Location -2 henceforth. As shown in Figure 4.56, on the surface the Y-crack width at Location-1 looked tight although there was evidence of small spalling right where the y-crack is formed as can be seen in the inserted picture in Figure 4.56. Coring was conducted at this section. The core shown in Figure 4.57 revealed that the Y-crack extended throughout the depth of the slab. Also, the Y-crack width at the top appeared wider than at the bottom of the core. The formation of the Y-crack as can be seen in Figure 4.57 was at the intersection of the longitudinal and transverse steel.

The Y-crack detected at Location-2 on IH 10 in El Paso district showed no distress formation or signs of spalling on the surface as shown in Figure 4.58. Again, after conducting coring at the Y-crack Location-2, the Y-crack was found to be formed at the intersection of longitudinal and transverse steel as shown in Figure 4.59.



Figure 4. 56 Coring Conducted at Y-crack Location on IH 10 in El Paso District – Location 1



Figure 4. 57 Y-crack at the Intersection of Longitudinal and Transverse Steel on IH 10 in El Paso District – Location 1



Figure 4. 58 Y-Crack on IH 10 in El Paso District – Location 2



Figure 4. 59 Core Taken at Y-crack Location 2 on IH 10 in El Paso District – Location 2

4.5 Test Section on FM 1938 in the Ft. Worth District

In order to study the behavior of CRCP leading to slab expansions and subsequent distresses, it was decided to monitor concrete strain in CRCP over a period of time through field testing. The field testing results from FM 1938 test section construction in Fort Worth district conducted

under TxDOT Research Project 5-6037: “Implementation of Alternatives to Asphalt Concrete Subbases for Concrete” were utilized. The slab thickness at these sections was 9 in. The two sections for this study are referred as FTW-I and FTW-II test sections and were constructed in Summer and Winter 2010 respectively.

4.5.1 FTW-I and FTW-II Test Sections - Testing Plan and Gage Setup

As shown in Figures 4.60 and 4.61, 3 VWSGs each were installed at FTW-I and FTW-II test sections in the longitudinal direction. The VWSGs were installed at a distance of 1 in., 4.5 in. and 8 in. from the base. The slab thickness for the test sections is 9 in. FTW-I test section was constructed on August 15, 2010 and FTW-II was constructed on March 17, 2010.

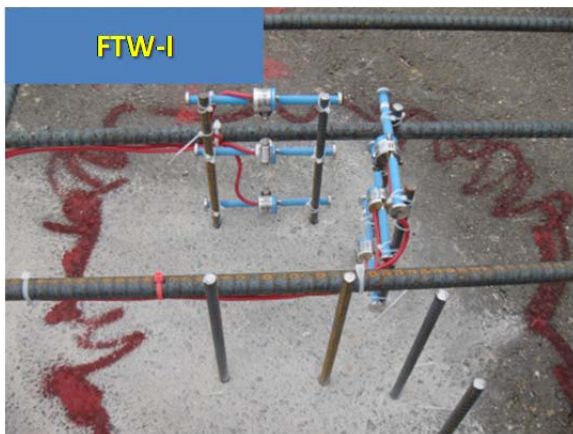


Figure 4. 60 Vibrating Wire Strain Gage Installation at FTW-I Test Section

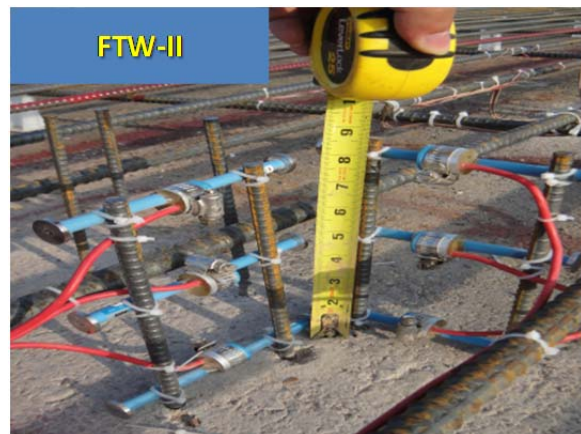


Figure 4. 61 Vibrating Wire Strain Gage Installation at FTW-II Test Section

Figures 4.62 and 4.63 show the transverse crack pattern near the VWSGs installed at FTW-I and FTW-II test section. At FTW-I, transverse cracks were observed at 5 ft. 3in. from the location of the VWSGs. At FTW-II, the transverse crack nearest to the VWSGs was at a distance of 2 ft. and 10 in.

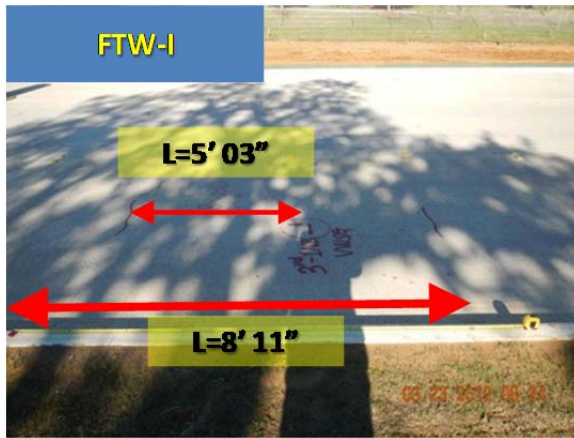


Figure 4. 62 Crack Location at FTW-I Test Section



Figure 4. 63 Crack Location at FTW-II Test Section

4.5.2 Concrete Strain Behavior at FTW-I and FTW-II Test Section

Concrete strain variation at mid-depth of the slab using the data from the VWSGs was evaluated. Specific temperature ranges were selected to see the behavior of concrete strain at each temperature range over a period of time. The data from FTW-I summer construction section was obtained 300 days after construction, whereas concrete strain data for FTW-II winter construction section was obtained 600 days after construction.

Figures 4.64, 4.65, 4.66 and 4.67 present the concrete strain at FTW-I summer test section at temperature ranges 60-62 °F, 70-72 °F, 80-82 °F and 90-92 °F respectively. At 60-62 °F, the concrete strain remains steady at around 150 micro strains in compression. At 70-72 °F, the concrete strain decreases from 100 micro strains in compression to around 125 micro strains in compression. At 80-82 °F, the concrete strain decreases from 75 micro strains in compression to 110 micro strains in compression. Also, at 90-92 °F, the concrete strain decreases from 50 micro strains in compression to 100 micro strains in compression. Thus, at each temperature range, the concrete strain over a period of 300 days is in compression. That means for the same temperature as the time passes, the concrete in CRCP continues to be in compression.

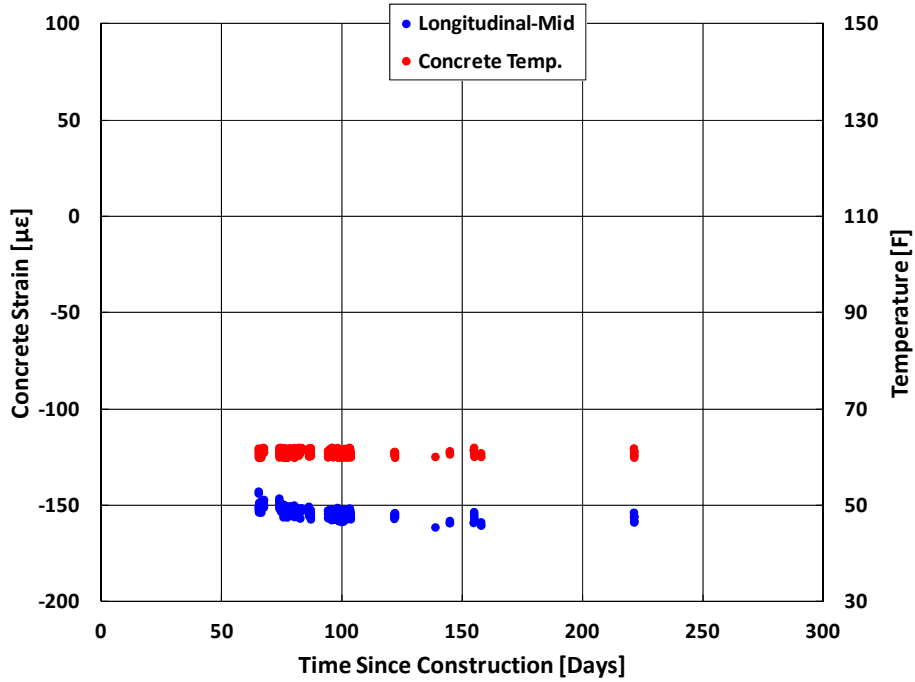


Figure 4. 64 Concrete Strain Variation on FM 1938 Summer Section at 60-62 °F

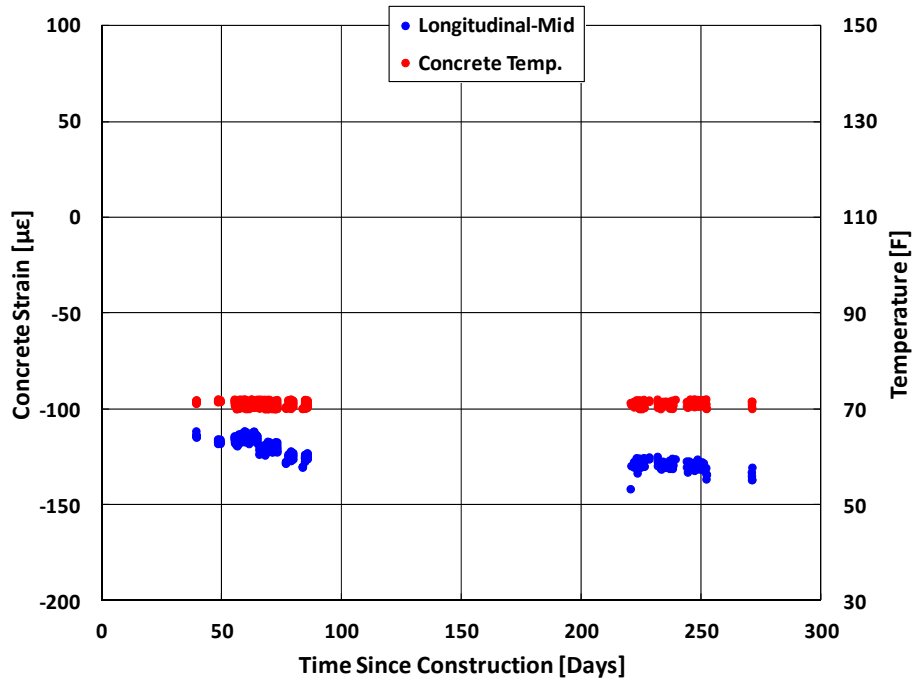


Figure 4. 65 Concrete Strain Variation on FM 1938 Summer Section at 70-72 °F

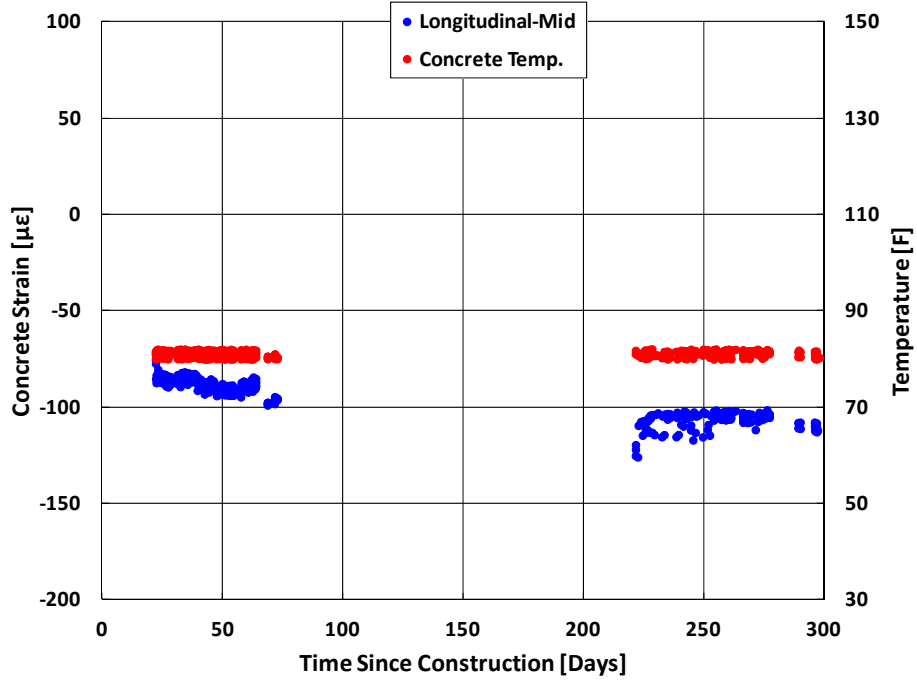


Figure 4. 66 Concrete Strain Variation on FM 1938 Summer Section at 80-82 °F

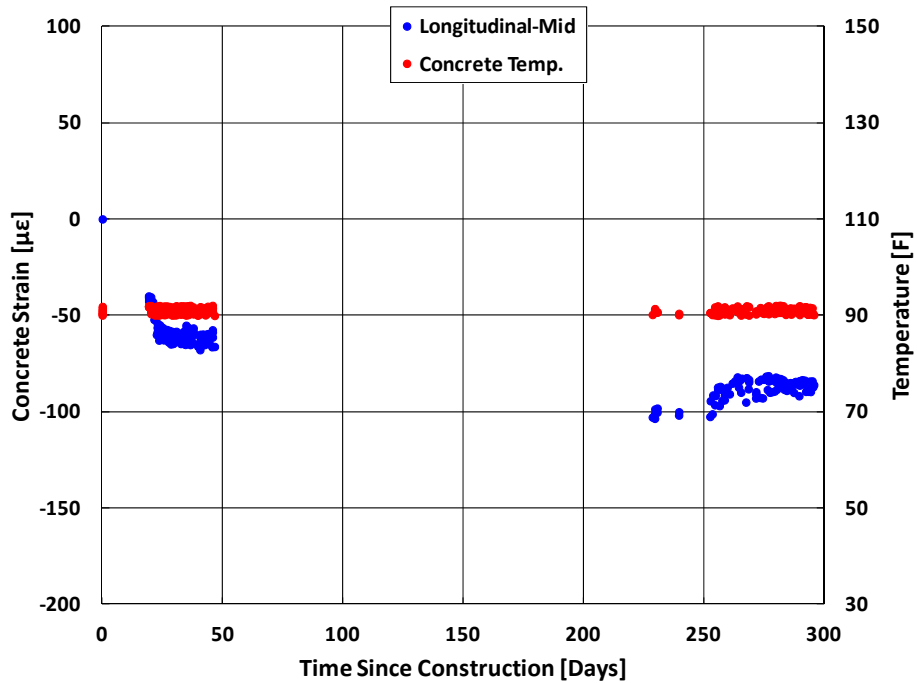


Figure 4. 67 Concrete Strain Variation on FM 1938 Summer Section at 90-92 °F

Figures 4.68 to 4.71 depict the change in concrete strain at specific temperature ranges at FTW-II winter construction section over a period of 600 days.

As shown in Figure 4.68, for concrete temperature range of 60-62 °F, the total concrete strain decreases from 30 micro strains in compression to 160 micro strains in compression. At 70-72 °F, the concrete strain decreases from 10 micro strains in tension to 120 micro strains in compression. Similarly, at the end of 600 days since construction for a concrete temperature range of 80-82 °F, the concrete strain is in constant compression up to 600 days since construction. Identical compressive concrete strain after 600 days since construction is seen at 90-92 °F temperature range in Figure 4.71.

The above data shows that for 300 days since construction in the summer season and 600 days since construction in the winter season, concrete strain was observed to be in constant compression at different concrete temperature ranges. This test result shows that slab expansion in CRCP may not be developed in the relatively early age compared to existing CRCP. Since data loggers are still in FM 1938, the data will be monitored for long-term strain variation continually.

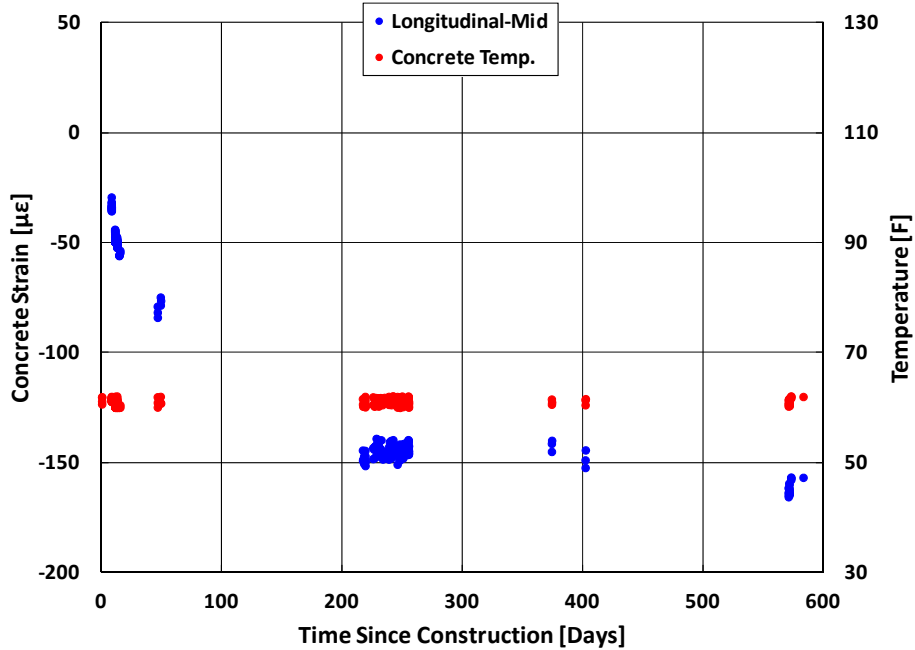


Figure 4. 68 Concrete Strain Variation on FM 1938 Winter Section at 60-62 °F

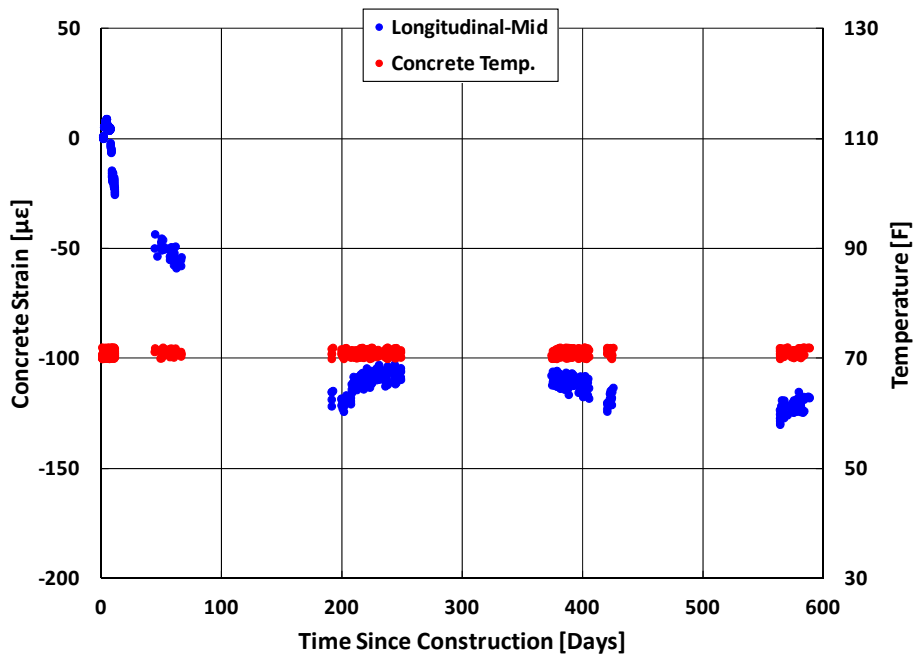


Figure 4. 69 Concrete Strain Variation on FM 1938 Winter Section at 70-72 °F

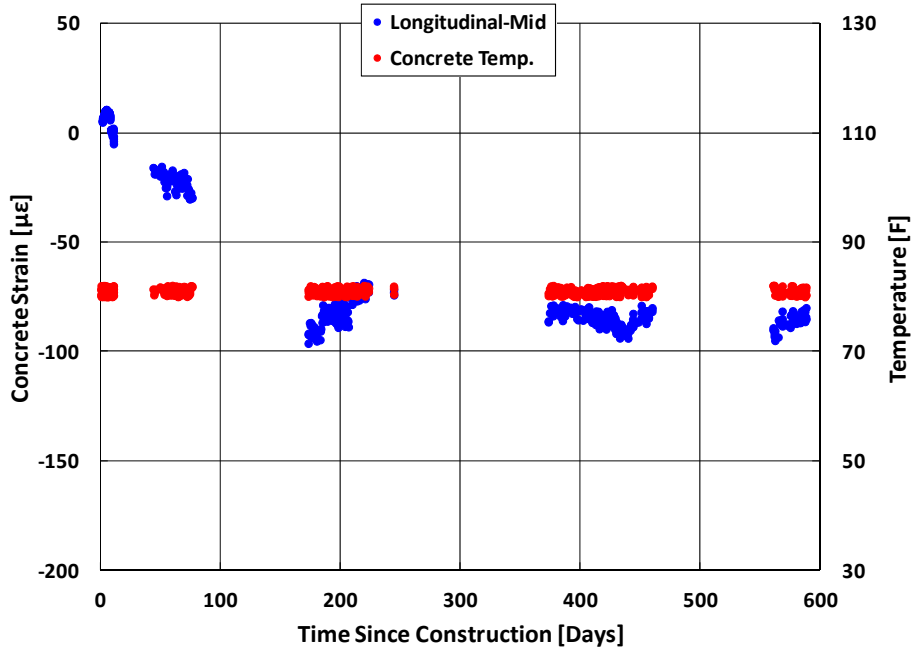


Figure 4. 70 Concrete Strain Variation on FM 1938 Winter Section at 80-82 °F

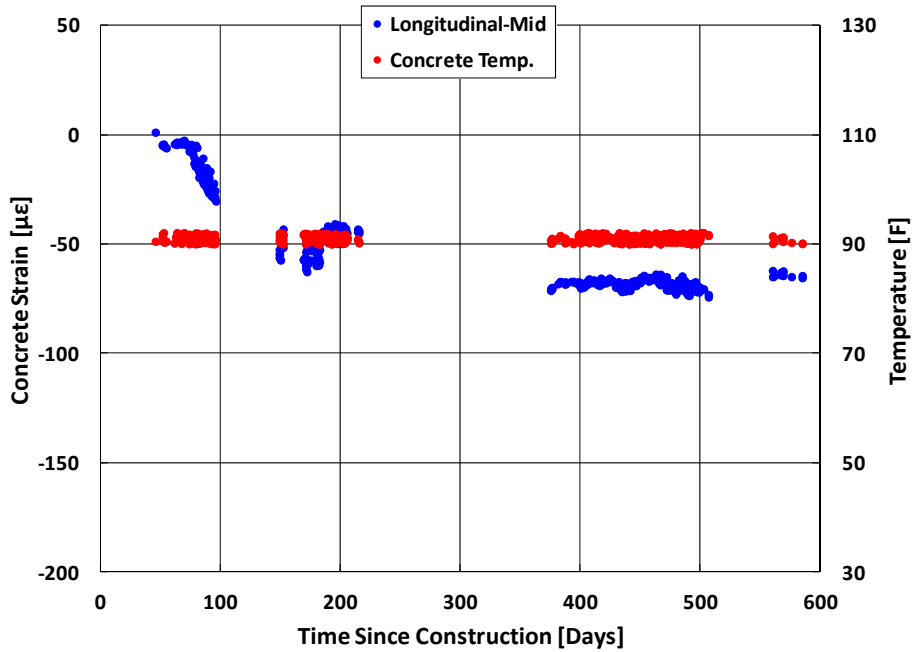


Figure 4. 71 Concrete Strain Variation on FM 1938 Winter Section at 90-92 °F

4.6 Distress Mechanisms at Longitudinal Joint

One of the premature distresses observed in Texas is distress near longitudinal construction joints (LCJs) or longitudinal warping joints (LWJs). To identify mechanisms of the distresses related to LCJs, 4 CRCP sections that experience distresses at LCJs and LWJs were identified. Figure 4.72 (a) illustrates distresses at LCJ on IH 27 in the Lubbock District before repair. According to TxDOT 2010 PMIS, these distresses were recorded as punchout. However these are not real punchouts but these distresses may have been caused by relative lane movement between inside and outside lane. Figure 4.72 (b) shows the picture after repair. As can be seen in Figure 4.73 (a), the relative movement between inside lane and outside lane was observed and the relative movement was almost 1 in. as can be seen from the tining spacing at LWJ. Longitudinal joint separation was also observed in this section. Figure 4.73 (b) illustrates the faulting at longitudinal joint. This section was overlaid with asphalt concrete as shown in Figure 4.74 (a). Figure 4.74 (b) shows the stitched longitudinal joint before asphalt overlay.



Figure 4. 72 LCJ Distresses on IH 27 in the Lubbock District



a. Joint Separation of LWJ and Relative Movement Between Slabs



b. Longitudinal Joint Faulting

Figure 4. 73 Longitudinal Joint Condition on IH 40 in the Amarillo District



a. Asphalt Overlay



b. Slot Stitching

Figure 4. 74 Asphalt Overlay over CRCP on IH 40 in the Amarillo District

Two sections were evaluated on IH 10 in the El Paso district for the distresses at LCJs. Figures 4.75 (a) and 4.75 (b) illustrate the distress and Portland cement concrete patch (PCP) on IH 10 eastbound at right after exit 22A, respectively. The longitudinal joint separation was also observed same as above mentioned IH 27 and IH 40. Figure 4.76 (a) is the pavement image of IH 10 westbound (reference marker from 26 to 27) from Google map. There are four lanes and the most of distresses is recorded in the second lane (L2) according to TxDOT 2013 PMIS as shown in Figure 4.76 (b). In general, since the trucks are usually passing through the outside lane, the most of punchouts was observed in the outside lane of CRCP. However, the majority of

Chapter 5 Conclusions and Recommendations

5.1 Conclusions

Extensive field investigations to study the behavior of steel and concrete in continuously reinforced concrete pavements leading to the formation of premature distresses were carried out. The mechanism of premature distresses near the transverse construction joint due to use of 50% additional steel at the transverse construction joint, construction of additional lane, construction and concrete material issues arising from manual placement of concrete near the transverse construction joint and the difference in behavior of concrete near the transverse construction joint depending on the construction season were studied. The slab movement at the construction joint when concrete is placed after a considerable period of time on the morning side of the slab was also evaluated. The longitudinal and vertical movement of the slabs tied at the longitudinal joint to the adjacent slab but in the absence of concrete on the morning side of the transverse construction joint was also studied. Forensic investigation of Y-crack and narrow transverse cracks in the field was conducted.

The following conclusions can be derived on the basis of field investigations and evidence collected:

- 1) Longitudinal tie bars at TCJs behave quite differently from longitudinal steel. It is primarily because longitudinal steel is continuous while tie bars are terminating at about 25 inches from TCJs. When the concrete temperature increases substantially from the setting temperature of concrete, tie bars actually could be in compression, potentially causing horizontal cracking of concrete at the depth of the steel placement and distresses.
- 2) Steel stresses at TCJ decrease over time, potentially due to the creep of concrete and the development of transverse cracks, which might invalidate the benefit of additional tie bars at TCJs.
- 3) The placement of additional tie bars at TCJs could interfere with concrete consolidation

operations near TCJs, creating poor quality concrete and potentially causing distresses in TCJs.

- 4) The rate of concrete strain variation with temperature near a TCJ is higher during the winter than during the summer season. It is due to the space available or joint widths at TCJs at different seasons. In the summer, joint widths get smaller, restricting the slab displacements when concrete temperature increases. On the other hand, joint widths get larger in the winter, allowing slab displacements with less restriction. However, this seasonal effect becomes less with pavement age.
- 5) When there is a significant time difference between the placements of concrete on either side of the construction joint, the newly placed concrete seems to pull the slab placed earlier on the other side of the TCJ due to drying shrinkage of newly placed concrete. Also, the old and new concrete slabs behave as a near composite structure with quite a small joint width, at least at early ages.
- 6) Due to the presence of additional steel at the TCJ, the compaction of concrete near the TCJ is hindered, resulting in formation of air voids and surface distresses near TCJs.
- 7) Y-cracks and narrow transverse cracks spacing that occur at early ages due to environmental loadings do not necessarily represent structurally weak elements. However, Y and narrow transverse cracks caused by repetitive overweight truck loadings exhibit distresses due to a presence of horizontal cracking.

5.2 Recommendations

Based on the conclusions derived from the field testing and investigations conducted, it is recommended that additional tie bars not be installed at TCJs. Also, in order to reduce stresses in longitudinal steel at TCJs, it is further recommended that transverse saw cuts be made at 5 ft. and 10 ft. from the TCJs in the morning placement side.

Further monitoring of steel and concrete strains over seasonal cycles at the transverse construction joint at all the test section locations needs to be continued to have a better in-depth understanding of steel and concrete behavior near the transverse construction joints. Condition surveys of these sections especially where different configurations of steel at the TCJ have been used at LBB-II test section should be periodically conducted.

References

- AASHTO, *AASHTO Guide for Design of Pavement Structures*. American Association of State Highway and Transportation Officials, Washington D. C., 1993.
- ARA, Inc., ERES Consultants Division. *Guide for Mechanistic-Empirical Design of New and Rehabilitated Pavement Structures, Part 3 – Design Analysis*. Champaign, Illinois, 2004.
- Nam, J.H. *Early-Age Behavior of CRCP and Its Implications for Long-Term Performance*. Ph.D. Dissertation, The University of Texas at Austin, Austin, Texas, 2005.
- Pavement Management Information System - Rater's Manual*. Texas Department of Transportation, Austin, Texas, 2009.
- Ryu, S.W., Saraf, S. and Won, M.C. *Project Level Performance Database for Rigid Pavements in Texas, II*. Publication FHWA/TX-11-0-6274-1, Texas Tech University, Lubbock, Texas, 2012.
- Ryu, S.W., Choi, PG., Zhou, W., Saraf, S. and Won, M.C. *Improvements of Full Depth Repair Practices for CRCP Distresses*. Publication FHWA/TX-11-0-6611-1, Texas Tech University, Lubbock, Texas, 2012.
- Zollinger, D., Won, M.C., Tyler Ley, Kyle Riding, Andrew Wimsatt, Zhou, W., Ryu, S.W., Choi, PG., *Implementation of Curing, Texturing, Subbase, and Compaction Measurement Alternatives for Continuously Reinforced Concrete Pavement.*, Publication FHWA/TX-13/5-6037-01-1, Texas A&M Transportation Institute, College Station, TX, 2013.
- Window, A. L., & Holister, G. S. *Strain Gauge Technology*. Applied Science and Publishers, London and New York, 1982.
- Won, M.C. *Just in Time Technology Transfer for Portland Cement Concrete Pavement Construction and Rehabilitation*. Publication FHWA/TX-12-5-9045-05-1, Texas Tech University, Lubbock, Texas, 2012.

Appendix A: Special Provision to Item 360

2004 Specifications

SPECIAL PROVISION
360---0xx
Concrete Pavement

For this project, Item 360, “Concrete Pavement” of the Standard Specifications, is hereby amended with respect to the clauses cited below, and no other clauses or requirements of this Item are waived or changed hereby.

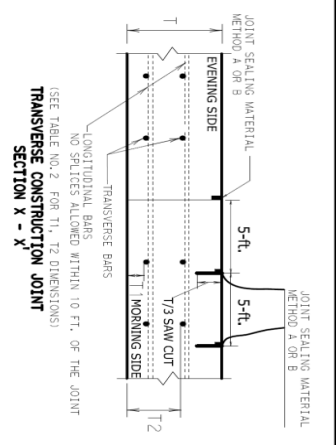
Article 360.4.D.2.a. Continuously Reinforced Concrete Pavement (CRCP) is voided and replaced by the following:

2. Transverse Construction Joints.

a. Continuously Reinforced Concrete Pavement (CRCP). Use a chalk line or string line to provide a true joint alignment. Saw transverse construction joint to the depth and width as shown on the plans within 24 hours of concrete finishing. Saw additional transverse joints at the locations and depth as shown on the plans within 24 hours of concrete finishing. Protect the reinforcing steel immediately beyond the construction joint from damage, vibration, and impact.

DISCLAIMER: The use of this standard is governed by the Texas Engineering Practice Act. No warranty of any kind is made by TxDOT for any purpose whatsoever. TxDOT assumes no responsibility for the conversion of this standard to other formats or for incorrect results or omissions resulting from its use.

DATE: _____
FILE: _____



* TIE BARS MAY BE IN SAME PLANE AS TRANSVERSE BARS

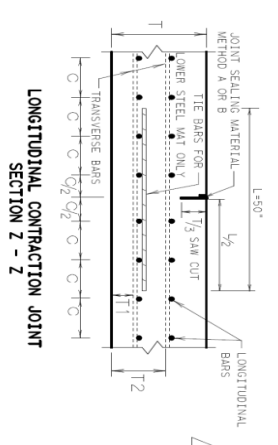
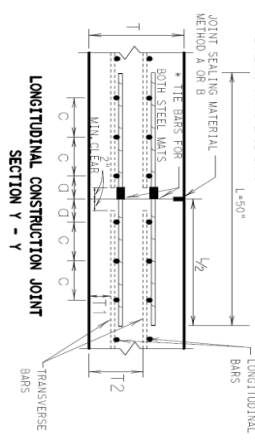
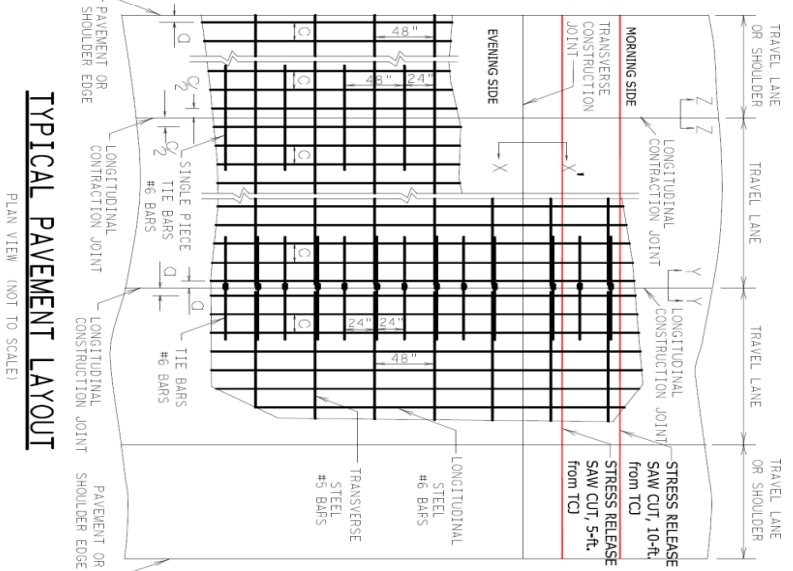


TABLE NO. 1 LONGITUDINAL STEEL

SLAB THICKNESS AND BAR SIZE	REGULAR STEEL BARS	FIRST SPACING AT EDGE OR JOINT	ADDITIONAL STEEL BARS AT TRANSVERSE CONSTRUCTION JOINT
T (IN.)	C	D	2 X C
BAR SIZE (IN.)	Ø	Ø	L
#6	10.5	3 TO 6	21
#5	9.5	3 TO 4	19
#4	8.5	3 TO 4	19

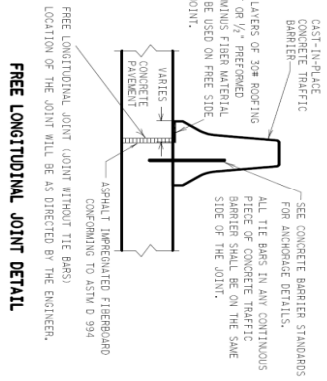
TABLE NO. 2 TWO LAYER STEEL PLACEMENT SPECIFICATIONS OF DIMENSIONS

THICKNESS (IN.)	T1 (IN.)	T2 (IN.)
14	4.5	8.0
15	5.0	8.5



TYPICAL PAVEMENT LAYOUT

PLAN VIEW (NOT TO SCALE)



FREE LONGITUDINAL JOINT DETAIL

GENERAL NOTES

1. THIS STANDARD IS FOR LOW CTE CONCRETE PAVEMENT ONLY. USE COURSE AGGREGATES TO PRODUCE CONCRETE WITH A COEFFICIENT OF THERMAL EXPANSION (CTE) NO GREATER THAN 4.0 X 10⁻⁶ IN./IN./°F.
2. SUPPLY AGGREGATES FROM SOURCES LISTED IN THE DEPARTMENT'S CONCRETE PAVED SOURCE QUALITY DATA. PROVIDE AGGREGATE CONSTRUCTION AND TESTING RECORDS TO THE ENGINEER BEFORE USE.
3. DETAILS FOR PAVEMENT WIDTH, PAVEMENT THICKNESS AND THE CROWN GROSS-SLOPE SHALL BE SHOWN ELSEWHERE IN THE PLANS. PAVEMENTS WIDER THAN 100 FT. WITHOUT A FREE LONGITUDINAL JOINT, ARE NOT COVERED BY THIS STANDARD.
4. THE DETAIL FOR THE JOINT SEALANT AND RESERVOIR 15 SHOWN ON STANDARD SHEET "CONCRETE PAVING DETAILS, JOINT SEALS."
5. ALL THE REINFORCING STEEL AND TIE BARS SHALL BE DEFORMED STEEL BARS CONFORMING TO ASTM A 615 (GRADE 60) OR ASTM A 996 (GRADE 60), USE #5 BARS FOR TRANSVERSE STEEL AND USE #6 BARS FOR LONGITUDINAL STEEL AND TIE BARS.
6. STEEL BAR PLACEMENT TOLERANCE SHALL BE +/- 1 IN. HORIZONTALLY AND +/- 0.5 IN. VERTICALLY. CALCULATED AVERAGE BAR SPACING (CONCRETE PLACEMENT WIDTH / NUMBER OF LONGITUDINAL BARS) SHALL CONFORM TO TABLE NO. 1 & 2 AND AS SPECIFIED.
7. PAVEMENT WIDTHS OF MORE THAN 15 FT. SHALL HAVE A LONGITUDINAL JOINT (SECTION Z-Z OR SECTION Y-Y). THESE JOINTS SHALL BE LOCATED 15 SHOWN ELSEWHERE ON THE PLANS.
8. THE SAW CUT DEPTH FOR THE LONGITUDINAL CONTRACTION JOINT AND STRESS RELIEF JOINT AT THE TRANSVERSE CONSTRUCTION JOINT SHALL BE ONE THIRD OF THE SLAB THICKNESS.
9. THE TRANSVERSE BAR SPACING SHALL BE 48 IN. FOR ALL THE CONCRETE PAVEMENT WIDTHS.
10. AT LONGITUDINAL CONTRACTION JOINTS, SINGLE PIECE TIE BARS SHALL BE USED. THE TIE BARS SHALL BE PLACED MIDWAY BETWEEN THE TRANSVERSE BARS AT 48 IN. SPACING FOR THE LOWER STEEL MAT ONLY. AT LONGITUDINAL CONTRACTION JOINTS, MULTIPLE PIECE TIE BARS SHALL BE PLACED AT 24 IN. SPACING FOR BOTH STEEL MATS. WHEN APPROVED BY THE ENGINEER, SINGLE PIECE TIE BARS MAY BE USED BY INSERTING INTO PLASTIC CONCRETE.
11. WHEN TYING CONCRETE CUTTER AT A LONGITUDINAL JOINT, THE TIE BAR LENGTH OR POSITION MAY BE ADJUSTED. PROVIDE 3 IN. OF CONCRETE COVER FROM THE BACK OF CUTTER TO THE END OF THE BAR.
12. MISSING OR DAMAGED TIE BARS SHALL BE REPLACED BY DRILLING AND EPON GROUTING AT THE CONTRACTION'S EXPENSE.
13. OMIT TIE BARS LOCATED WITHIN 18 IN. OF THE TRANSVERSE CONSTRUCTION JOINTS. USE HAND-OPERATED DIMENSION VERIFIERS TO CONSOLIDATE THE CONCRETE ADJACENT TO ALL PAVED JOINTS.
14. OBTAIN THE ENGINEER'S WRITTEN APPROVAL, IF THE CONCRETE MIX DESIGN USES MORE THAN 5.5 SACKS/CY.
15. LONGITUDINAL REINFORCING STEEL SPLICES SHALL BE A MINIMUM OF 25 IN.

Texas Department of Transportation
Design Division Standard

CONTINUOUSLY REINFORCED CONCRETE PAVEMENT TWO LAYER STEEL BAR PLACEMENT T-14, & 15 INCHES FOR LOW CTE CONCRETE CROP (2A) -13

DATE:	BY:	CHK:	APP:



TEXAS TECH UNIVERSITY
Multidisciplinary Research in Transportation

Texas Tech University | Lubbock, Texas 79409
P 806.742.3503 | F 806.742.2644